



universität  
wien

# DISSERTATION

Titel der Dissertation

„Role of Sprouty proteins as antagonists of RTK signaling“

Verfasser

Mag. rer. nat. Christoph-Erik Mayer

angestrebter akademischer Grad

Doktor der Naturwissenschaften (Dr. rer. nat.)

Wien, 2008-11-21

Studienkennzahl lt. Studienblatt:	A 091 419
Dissertationsgebiet lt. Studienblatt:	Chemie
Betreuerin / Betreuer:	Ao. Prof. Dr. Fritz Pittner



## Danksagungen

Meiner Familie (Mama, Papa, Oma, Opa, Alex, Thesi und Carina), für ihre Hilfe und Unterstützung in allen Lebenslagen. Speziell möchte ich meine Dissertation meinem Opa widmen.

Edda, für die vielen gemeinsamen Erlebnisse und Ziele, die uns verbinden und mein Leben verschönern. Außerdem möchte ich auch ihrer Familie danken, die mich mit offenen Armen aufgenommen hat.

Allen meinen FreundInnen, die mich oft besser kennen, als ich mich selbst.

Ao. Prof. Pittner, für die Betreuung meiner Dissertation.

Priv. Doz. Univ.-Lektor Dr. Hedwig Sutterlüty, für die tolle Betreuung, Geduld und Arbeit, die sie in den fünf Jahren „Sprouty“ in mich investiert hat.

Meinen Arbeitskollegen Flo, Gerald, Babs und Ilse, für die schöne Zeit und das tolle Arbeitsklima.

Ao. Prof. Walter Berger und seinen Mitarbeitern (Sigrid, Rita, Hendrik, Christine, Petra, Sabine, Christian, Vera, Flo, Dani und Ute), Prof. Micksche, den Gruschen, Mikulitsen, Gsurlis, Marians, Elblings, Grasl-Kraupps und Holzmännern, Silvia und Gerti für die gute Zusammenarbeit und Hilfe.

Ass. Prof. Tesfaye Mengiste und seinem Labor, für die tolle Zeit in Purdue

Allen Menschen, denen ich hier gerne persönlich Danken würde, aber leider keinen Platz dafür finde.

# Table of Contents

<b><u>DANKSAGUNGEN.....</u></b>	<b><u>3</u></b>
<b><u>TABLE OF CONTENTS.....</u></b>	<b><u>4</u></b>
<b><u>1 ZUSAMMENFASSUNG/ ABSTRACT .....</u></b>	<b><u>6</u></b>
1.1 ZUSAMMENFASSUNG .....	6
1.2 ABSTRACT .....	7
<b><u>2 INTRODUCTION.....</u></b>	<b><u>9</u></b>
2.1 DEREGULATED SIGNALING IN CANCER .....	9
2.1.1 RECEPTOR TYROSINE KINASE-MEDIATED SIGNALING .....	10
2.1.2 RAS AND RAS-INDUCED PATHWAYS .....	12
2.2 SPROUTY PROTEINS .....	17
2.2.1 SPROUTY FAMILY MEMBERS .....	17
2.2.2 SPROUTY EXPRESSION DURING EMBRYOGENESIS .....	19
2.2.3 SPROUTY GAIN AND KNOCK-OUT STUDIES.....	20
2.2.4 REGULATION OF SPROUTY FUNCTION AND ACTIVITY.....	22
2.2.5 ROLE OF SPRY PROTEINS DURING NEOPLASTIC TRANSFORMATION.....	27
<b><u>3 AIMS OF THE STUDY.....</u></b>	<b><u>29</u></b>
<b><u>4 MATERIALS AND METHODS .....</u></b>	<b><u>30</u></b>
4.1 COMPETENT BACTERIA .....	30
4.2 TRANSFORMATION BY HEAT SHOCK .....	30
4.3 POLYMERASE CHAIN REACTION (PCR)-BASED TECHNIQUES.....	30
4.4 RESTRICTION DIGESTION AND CLONING.....	32
4.5 STETL, MIDI, MAXI AND CsCL PLASMID DNA PURIFICATION .....	33
4.6 CELL CULTURE .....	34
4.7 CONSTRUCTION OF ADENOVIRUSES .....	35
4.7.1 PREPARATION OF $\Psi$ 5 DONOR VIRUS DNA .....	35
4.7.2 PREPARATION OF THE TARGET RECOMBINANT VIRUS.....	36
4.8 CLONOGENIC ASSAY, GROWTH CURVE, SCRATCH ASSAY .....	36

4.9	FLOW CYTOMETRY .....	37
4.10	GENERATION OF SPRY-SPECIFIC ANTIBODIES.....	37
4.11	IMMUNOBLOTTING .....	39
4.12	IMMUNOPRECIPITATION .....	39
4.13	NORTHERN BLOTTING AND <sup>32</sup> P-LABELING.....	40
4.14	STATISTICS.....	41
4.15	CONSTRUCTION OF A HUMAN LUNG CDNA LIBRARY .....	41
4.16	YEAST QUICK TRAF0 .....	41
4.17	LACZ ASSAY .....	42
<b>5</b>	<b><u>RESULTS .....</u></b>	<b>44</b>
5.1	MANUSCRIPT 1: DOWN-REGULATION OF SPROUTY2 IN NON-SMALL CELL LUNG CANCER CONTRIBUTES TO TUMOR MALIGNANCY VIA EXTRACELLULAR SIGNAL-REGULATED KINASE PATHWAY-DEPENDENT AND -INDEPENDENT MECHANISMS.....	44
5.2	MANUSCRIPT 2: RAS SIGNALING HAS A CLEARLY DISTINGUISHABLE IMPACT ON SPROUTY1, 2 AND 4 EXPRESSIONS .....	57
5.3	UNPUBLISHED DATA .....	73
5.3.1	CELL CYCLE-SPECIFIC REGULATION OF SPRY PROTEINS.....	73
5.3.2	CONSTRUCTION OF A HUMAN LUNG CDNA LIBRARY .....	78
5.3.3	pBD-GAL4-hSPRY2 BAIT LACZ SCREEN .....	82
<b>6</b>	<b><u>SUMMARY AND DISCUSSION .....</u></b>	<b>83</b>
<b>7</b>	<b><u>ABBREVIATIONS.....</u></b>	<b>90</b>
<b>8</b>	<b><u>REFERENCES.....</u></b>	<b>92</b>
<b>9</b>	<b><u>CURRICULUM VITAE.....</u></b>	<b>102</b>

# 1 Zusammenfassung/ Abstract

## 1.1 Zusammenfassung

Krebszellen sind durch eine weitgehende Unabhängigkeit von Wachstumsfaktorstimuli und eine starke Überaktivierung von wachstums- und überlebens-promovierenden Signalübertragungssystemen gekennzeichnet. Auch die verminderte Expression der Sprouty (Spry) Proteine trägt nachweislich in malignen Tumoren verschiedener Gewebe zu diesem Phänotyp bei. In normalen Zellen fungieren die Spry Proteine, hauptsächlich über ihre hemmende Wirkung auf die Ras/Raf/MAPK Signalkaskade, als Modulatoren von Rezeptor-Tyrosin-Kinasen-aktivierten Signalwegen.

In dieser Arbeit konnten wir zeigen, dass die Expression von Spry2, aber nicht von Spry1, im Nicht-kleinzelligen Lungenkarzinom (NSCLC) im Vergleich zum normalen adulten Lungenepithelium signifikant reduziert ist. Basierend auf dieser Erkenntnis, untersuchten wir den Einfluss der Spry2 Expression auf den malignen Phänotyp von NSCLC in Abhängigkeit von wildtyp (wt) und konstitutiv aktivem K-Ras. Während die verminderte Aktivität der MAPK Kaskade und die herabgesetzte Geschwindigkeit der Zellwanderung nach ektoptischer Expression von Spry2 ausschließlich in K-Ras wt Zellen beobachtet wurde, war die Hemmung von Zellvermehrung und Tumorformation in der Maus bei der Re-expression von Spry2 unabhängig vom K-Ras Status. Die gewonnenen Daten legen nahe, dass Spry2 neben der Ras/Raf/MAPK Kaskade eine zweite regulatorische Funktion wahrnimmt. Erhärtet wird diese Annahme durch Versuche mit einer Spry2 Mutante, die zwar nicht in der Lage war die Signalintensität der MAPK zu inhibieren, aber dennoch signifikant, wenn auch schwächer als Spry2 wt, die Zellvermehrung hemmte.

Da alle Sprouty Proteine als Teil einer auto-regulatorischen Rückkoppelungsschleife beschrieben wurden, untersuchten wir in weiterer Folge die molekularen Grundlagen der Expressionsregulation verschiedener Spry Familienmitglieder. Erhöhte Spry2 und Spry4 Levels korrelierten signifikant mit der Expression von aktiviertem endogenen und ektoptisch expremierten K-Ras in NSCLC-Zelllinien bzw. nicht-malignen Fibroblasten, während Spry1 nicht erhöht vorgefunden wurde und nicht direkt durch Ras-induzierte Signalwege reguliert wird. Durch die Verwendung verschiedener Wachstumsfaktoren und spezifischer Ras Mutationen konnten wir weiters zeigen, dass Spry2 hauptsächlich über aktivierende Ras/ Erk Signale reguliert wird, während bei Spry4 die Induktion der Spry4 Expression fast ausschließlich durch Serum angeregt und über mehrere Ras-aktivierte Signalwege beeinflusst wird.

Bezüglich der Expressionsmuster während eines Zellzyklus zeigten alle untersuchten Spry Familienmitglieder phasenspezifisch fluktuierende und voneinander merklich unterschiedliche Expressionsprofile. Außerdem legen unsere Daten nahe, dass Spry1 und Spry2 über die Ebene der Transkription reguliert werden, da mRNA und Proteine übereinstimmend voneinander exprimiert vorliegen. Im Gegensatz dazu wird Spry4 eher durch post-translatorische Mechanismen stabilisiert. Über die exogene Expression von wildtyp und dominant negativem cCbl untersuchten wir den Einfluß von cCbl auf die Zellzyklusphase-abhängige Expression von Spry1, 2 und 4, v.a. zwischen später G1 und früher S Phase. Dabei konnten wir zeigen, dass die Herunterregulation von Spry2 während dieses Phasenfensters durch cCbl erfolgt, während Spry1 und Spry4 keine direkten Substrate von cCbl sind.

Zusammenfassend, Spry2 wirkt der Erk Phosphorylierung entgegen und wird selbst durch Ras über den MAPK Signalweg induziert. Weiters inhibiert Spry2 die Zellproliferation über einen noch nicht beschriebenen Signalweg. Außerdem konnten wir zeigen, dass verschiedene Sprys über unterschiedliche Mechanismen in verschiedenen Zellzyklusphasen induziert werden. Auf Grund dieser Erkenntnisse liefern unsere Daten einen wichtigen Beitrag zum Verständnis der Rolle von Spry Proteinen, vor allem im Hinblick auf ihre Rolle in der Krebsentstehung und -progression.

## 1.2 Abstract

Self sufficiency of growth signals and desensitized signal transduction systems are hallmarks of human cancer. One group of proteins shown to be deregulated in malignant tumors of diverse tissues are members of the Sprouty (Spry) protein family. Sprys function as modulators of receptor tyrosine kinase (RTK) signaling mainly by interfering with the Ras/Raf/mitogen-activated protein kinase (MAPK) cascade as part of an auto-regulatory feedback loop.

In this study, we show that Spry2, but not Spry1 expression, is consistently lowered and significantly reduced in non-small cell lung cancer (NSCLC) compared to the normal adult lung epithelium. Based on this finding, we investigated the influence of Spry2 expression on the malignant phenotype of NSCLC cells in the background of wild type (wt) or constitutive active K-Ras. Ectopic expression of Spry2 antagonized extracellular-regulated kinase (Erk) activity and cell migration just in K-Ras wt cell lines. In contrast, inhibition of cell proliferation and tumor formation in mice in response to Spry2 re-expression was observed

independently of the K-Ras status. In corroboration, a Spry2 mutant unable to inhibit MAPK phosphorylation still reduced cell proliferation significantly but less pronounced compared with the Spry2 wt protein.

Since all Sprouty proteins had been suggested to be regulated as part of an auto-regulatory feedback loop, further experiments were designed to explore the precise requirements for induced expression of the Spry proteins. Increased Spry2 and Spry4 levels significantly correlated with the expression of activating endogenous and ectopic expressed K-Ras mutations in NSCLC cells and non-malignant fibroblasts, whereas Spry1 was not found elevated and was not regulated directly via Ras-mediated signaling cascades. Using different growth factors and ectopic expression of Ras mutant forms, our data revealed that induction of Spry2 is exclusively dependent on Erk activation via Ras-dependent signaling, while induction of Spry4 expression was almost exclusively activated by serum and/or several Ras-influenced signaling cascades.

Throughout the cell cycle all investigated Spry proteins showed clear and reproducible fluctuations, but interestingly their cell cycle-specific expression patterns differed markedly. Further, we demonstrate that Spry1 and Spry2 levels are mediated by transcriptional activation, since mRNA and protein levels were found coregulated, while Spry4 is stabilized by post-translatory modifications. Finally, we investigated the influence of ectopically expressed wildtype and dominant negative cCbl on the cell cycle-specific expression of Spry1, 2 and 4, especially between late G1 and early S phase. Our data indicate that Spry2 downregulation within this specific time-frame is mediated by cCbl, whereas Spry1 and Spry4 are not direct substrates of cCbl.

Summarizing, Spry2 antagonizes Erk phosphorylation and is itself induced by Ras via MAPK activation. Furthermore, Spry2 inhibits cell proliferation by another yet unidentified pathway. In addition, we showed that Sprys are induced by different mechanisms, during different phases of the cell cycle and are independently deregulated in tumor cells. Therefore our data make an important contribution to understand the role of Spry proteins.



## 2 Introduction

### 2.1 Deregulated signaling in cancer

Cancer is a multi-step process developing as a consequence of stepwise accumulation of mutations in several genes. The modern definition of a neoplastic cell is one that has clonally expanded as a result of somatic mutations<sup>1, 2</sup>. Since cancer is not caused by a single gene defect, each mutation contributes to malignancy<sup>3</sup> and each new step leads to a clonal expansion of cells harboring the new mutation: in this way the probability that multiple mutations occur in the same cell is greatly increased<sup>4</sup>. The first somatic mutation that causes a clonal expansion initiates the neoplastic process<sup>2</sup>. Subsequent somatic mutations result in additional rounds of clonal expansion-tumor progression<sup>1</sup>. The clonal evolution model involves mutations in three major types of genes, which are required for a selective advantage to the neoplasm over adjacent normal cells. Among the first group are genes taking part in both positive and negative regulation of cell growth and survival<sup>2</sup>. Within the second group, genes and their respective protein products are involved in genetic stability regulating DNA synthesis and repair and control processes responsible for mitotic recombination and chromosomal segregation. Alterations in the mitotic process lead to chromosome rearrangements and aneuploidy observed in nearly all solid tumors<sup>5</sup>. Aneuploidy itself increases the possibility for further gains or losses of chromosomes during the mitotic process<sup>6</sup> and to a higher mutation rate in other genes<sup>7</sup>. The third group mediates tumor invasion and metastasis: abnormalities in cell adhesion proteins, proteolytic enzymes that enhance the capability to invade adjacent tissues and changes molecules associated with blood clotting and angiogenesis<sup>8,9</sup>.

Oncogenes and tumor suppressor genes function similarly at the physiologic level and alterations lead to a selective advantage during the clonal selection process. Oncogenes are mutated to render genes constitutively active or active under conditions in which the wild-type gene is not and can result from chromosomal translocation, gene amplification and mutations of crucial residues within the coding sequence. Usually one mutated allele of an oncogene is sufficient to confer a selective growth advantage. Alterations within tumor-suppressor genes reduce their activity to inhibit tumor formation and result from missense mutations, truncated versions, deletions and insertions or epigenetic silencing. Mutated cancer genes enhance net cell growth, but there are many fewer pathways than genes and mammals have multiple safeguards to protect the cell. Since intracellular pathways intersect at multiple levels they cannot be considered separately. For example, several genes

directly control transitions from resting stage (G<sub>0</sub>, G<sub>1</sub>) to replicating phase (S) of the cell cycle: cyclin-dependent kinase 4 (CdK4), CyclinD1 which activates CdK4, the transcription factor retinoblastoma (Rb) and p16 (inhibits CdK4)<sup>10-12</sup>. Genes-encoding p16 and Rb are tumor suppressor genes inactivated by mutation, whereas mutations in CdK4 and Cyclin D1 are activating those oncogenes. There is leading evidence that these four genes function in a single pathway in human cancer and show an “exclusivity” principle: since the functional effect of each mutation is similar only one of the four genes is usually mutated.

Further, solid tumors consist of two compartments – neoplastic epithelial cells and surrounding stroma cells. During the last years it became evident that the stroma participates in many supportive functions such as angiogenesis and plays an active role in tumorigenesis<sup>13</sup>. Usually, cell maintenance and intracellular communication is precisely coordinated by positive and negative feedback loops providing the cells with the ability to adjust its output in response to monitoring itself. Further, spatial regulation of signaling events are also regulated by feedback loops<sup>14</sup>. Therefore such feedback loops are very often found deregulated in neoplastic lesions. Negative feedback occurs when e.g. a signal induces the expression of its own inhibitor to limit and/or dampen signaling. In healthy cells, p53 is maintained safely beyond its functional threshold by action of a negative feedback involving Mdm2, whose transcription is activated by p53<sup>15, 16</sup>. Since p53 mediates cell-cycle arrest and/or cell death upon damage, cells that cannot escape the Mdm2/p53 feedback loop are in danger of losing control of normal growth and development as they cannot respond to potentially carcinogenic damage and subsequently, the activity of p53 is lost in the majority of human cancers<sup>17</sup>. A signal activating positive feedback loop amplifies/stabilizes the initial signal to prolong signaling. Thus, a number of tumors contain amplified or overexpressed Mdm2, which is sufficient to block the response of wild-type p53 upon damage and also leads to tumor progression. Other examples are autocrine, positive feedback loops which mediate the induction of expression of more signaling molecules through the activation of intracellular signaling kinases.

### **2.1.1 Receptor tyrosine kinase-mediated signaling**

Signal transmission cascades are usually initiated by a specific extracellular polypeptide ligand binding to membrane spanning cell surface receptors. Receptor tyrosine (Tyr) kinases (RTKs) play an essential role in the complex network of cell communication by converting extracellular signals into intracellular ones. They control fundamental processes including cell cycle, cell migration, cell metabolism, cell survival, cell proliferation, cell differentiation and

hence tissue homeostasis. They are transmembrane glycoproteins that consist of an extracellular ligand binding domain, a membrane-spanning transmembrane helix and a cytoplasmic domain with a conserved protein kinase domain core subjected to autophosphorylation and phosphorylation by heterologous protein kinases<sup>18, 19</sup>. The polypeptide ligands for RTKs, mostly growth factors, comprise a large variety of different signal proteins which act as local mediators at very low concentrations ( $10^{-9} - 10^{-11}$  mol/L). Ligand binding to the corresponding receptor induces the formation of RTK dimers or oligomers, or causes conformational change of already preformed receptor complexes and leads to RTK activation by cross-phosphorylation (autophosphorylation) of the neighboring cytosolic kinase domain.

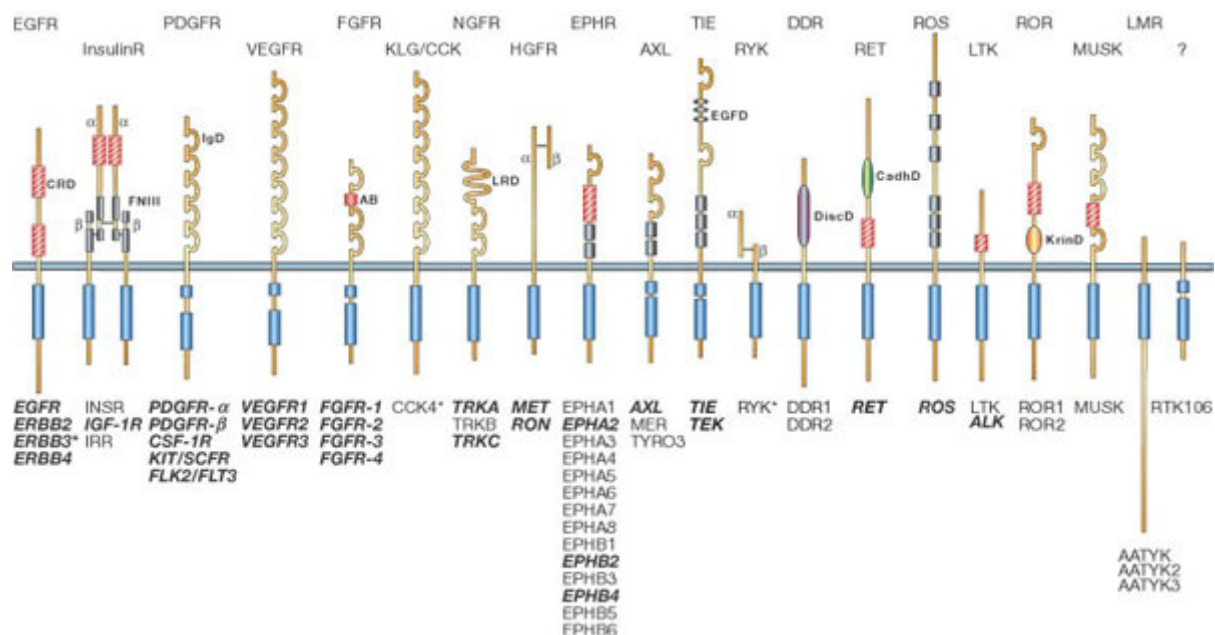


**Figure 1** Structure of diverse RTKs<sup>20</sup>

Tyr phosphorylation within the kinase domains increases the enzymatic activity and catalyzes the transfer of the  $\gamma$ -P of ATP to hydroxyl groups of Tyrs to activate specific proteins<sup>19</sup>. Further, autophosphorylation of Tyr residues outside the kinase domain creates high-affinity binding sites which are targeted by Src homology region 2 (SH2)- and phospho-tyrosine binding (PTB)-interacting motifs found in adaptor proteins, such as growth factor receptor-bound protein 2 (Grb2) and fibroblast growth factor receptor substrate 2 (FRS2)<sup>21</sup>. Under non-malignant conditions, RTKs are under tight control, since these phosphorylation binding domains are also recognized by proteins leading to receptor downregulation. One example is the casitas B-lineage lymphoma (cCbl) protein which targets activated epidermal growth factor receptor (EGFR) promoting ubiquitination and degradation<sup>22</sup>. Nevertheless, RTKs were

found to play a decisive role during carcinogenesis. Many of the known RTKs have been found either mutated or overexpressed in human cancers<sup>20</sup>.

Downstream-signaling cascades drive tumorigenesis through coordinated phosphorylation of proteins regulating protein synthesis, cell-cycle progression and metabolism, and of transcription factors that induce the expression of genes involved in these processes<sup>4, 23</sup>.

The best known signaling cascades activated by RTKs and often found deregulated in cancer are the mitogen-activated protein kinase (MAPK) and the phosphatidylinositol 3-kinase (PI3K) pathway with the Ras protein, functioning as the major integrator between extracellular signals and intracellular response.

### 2.1.2 Ras and Ras-induced pathways

Ras genes were identified as retroviral oncogenes in the 1960/70s from the genome of Harvey and Kirsten rat sarcoma viruses<sup>24, 25</sup>. During the 1980s Ras activating mutations were identified in human tumors leading to intensive studies concerning Ras-mediated signaling. Today, it is estimated that 20% of all human tumors have activating mutations in one of the Ras genes. Germline mutations in Ras pathway-genes result in phenotypically overlapping neuro-cardio-facial-cutaneous developmental syndromes<sup>26</sup>: Neurofibromatosis Type I, Noonan syndrome, LEOPARD syndrome, Cardio-facio-cutaneous syndrome and Costello syndrome<sup>27, 28</sup>. In general, patients are characterized by facial dysmorphisms, heart defects and short stature, skin and genital malformations, mental retardation, and predisposition to certain malignancies<sup>26</sup>.

Ras belongs to a large family of monomeric guanosine triphosphatases (GTPases) functioning as switches between an active GTP and an inactive, non-promoting conformation. Hexa-coordinated  $Mg^{2+}$  within small G-proteins provides tight association with guanine nucleotides (dissociation constants of GDP and GTP -  $K_D \sim 10-100pM$ )<sup>29</sup>. Two so called switch regions of Ras undergo dramatic structural changes depending on the type of bound nucleotide: switch region I (aa 30-38) and switch region II (aa 59-67). Upon GTP-binding these two domains form a surface for effector molecule binding<sup>30</sup>. Ras has a measurable intrinsic GTPase activity (GTPase hydrolysis rate constant 0.028/min)<sup>31</sup>, but GTPase accelerators – GTPase activating proteins (GAPs) - increase GTPase activity 10<sup>5</sup>-fold<sup>32</sup>. Recharge is catalyzed by guanine-nucleotide exchange factor (GEF) activity generating RasGTP. Activated RTKs are targeted by Grb2 which recruits son of sevenless (Sos)-GEF to the plasma membrane as a result of its constitutive interaction with Grb2. Upon Ras binding, Sos is maintained in an autoinhibitory state. At first, RasGDP binds Sos at an allosteric site distal to the catalytic domain to induce

low GEF activity<sup>33-35</sup>. The generated RasGTP then binds with higher affinity to the same allosteric Sos domain to fully relieve steric occlusion of the active site inducing high GEF activity<sup>36, 37</sup>. Significantly, activating mutations in Sos have been identified in patients with Noonan's syndrome<sup>38, 39</sup> highlighting the role of Sos in regulating duration, amplitude and output of Ras signaling<sup>40</sup>. General Ras expression was shown to be modulated by small non-coding RNAs (microRNAs), e.g. the microRNA let-7, downregulating Ras mRNA at a post-transcriptional level<sup>41, 42</sup>.

Ras isoforms were found localized at various intracellular membranes including Golgi, endoplasmic reticulum (ER) and endosomes<sup>43-45</sup>. Different localization is mediated by post translational modification (farnesylation and carboxymethylation) of the hypervariable c-terminal region of Ras and influences strength, duration and the functional diversity of Ras proteins<sup>46-48</sup>. In H-Ras and N-Ras the hypervariable cysteine-rich region is palmitoylated and constantly shuttles between Golgi and plasma membrane upon de-/repalmitoylation cycles<sup>49, 50</sup>. In contrast, K-Ras possesses a region of polybasic amino acids and primarily localizes to the plasma membrane, but when phosphorylated re-localizes to other endomembrane compartments (ER, mitochondria, Golgi)<sup>51, 52</sup>. Further, spatio-temporal activation, specificity and intensity of Ras signaling is influenced by distinct microdomains such as lipid rafts and caveolae within the plasma membrane<sup>53</sup>. 50% of GDP-H-Ras is localized to caveolae and upon activation GTP-N-Ras and GTP-H-Ras are mostly located to lipid rafts, while K-Ras is not predominantly localized to lipid rafts irrespective of its activation status<sup>54, 55</sup>. Additionally, Ras proteins are differently expressed in diverse tissues and probably exhibit cell type- and tissue-specific functions. In mice, H-Ras is highly expressed in brain, muscle and skin and lowest in liver, while K-Ras is readily detected in gut, lung and thymus. N-Ras is primarily expressed in testis and thymus<sup>56</sup>. Although mutated Ras genes produce the same phenotypes *in vitro*, altered K-Ras proteins are prevalent in tumors of epithelial origin such as colon<sup>57</sup>, lung<sup>58</sup> and pancreatic<sup>56</sup> tumors, H-Ras in bladder carcinoma<sup>59, 60</sup> and N-Ras is often found mutated in liver cancer<sup>61</sup> and tumors of the hematopoietic system<sup>62</sup>. Interestingly, knock-out studies in mice revealed viable phenotypes when H- or N-Ras expression is lost, whereas lack of K-Ras is embryonically lethal<sup>63-66</sup>.

Somatic and germline mutations in all Ras proteins have been found at residues 12, 13, 59, 61 with position 12, 13 and 61 being the most common<sup>67, 68</sup>. The substitutions prevent the intrinsic and GAP-catalyzed hydrolysis of GTP leading to constitutively active Ras<sup>69</sup>. Wild-type G12 and G13 are required for proper insertion of the positively charged "arginine finger" of GAP to neutralize and cleave the bond between  $\beta$  and  $\gamma$ -phosphate of GTP. RasQ61 is

located within the switch II domain (Q61 is the most conserved residue among all small G-proteins) and activates H<sub>2</sub>O to target the  $\gamma$ -P of GTP<sup>70</sup>. Prolonged activation of Ras is also achieved by other mechanisms than Ras mutations: e.g. mutated Ras-GAP neurofibromin-1 (NF1) (interestingly, none of the other 12 identified RasGAPs have been found mutated in human cancer)<sup>71</sup> and reduced expression of a let-7 microRNA<sup>42</sup>. Next to activating mutations, also dominant negative Ras isoforms were characterized in vitro. Through mutations in codon 15, 16 and especially serine (Ser) to asparagines in codon 17 the coordination to Mg<sup>2+</sup> is weakened and the RasGDP-GEF complex is stabilized and inhibits downstream effector protein binding. Overexpression of S17N mutants inhibits the functions of wild-type (wt) protein by sequestering GEF proteins<sup>72-74</sup>.

Ras is a general linkage protein and plays a major role in intracellular signaling cascades by activating different downstream effector proteins, such as Raf kinase, PI3K and RalGDS.

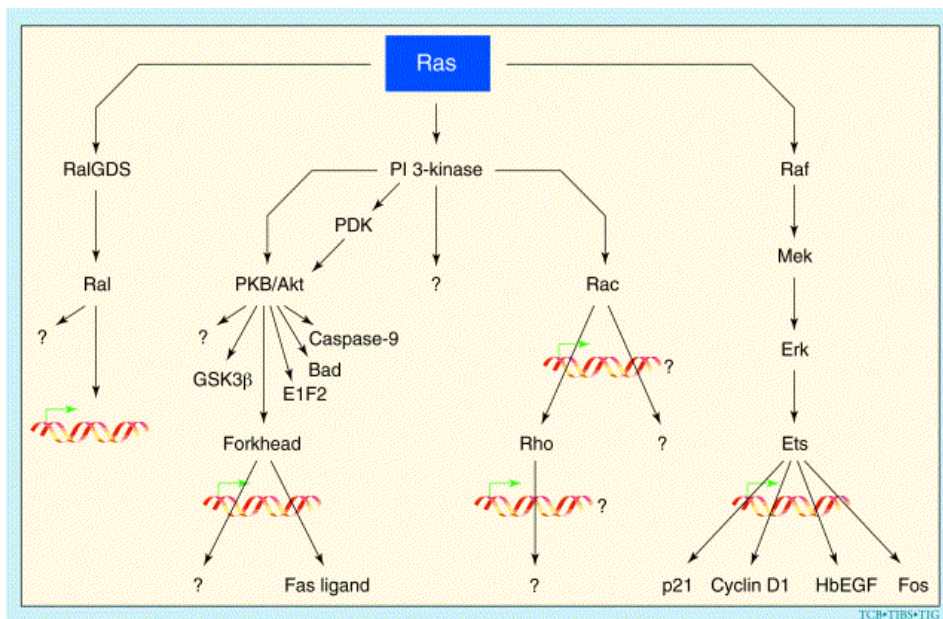


**Figure 2** Downstream effector pathways of Ras<sup>4</sup>

All Ras proteins can interact directly with Raf family kinases. Raf is maintained in an auto-inhibited state within the cytosol with the N-terminal domain preventing the activity of the C-terminal kinase domain. 14-3-3 dimers bind to phosphorylation sites of Raf to stabilize the auto-inhibited state<sup>75, 76</sup>. RTKs mediate phosphorylation, as well as Ras-binding, release of 14-3-3 and membrane lipid interaction to disrupt auto-inhibition of Raf and stabilize the active conformation of the kinase domain<sup>21</sup>. Different Ras proteins activate Raf with various intensities. K-Ras is the most potent activator of c-Raf, followed by N- and H-Ras<sup>77</sup>. Several

mutations in one of the Raf isoforms have been characterized: e.g. B-Raf has been found in over 60% of malignant melanomas and rarely in colon, thyroid and lung tumors<sup>78</sup>.

Once activated, all Raf family members activate mitogen-activated protein kinase (MAPK) cascade simply by phosphorylating mitogen-activated protein kinase-kinase MEK and consecutively extracellular-regulated kinase (Erk) residues in their respective kinase domains<sup>79-82</sup>. MAPK scaffolds, such as the leucine-rich repeat protein Sur-8<sup>83</sup>, act as docking platforms<sup>84, 85</sup> to facilitate MAPK activation and provide specificity. Once activated, Erk translocates into the nucleus and activates the transcription of a set of immediate early genes, such as Myc, Ets, c-Fos and c-Jun.

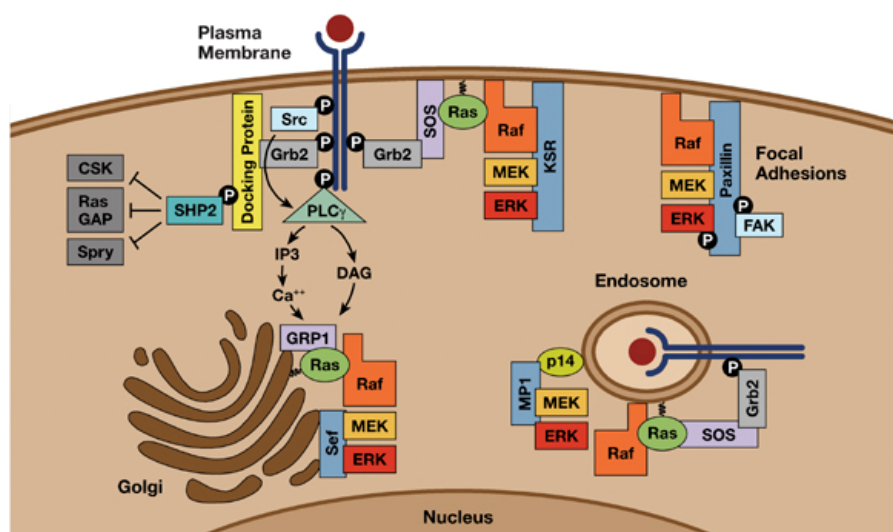


**Figure 3** RTK-Ras-ERK signaling cascade<sup>21</sup>

Another effector pathway of Ras activates PI3K-mediated signaling<sup>86</sup>. Usually Ras plays a minor role in mediating PI3K downstream responses from RTKs<sup>87</sup>, while oncogenic Ras efficiently activates PI3K<sup>88</sup>. Notably, H-Ras is a more potent activator of PI3K than K-Ras<sup>89</sup>. PI3Ks, assembled by the p110 catalytic and an adaptor/regulatory (p85 $\alpha$ ,  $\beta$  and p55 $\gamma$ ) subunit, mediate the phosphorylation of the 3'-OH group of the inositol ring in phospholipids. The major pathway of PI3K activation is initiated by phosphorylated RTKs, which are targeted by the SH2-containing adaptor subunit of PI3K leading to allosteric activation of the catalytic subunit. Alternatively, but insignificant under normal conditions, Ras-GTP can induce the p110 subunit of PI3K. Activation of PI3K results in production of phosphatidylinositol 3, 4, 5-triphosphate (PIP<sub>3</sub>), out of which 5'-inositol lipid phosphatases further generate phosphatidylinositol 3, 4-biphosphate (PIP<sub>2</sub>). Both are targeted by highly-basic pleckstrin-

homology (PH)-containing domains, found in 3'-phosphoinositide-dependent kinase-1 (PDK-1) and Akt/protein kinase B (PKB) (summarized in<sup>20</sup>).

PKB/Akt is assembled by an N-terminal PH domain, a central kinase domain (Thr308) and a regulatory (Ser473) C-terminus. PDK-1 activates Thr308-Akt<sup>90</sup>. When Akt is targeted to the inner membrane it is activated by constitutive active PDK-1, which is consequently localized at the plasma membrane showing a 10-fold higher affinity to PIP<sub>3</sub> than Akt. Upon Ser473 phosphorylation, Akt translocates to the nucleus and is involved in mediating the transcription of specific genes to regulate cell survival (Forkhead transcription factors, pro-apoptotic Bcl-2 family member Bad and the cyclicAMP response element-binding protein (CREB)), cell-cycle progression (including Cyclin D1), cell growth and cell metabolism (including protein synthesis and glycogen metabolism)<sup>91</sup>.

Mutations in PI3K pathway components account for 30% of all human cancers<sup>23</sup>, including gene amplification of p110<sup>PI3K</sup> and Akt in ovarian, breast and pancreatic tumors<sup>23, 92-94</sup> and p85<sup>PI3K</sup> mutations in colon and ovarian tumors<sup>95</sup>. Nevertheless, inactivation of Phosphatase and Tensin homolog (PTEN)-protein mainly accounts for deregulated signaling via the PI3K pathway and is thought to be the second most mutated tumor suppressor in humans after p53<sup>4</sup>. PTEN dephosphorylates the 3'-OH position of the inositol ring in PIP<sub>3</sub> and PIP<sub>2</sub>. Consequently, loss of function of PTEN leads to overactivity of Akt through accumulation of PIP<sub>3</sub> and PIP<sub>2</sub> and mutations are detected in a high percentage of human tumors, including breast, ovarian and colon cancers and glioblastoma<sup>96</sup>. Germline mutations of PTEN were found in Cowden's disease and Bannayan-Zonana syndrome<sup>97</sup>.

Downstream of Akt, activation of mTOR induces the phosphorylation of the inhibitor eukaryotic initiation factor 4E (eIF4E)-binding protein (4E-BP) to release eIF4E. Subsequently, eIF4E initiates protein translation of highly structured 5'-untranslated regions found in the mRNA sequences of c-Myc and CyclinD1 involved in cell cycle progression. Using the mTOR inhibitor rapamycin, mTOR was also shown to regulate transcription of c-Myc and activation of signal transducer and activator of transcription (Stat) 3 and PKCs. P70<sup>S6K</sup>, activated by PDK-1, phosphorylates S6 protein of the 40S ribosomal protein subunit. Induced S6 drives the translation of 5'-terminal oligopyrimidine-rich tract (5'-TOP) mRNAs, which encode for other ribosomal proteins and other components of the translational machinery<sup>98</sup>. Data illustrating that mTOR mediates transformation induced by PI3K and Akt through activation of p70<sup>S6K</sup> and 4E-BP-1, highlights the cooperation between PI3K, Akt, p70<sup>S6K</sup> and mTOR in oncogenesis<sup>99</sup>.



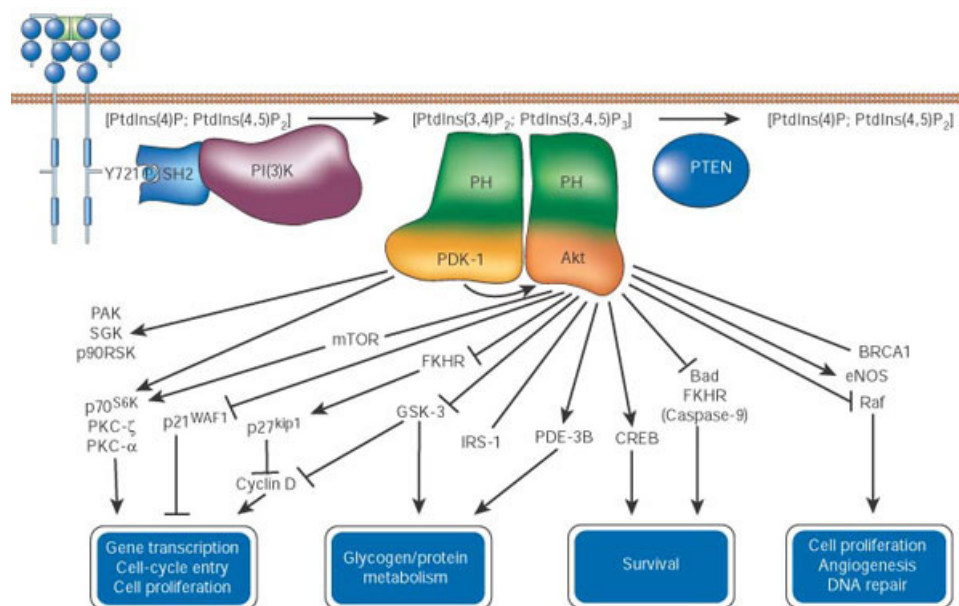


**Figure 4** *RTK-Ras-PI3K-induced signaling cascade*<sup>20</sup>

Under normal conditions activation of Ras is triggered by external growth factors in a precise-temporal manner. In primary cells, activated Ras promotes cell-cycle arrest and senescence<sup>100</sup>. In contrast, oncogenic Ras proteins are persistently switched on and mediate the activation of diverse downstream pathways. In doing so, Ras effector pathways interact in a concerted manner during transformation at least in cell culture models, because each downstream pathway activates the transcription of sets of genes regulating cell proliferation and apoptosis that are not expressed in normal cells. Such synergistic interactions have been noted for Rho and Raf<sup>101</sup>, PI3K and Raf<sup>102</sup>, and RalGDS and ERK<sup>103</sup>. Corroborating, Ras transformation can be strongly inhibited by blocking any of these downstream pathways.

## 2.2 Sprouty proteins

### 2.2.1 Sprouty family members

The members of the Sprouty (Spry) protein family function as regulators of RTK-mediated signaling in a receptor- and cell type-specific manner. Their main mode of action was described to inhibit MAPK activation in response to RTK/Ras/Erk-mediated signaling<sup>104</sup>. Further, Spry expression was shown to repress branching morphogenesis<sup>105</sup>, to inhibit angiogenesis<sup>106-108</sup> as well as cell proliferation<sup>108-112</sup> and migration<sup>107-112</sup>. The first Spry protein to be discovered was the 63kDa *Drosophila melanogaster* dSpry<sup>113</sup>. Branchless (Bnl)/breathless (Btl) (homologues of human fibroblast growth factor (FGF)/FGF receptor (FGFR)) signaling plays a key role in activating branching morphogenesis in *Drosophila*<sup>114</sup>. Spry got

its name from a genetic screen showing that dSpry<sup>-/-</sup> mutants caused excessive trachea branching from the stalks of primary branches close to the tips where secondary branches normally divide. Further, the authors could show that dSpry expression itself was induced by Bnl signaling or the pointed Ets-domain transcription factor and suggested that dSpry localized to the plasma membrane with a small portion being released into the extracellular environment and compete with FGF ligand for binding to its receptor<sup>113</sup>. Subsequent studies confirmed that Spry expression is induced by RTK signaling, but located Spry to function within the cell as part of a negative feedback loop fine-tuning the activity of intracellular signaling pathways<sup>105</sup>.

Sprouty homologues were found in *Xenopus laevis*<sup>115</sup>, chicken<sup>116, 117</sup>, zebrafish<sup>118</sup>, rat<sup>119</sup>, mouse<sup>116, 120, 121</sup> and humans<sup>113, 122</sup>. Murine Spry homologues (termed mSpry1-4) were found to be expressed in most fetal and adult tissues: Spry1, 2 and 4 were detected in lung, brain, heart, kidney, skeletal muscle, colon, placenta, testis, uterus and limbs, while Spry3 expression is restricted to brain and testis in adults<sup>116, 120-125</sup>. In humans, also 4 homologues of *Drosophila* Sprouty were identified<sup>113, 120, 123</sup>, sharing an unique cysteine-rich C-terminal domain and a small, highly conserved N-terminal domain, which are both necessary for Spry function.

Within the N-terminal domain all Spry proteins share a conserved Tyr residue which is activated upon RTK-activation promoting interaction with SH2-containing molecules<sup>126-128</sup>.

The rest of the N-terminal sequence diverges within the four Spry proteins.

mSpry2	MEARAQSG-NGSQPLLQTAHDSGR---QRGEPDPRDALTQQVHVLSLDQIR--AIRNTNEYTEGPTVVPRPGLKPAPRPSTQHKHE	80
hSpry2	MEARAQSG-NGSQPLLQTPRDGGR---QRGEPDPRDALTQQVHVLSLDQIR--AIRNTNEYTEGPTVVPRPGLKPAPRPSTQHKHE	80
mSpry1	MDSPSQHGSHSTSLVVIQPPAVEGR---QRLDYD-RD--TQPATILSLDQIK--AIRGSNEYTEGPTSVARRPAPRTPAPRPEKQERTH	78
mSpry4	MEPPVPQS---SFPVNPSSVMVQP---LLDSRAPHSRLQHPLTILPIDQMK--TSHVENDYIDNPSLAPATGPK---RP--RGGPP	73
mSpry3	MDATVID-----SFPVNPSSVMVQP---LLDSRAPHSRLQHPLTILPIDQMK--TSHVENDYIDNPSLAPATGPK---RP--RGGPP	51
dSpry	SGSGVSGSSSFTRRRPPAPVR[ 21 ]QSAEPASNALGQPPASPVTLAQPRPESERLTNEYVDTELQHATRSHQHPAGQDNGQTTT	226
mSpry2	RLHGLPEHRQPPRLQPSQVHSS-RAPLSRSISTVSSGSRST-RTSTSSSSSEQRLLGSPFSHCPA---AADGIIRVQPKS-ELKP	160
hSpry2	RLHGLPEHRQPPRLQPSQVHSSARAPLSRSISTVSSGSRST-RTSTSSSSSEQRLLGSPFSHCPA---AADGIIRVQPKS-ELKP	160
mSpry1	EIIPANVNSYEHPRPASHPGNARGSVLSRSTSTGSAASSG----SSSSVSEQGLLGRSPPTRP IPGHRSDRVRTQPK-QLLV	157
mSpry4	ELAPTARCD---QDITHHWIS---FSGRPSSVS-----SSSTSSDQRLLDHMAPP-PVAEQASPRAVRLQPKVHVCKP	141
mSpry3	DWSLATMPTALP-RSISQCHQLQP--LPQHLSQSSISSS-----MSQSTTASDGRLLASITPS-P----SGQSIIRTPQGAGAHPK	124
dSpry	HLLLLLQQRNHLHLLQHQ[ 28 ]ARLATTTQATSVSGSDHTDGLLHSHLQNSTTKPPASKQPALPRL[ 13 ]QPIITQPTPATQKE	345
mSpry2	GD--VK-----PLSK---DDLGLHAYRCEDCGKCKCKECTYPRPLPSDWICDKQCLCSAQNVIDYGTVCVCKGLFYHCSNDDDED--	235
hSpry2	GE--LK-----PLSK---EDLGLHAYRCEDCGKCKCKECTYPRPLPSDWICDKQCLCSAQNVIDYGTVCVCKGLFYHCSNDDDED--	235
mSpry1	ED--LK-----ASLK---EDPTQHKFIEQCCKCKCKGECTAPRALPSCLAGDRQCLCSAESMVEYGTCLMGLVKGI FYHCSNDDDGG-	233
mSpry4	LD--LK---GPTAP--PELDKHFLLAEACGKCKCKEASPRTPSPCWVQNECLCSAQTLVNIYGTCLMGLVQGI FYHCSNDDDEG-	218
mSpry3	VDGALK---GEAEQSVGHSSDHLFIIEECGCKCKVCPCTAVRPLPSCWMCNQCLCSAESLLDYGTCLMGLVQGI FYHCSNDDDED--	204
dSpry	RMHALE[ 12 ]GPLVMAGDPSLLNP IVCPRCGRRCRCEQCSPPLEQTWVKNKTCCLCSAESVIDYASCLCAKALFYHCSNDDARDND[ 9 ]	445
mSpry2	NCADNPSCSQSHCCTFWSAMGVMSLFLPCLWCLFAKGLKLCQGCYDRVNRPGCRCK-NSNTVCCKVPTVPPRN---FEKPT-	315
hSpry2	NCADNPSCSQSHCCTFWSAMGVMSLFLPCLWCLFAKGLKLCQGCYDRVNRPGCRCK-NSNTVCCKVPTVPPRN---FEKPT-	315
mSpry1	SYSDNPSCSQSHCCSRYLCMGALSCLPCLLCYPPAKGQLKLCRCGYDWHRRPGCRCK-NSNTVYCKLES CSPRA---QGLKS-	313
mSpry4	SCADHPSCSQSNNCCARWSFMGALS VVLPCLLCLEPATGVKLAQRGYDRLRRPGCRCK-HTNSVICKAASGDTKTSRS DKPF-	300
mSpry3	NCADNPSCSQSPSCFIRWAAMSLISLFLPCLCCLEPTRGLHMCQQGYDSLRRPGCRCKRHHTNTVCRKISSSSFPFKAQEKSV	288
dSpry	PCVDNPSCSGPYKRTQRWGWLGALSIFLPCLWFWEMRGMKLCCKCYGRFAGRGRC[ 66 ]RSILRKGDLTPKRLDSSPDY	591

**Figure 5** Sequence match of conserved key functional amino acids<sup>129</sup>

Membrane localization of Spry proteins is a conserved mechanism induced by RTK signaling<sup>126, 128, 130</sup>. hSpry2 colocalized with microtubules and translocated to membrane ruffles upon growth factor stimulation<sup>110, 131</sup>. Since membrane targeting was not in all cases dependent on N-terminal Spry Tyr phosphorylation<sup>127, 128, 132</sup>, the C-terminus was shown to be sufficient to mediate localization of Spry proteins to membrane structures upon activation where they interact with target proteins<sup>110, 127, 130, 133</sup>. The membrane-binding domain encompasses residues 178-221 which binds to PIP<sub>2</sub> in vitro and colocalizes with the PH-domain of proteinlipase C- $\gamma$ <sup>133</sup>. Further it was demonstrated that ectopically expressed Spry1 and 2 are modified by palmitoylation which would serve as an anchorage for membrane targeting<sup>106</sup>. In addition, hSpry2 harboring an R252D mutation fails to translocate to the plasma membrane and is therefore impaired in its ability to inhibit FGF-mediated signaling<sup>133</sup>. Accordingly, ectopically expressed C-terminal truncated versions of Spry2 are unable to inhibit cell migration, cell proliferation and MAPK activation in response to diverse growth factor stimuli<sup>110, 127</sup>.

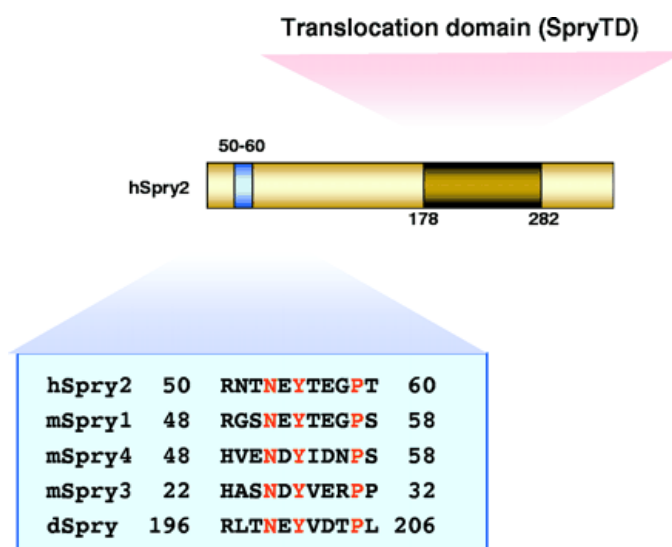


**Figure 6** The two functional conserved Spry domains<sup>129</sup>

### 2.2.2 Sprouty expression during embryogenesis

As negative feedback regulators of RTK-signaling, Spry proteins are expressed mainly at sites of excessive FGF signaling during organogenesis in mouse, rat and chicken<sup>116, 117, 119, 121, 134-136</sup>. During lung morphogenesis, Spry2 was expressed in a spatio-temporal manner in the epithelium during lateral outgrowth and in close proximity to known sites of FGF10 signaling and in distal airways<sup>119, 122, 135</sup>. Also Spry1 and Spry4 show overlapping, but not identical expressions patterns to FGF10 during organogenesis<sup>119, 120</sup>. Ectopically implanted FGF10

beads upregulated *Spry2* expression<sup>135</sup> and mediated Tyr phosphorylation of m*Spry2*, membrane localization and increased the interaction with Grb2, FRS2 and Raf in contrast to SH2-containing Tyr phosphatase 2 (Shp2) and GAP1<sup>137</sup>. Accordingly, lower levels of FGF10 inhibited branching (and decreased *Spry2* levels) in the same way as overexpressed *Spry2*, which inhibited epithelial cell proliferation<sup>135</sup> and MAPK activation<sup>137</sup>. Decreased levels of m*Spry2* using anti-sense oligonucleotides caused excessive branching and increased proliferation and the production of surfactant proteins, which play an essential part during lung maturation<sup>122</sup>. Continuous expression of *Spry4* during development lead to relatively normal lung histology, but reduction in pulmonary lung parenchyma, hypoplastic lungs and inhibited vascular development and branching events (lungs with 3 instead of 5 lobes). During E12.5-E13.5 lungs were most sensitive to excessive *Spry4* in terms of branching and growth, whereas overexpression between E16.5-18.5 reduces weight. In vitro, overexpressed *Spry4* inhibited the effect of FGF7<sup>138</sup>. During brain development in mouse and chicken, *Spry1* and *Spry2* expression overlapped with or was immediately adjacent to expression domains of one or more FGF genes and especially apparent to known sites of FGF8<sup>116, 117</sup>. FGF8 also strongly induced *Spry2* expression as immediate-early response in chicken<sup>134</sup>. Furthermore, overexpression of m*Spry2* and m*Spry4* during organogenesis in chicken lead to reduction of limb bud size of developing wing and prevented differentiation of proliferation chondrocytes, leading to reduction in skeletal element size<sup>116</sup>. These data also emphasized the evolutionary conserved role of *Spry* proteins as mediators of RTK signaling.

### 2.2.3 Sprouty gain and knock-out studies

In *Drosophila*, d*Spry*<sup>-/-</sup> knockout caused excessive trachea branching as a consequence of aberrant FGF signaling during development<sup>113</sup>. In other reports, overexpression and loss of function studies of d*Spry* showed opposing phenotypes during imaginal disc, nervous system and wing vein development, respectively and d*Spry* overexpression especially mimicked those effects found in a lost or mutated EGFR pathway background<sup>130, 139, 140</sup>. In their reports, d*Spry* expression was detected from stage 7 of oogenesis onwards<sup>130, 140</sup>, which was not always dependent on EGFR, but never on Heartless (Htl) and Btl (both homologues of human FGFR) signaling. Nevertheless, overexpressed d*Spry* in embryos inhibited Htl, Btl and EGFR-mediated induction of MAPK and the authors suggested additional factors to be necessary, depending on the cellular context, to induce d*Spry* expression. During oogenesis removal of d*Spry* gave rise to phenotypes consistent with hyperactivated EGFR<sup>140</sup>. During wing development d*Spry* was induced by EGFR signals within the wing veins and d*Spry*

overexpression lead to loss of wing size and reduction or elimination of wing veins<sup>130, 140</sup>. Furthermore, dSpry followed EGFR signaling in the developing eye and follicle cells where it inhibited Torso-EGFR-mediated downstream activation. dSpry<sup>-/-</sup> *Drosophila* died as pupae and had supernumerary photoreceptors, cone cells, pigment cells (non-photoreceptor cells in pupal retina) and extra wing veins and overexpression reduced the number of photoreceptors in the eye<sup>130, 139</sup>. *Drosophila* lacking dSpry further developed phenotypes in the larval peripheral nervous system (extra chorodotonal organs) and embryonic central nervous system (extra midline glial cells) closely related to those of hyperactivated EGFR.

Loss of Spry2 in mice caused phenotypes correlated to excessive signaling via growth factors. Whereas most of the knock-out mice died within the first weeks, many of the remaining survived for at least 6 months, but were significantly smaller than +/+ and +/- littermates<sup>141</sup>. The knock-out mice suffered from esophageal achalasia and intestinal movements defects (resembling human Hirschsprung disease) as a consequence of an increased enteric neuronal network and hypertrophic ganglion strands. Increased Erk and Akt activation was detected in the colon ganglia and at the level of single nerve cells in response to hypersensitivity of the enteric nervous system to glial cell line-derived neurotrophic factor (GDNF) and its receptor rearranged during transfection (Ret)<sup>141</sup>. Furthermore, Spry2 <sup>-/-</sup> mice suffered from hearing defects<sup>141, 142</sup>. Subsequent studies accounted Spry2 with two functions pre- and postnatal in the organ of corti. During postnatal differentiation one Deiter's cell (a progenitor of outer hair cells) transformed into an extra pillar cell, because of aberrant FGF8 signaling from adjacent inner hair cells, which was the possible cause of deafness. This Spry2 loss phenotype could be rescued by decreasing the dosage of FGF8 produced by inner hair cells, suggesting that FGF8 promotes pillar cell differentiation and Spry2, produced by Deiters' cells, prevents a Deiters' cell to become a pillar cell<sup>142</sup>. Furthermore, Spry2 was shown to play a role during craniofacial development<sup>143, 144</sup>. Lack of Spry2 resulted in increased proliferation due to enhanced expression of FGF signaling-induced genes in the epithelium and mesenchyme and the discoordination of palate growth and morphogenic movements necessary for midline contact<sup>144</sup>. Since cleft palate was also observed in 40% of FGF9 null mice<sup>145, 146</sup>, the authors suggested Spry2 to be a strong candidate to regulate FGF9-mediated signaling. Additionally, overexpression of Spry2 before stage 10 resulted in defects in bone architecture and a completely open palate with nasal turbinates, whereas at later stages Spry2 overexpression caused no defects, resembling a stage-specific role of Spry2 mainly during early stages of craniofacial development<sup>143</sup>. Loss of Spry2 was further associated with malformations during teeth development. Spry2 null mice developed an additional diastema tooth in the lower jaw

without significantly changing the shape of other teeth. The absence of Spry2 function rendered the diastema bud epithelium hypersensitive to FGF signaling from the adjacent mesenchyme and maintained expression of sonic hedgehog homolog (Shh)<sup>147</sup>. Spry2<sup>+/-</sup> mice showed normal dentition.

Spry4 null mice were viable and fertile and 16% of the investigated mice carried a, mostly unilateral, supernumerary tooth, which probably resulted from maintained mesenchymal FGF signaling during morphogenesis<sup>147</sup>. Another report showed that loss of Spry4 function lead to reduced body weight and post-natal growth in the F7 generation. Further, they developed duplicated digits at the forelimb, but were fertile and harbored no gross abnormalities in any other major organ (e.g. no enhanced lung branching). Knock out- and wt-derived mouse embryonic fibroblasts (MEFs) showed sustained Erk signaling upon FGF, but not EGF, signaling and Spry4 was induced by Wnt-3a in wt MEFs. Spry2/Spry4 double knock out mice were embryonic lethal by E12.5 and showed severe abnormalities in craniofacial and limb morphogenesis and defects in brain and lung<sup>148</sup>.

Loss of function studies focusing on Spry1 revealed that Spry1 is involved in regulating ureter-kidney development<sup>149, 150</sup>. Most Spry1<sup>-/-</sup> mice died within the first 5 months and featured phenotypes of uni- or bilateral ureter (multiple ureters, hydroureter) and kidney malformations (nephrons not restricted to cortex, multiple epithelial cysts, several kidney primordia fused together) characteristic of the human Congenital Anomalies of the Urinary Tract and Kidney (CAKUT) disease<sup>149</sup>. Further, the renal epithelia in Spry1 null newborns exhibited structural and molecular changes characteristic of cystic kidney disease<sup>150</sup>. It was shown that Spry1 functions as feedback antagonist of GDNF/Ret/Wnt11 signals during kidney development<sup>149, 150</sup>. Consequently, lowered GDNF dosages rescued the Spry1<sup>-/-</sup> phenotype<sup>149</sup>. Furthermore, Spry1 was shown to limit the action of wilms tumor suppressor gene 1 (WT1) in the condensing mesenchyme during nephrogenesis and downregulation of Spry1 limited the number of nascent glomeruli<sup>151</sup>.

#### **2.2.4 Regulation of Sprouty function and activity**

Several proteins have been identified to modulate the mode of action of Spry proteins. Most reports focused on the role of Spry family members during intracellular signaling within the RTK/Ras/MAPK cascade, but contradictorily data have been published to locate the step of Spry interference upstream or downstream of Ras (summarized in<sup>105</sup>).

In vitro, Spry expression was mostly induced in response to growth factors. Increased levels either on mRNA or protein levels were detected upon activation using FGF2, EGF, platelet-

derived growth factor (PDGF), vascular-endothelial growth factor (VEGF) and hepatocyte growth factor/ scatter factor (HGF/ SF)<sup>106, 109, 111, 152-154</sup>. These growth factors mainly induced Spry expression through activation of the MAPK signaling cascade. Correspondingly, it was shown that activated Erk is necessary to induce Spry gene expression<sup>152</sup>. In addition, expression of the dominant active, oncogenic Raf1-CAAX caused an increase of Spry2 and Spry4 mRNA<sup>155</sup>. In vivo, transgenic mice expressing the constitutive active K-Ras<sup>G12D</sup> mutant showed increased expression of Spry2 in the lung epithelium<sup>156</sup>. Furthermore, Wnt3a and co-expression of Wnt7a and Fzd9 upregulated Spry4, but not Spry1 and 2, respectively<sup>148, 157</sup>. Within the N-terminal fraction of Spry proteins a conserved Tyr residue was shown to be crucial for its inhibitory action upon phosphorylation mediated by diverse growth factors, ectopically expressed RTKs, or Src-like kinases<sup>127, 128, 132, 154, 158</sup>. Correspondingly, in many cases mutations of this specific Tyr to alanine or phenylalanine, respectively, abrogated or diminished the functions of Spry proteins in a dominant negative manner on MAPK activation and cell proliferation in vitro and in vivo<sup>112, 132, 153, 154, 159, 160</sup>.

Promoter studies showed that WT1 directly targets Spry1 promoter and upregulates Spry1<sup>151</sup>. Sequence analysis of the Spry2 and 4 promoter revealed that the functionally important proximal region neither contains TATA nor CAAT box but an initiator element around the transcription start site<sup>146, 161, 162</sup>. Several cis-acting elements were shown to be present in the proximal region of Spry2, including activator protein 2 (AP2), CREB, stimulating protein 1 (SP1) and Ets-1<sup>161</sup>. Further, hepatic nuclear factor 1, SP1, AP2, Elk-1, E47/Thing 1, CCAAT-enhancer binding protein- $\beta$ , WT1, sterol regulatory element binding protein, Myc-associated zinc finger protein, PBX-1, zinc-finger protein ZF5, Stat5 and hypoxia-inducible factor 1 (HIF-1) were found in the 5'prime region of Spry4<sup>162</sup>. However, the factors controlling tissue-specific expression of Spry genes remain to be identified.

Only in some cases, decreased Spry levels were observed after growth factor addition. In endothelial and NIH3T3 cells, Spry1 mRNA was highest in starved cells and showed decreased expression after stimulation<sup>106, 109</sup>. Spry2 was downregulated by the addition of cytokine TGF- $\beta$ 1 and TNF- $\alpha$  by independent mechanisms<sup>163, 164</sup>. TGF- $\beta$ 1 increased the turnover rate of Spry2 via a lysosomal-dependent mechanism and decreased Spry2 transcription possibly by Smad and TGF- $\beta$ 1-mediated recruitment of HDACs<sup>164</sup>. TNF- $\alpha$  induced downregulation of Spry2 via p38 MAPK signaling on the level of translation. When Spry2 was overexpressed, it inhibited TNF- $\alpha$  mediated apoptosis, suggesting that Spry2 plays a role in controlling apoptotic action of TNF- $\alpha$ <sup>163</sup>.

In *Drosophila*, Drk (Grb2 homologue) and GAP1 were shown to bind directly to dSpry<sup>130</sup>. Whereas Grb2 was also found to bind to Spry in mammalian systems, no further evidence was reported in the case of GAP1. Some studies described the interaction of ectopically expressed isoforms of Spry proteins to be dependent on prior phosphorylation and the sequence surrounding the N-terminal conserved Tyr residue, which was targeted by the SH2 domain of Grb2, whereas others also detected an interaction in non-activated cells or in cells expressing dominant negative Spry, respectively<sup>109, 132, 154</sup>. A recent report demonstrated that the SH3 domain of Grb2 specifically targets the PxxPxR motif exclusively found in the C-terminal domain of Spry2 which competes with Grb2 binding to the proline-rich domain found in Sos, but not FRS2<sup>165</sup>. Spry2 was further co-localized to FRS2<sup>132</sup>. In some reports these interactions inhibited the complex formation of FRS2-Grb2-Sos (and –Shp2)<sup>127</sup>, whereas in others these complexes still formed<sup>132</sup> in the presence of overexpressed Spry. Spry-Raf interaction was described to be enhanced in a FGF signaling-dependent manner<sup>137</sup>, or mediated via a Ras-independent mechanism<sup>166</sup>. In the latter, Spry4 bound to Raf via a conserved C-terminal Raf-binding domain upon vascular endothelial growth factor receptor (VEGFR)-mediated PLC- $\gamma$ 1-PKC pathway activation<sup>166</sup>. Intracellular phosphatases were also shown to regulate the Spry function. Protein-Tyr phosphatase-1B (PTP1B) was increased in the soluble fraction of cells in association with Spry2 expression and contributed to the anti-migratory action of hSpry2<sup>167</sup>. Shp2 acts as positive regulator of FGF signaling and dominant active Shp-2 dephosphorylated mSpry2 and xSpry1 in vitro and in vivo, induced dissociation of both Spry proteins from Grb2 and reversed the inhibitory effect of xSpry1 on neurite outgrowth in response to FGF stimulation in PC12 cells<sup>168</sup>.

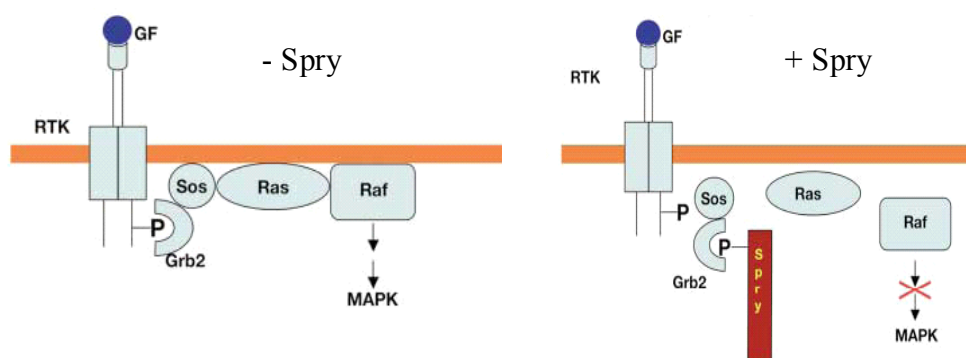


**Figure 7** Inhibition of signaling by Spry<sup>169</sup>

Further complexity was added when it was shown that in mammals Spry interferes differently within FGF- and EGF-mediated downstream signaling. Whereas in all cases, Spry



expression inhibited MAPK activation upon FGF stimulation, ectopically expressed Spry sustained EGF-induced MAPK induction<sup>106, 126, 128, 166, 170-172</sup>. These observations are in contrast to the above mentioned role of Spry in *Drosophila*, where it also negatively regulates EGFR signaling during development<sup>130, 140</sup>. This is of special interest since Spry2 is activated by Tyr55 phosphorylation (pTyr55) in both ways, but leading to different outcomes<sup>126-128, 173</sup>. In mammals, the different effect of Spry on EGFR activity was associated on its interaction with the ubiquitin E3 ligase cCbl, which mediates protein degradation of protein Tyr kinases<sup>174</sup>. Spry2 was shown to bind to cCbl and Cbl-b in unstimulated, but much stronger in EGF-induced cells<sup>128, 175</sup>.

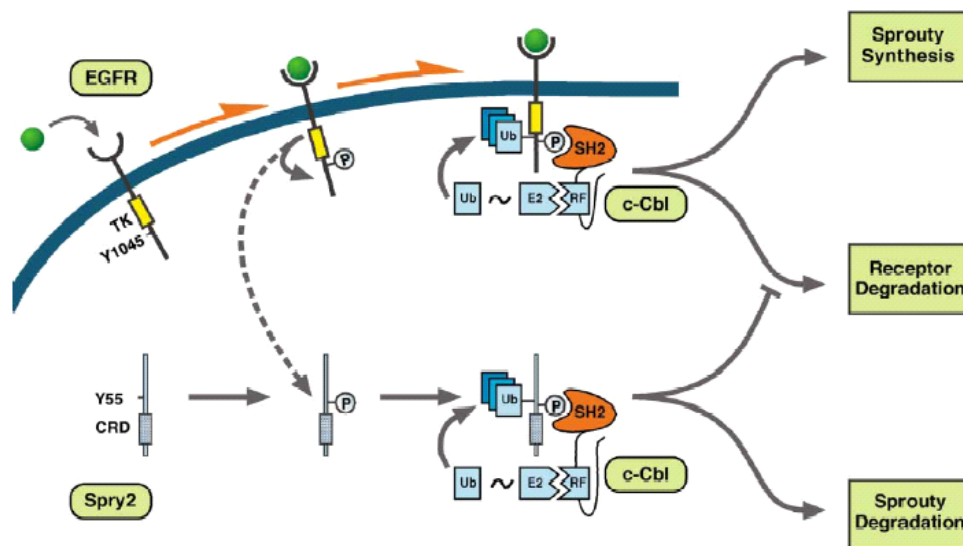


**Figure 8** Inhibition of EGF signaling attenuation by Sprouty<sup>128</sup>

Subsequent studies established three different mechanisms of how Spry2 intercepts cCbl-mediated EGFR degradation. In the first, Spry2 pTyr55 is targeted by the SH2 domain of cCbl. Since the sequence around Spry2 Tyr55 (pYxxxP – also found in EGFR around Tyr1045) is a known site for interaction between cCbl and phosphorylated Tyr proteins, cCbl initiates poly-ubiquitination and proteosomal degradation of pTyr55 Spry2 instead of pEGFR<sup>126, 128, 173</sup>. In the second mechanism, Spry2 competes with UBCH7, an E2 ubiquitin conjugating enzyme which mediates ubiquitination, for binding to cCbl's Ring Finger domain. Further, the interaction between Spry2 and the Ring Finger domain has been described as specific, but independent of growth factor signaling<sup>171</sup>. In the latter way, Spry2-cCbl interaction is mediated by CIN85<sup>172</sup>. CIN85 possesses three SH3 domains which bind to atypical proline-arginine motifs (PxxxPR) present in the C-terminus of cCbl and Cbl-b. In this way, CIN85 clusters Cbl molecules to target activated EGFR for endocytosis and

degradation<sup>176</sup>. Spry2 contains two such motifs and constantly interacts with 2/3 CIN85 SH3 domains, whereas Cbl joins this complex upon EGF stimulation<sup>172</sup>. Nevertheless, in all ways ectopically expressed Spry2 prolonged EGFR-mediated downstream signaling. Additionally, Spry1 was also shown to be a target of cCbl upon growth factor activation, but not Spry4, possibly because it lacks crucial residues in the conserved N-terminal domain<sup>132</sup>.

Several studies showed direct interaction between all human Spry proteins and the serine/threonine testicular protein kinase 1 (Tesk1)<sup>123, 177, 178</sup>. While it was shown that Tesk1 kinase activity was not necessary for complex formation<sup>177, 178</sup>, EGF stimulation increased the interaction between Tesk1 and Spry<sup>123</sup>. Furthermore, it was reported that Tesk1 altered Spry2 localization to cellular vesicles instead of membrane ruffles and inhibited Spry2 to bind to Grb2 upon FGFR1 induction. Therefore Spry2 was not able to reduce MAPK activity and to inhibit growth factor-mediated neurite outgrowth in PC12 cells, but Tesk1 did not affect the interaction between Spry2 and cCbl to sustain EGFR signaling upon EGF ligand stimulation<sup>177</sup>. On the other hand, Spry4 targeted Tesk1 in a dose-dependent manner to inhibit Tesk1-mediated cell spreading. Activation of MAPK was not essential for this mechanism<sup>178</sup>. Notably, due to its different C-terminal domain to Tesk1, no interaction between any member of the Spry family and Tesk2 was described<sup>177</sup>.

Next to the crucial Tyr55 within the conserved N-terminal box, also other phosphorylation sites have been demonstrated to regulate Spry2 function. Additionally to Tyr55, c-Src further phosphorylated Tyr residues within the C-terminal domain induced by FGF, but not EGF, linked to the inhibitory action of Spry2 on MAPK activation in response to FGF-, but not EGF-mediated signaling. Among them, Tyr227 and to a lesser extent also Tyr269 and Tyr283 mainly contributed to the action of Spry2, but were not involved in Spry2' cellular localization or interaction with Grb2<sup>154</sup>. In an early report Spry proteins were also subjected to serine (Ser) phosphorylation<sup>106</sup>. Accordingly, Spry proteins were shown to be phosphorylated within a Ser-rich domain in the center of the Spry locus upon EGF and FGF signaling<sup>179, 180</sup>. One report demonstrated that MAPK-interacting kinase 1 (Mnk-1) phosphorylates hSpry2 on serine 112 and 121 resulting in decreased EGF-induced degradation by cCbl. Furthermore, okadaic acid, a specific inhibitor of serine/threonine phosphatases, lead to the accumulation of the slow-migrating form of hSpry2. Since okadaic acid was observed to specifically inhibit protein phosphatase 2A (PP2A), the authors raised the possibility that hSpry2 might be a substrate for PP2A<sup>179</sup>. This interaction was confirmed by another report proposing a mechanism where Spry2 is phosphorylated on Ser112, 115 and 138 in unstimulated cells. As a consequence of FGFR1 signaling, PP2A is activated and the interaction with Spry2

increased to mediate dephosphorylation of Ser112 and 115 (Ser138 remains phosphorylated). FGFR1 on the other hand also mediates phosphorylation of Ser 156, 167, 197, threonine 190 and Tyr 176 and 190 on Spry2 which thereafter limits FGF-activated MAPK signaling. Then cCbl, which competes with PP2A to bind to a specific region between Spry2 residues 50-60, mediates Spry2 downregulation. Furthermore, in their report overexpression of cCbl's Tyr kinase binding domain abrogates Spry2 to inhibit FGFR1-induced ERK activation, neurite outgrowth and Spry2 is accumulated in the slower migrating band in a Spry2-specific immunoblot<sup>180</sup>.

At last, Spry family members were reported to complex as homo- and heterodimers<sup>132, 153</sup>, which serves as an additional step to be considered investigating of how Spry proteins finetune several RTK-mediated processes.

### 2.2.5 Role of Spry proteins during neoplastic transformation

Several studies focused on the role of Spry during tumorigenesis of diverse tissue. Spry1, 2 and 4 are downregulated in prostate cancer<sup>181-183</sup>. Reduced levels of Spry2, and in some cases also Spry4<sup>183</sup> were a direct consequence of silencing by promoter hypermethylation and treatment with de-methylating agent 5-aza-2'-deoxycytidine (AZA) increased Spry2 expression in vitro<sup>182</sup>. Further, 27-40% of loss of heterozygosity (LOH) was demonstrated for Spry2 with tightly flanking markers<sup>182</sup>. In breast cancer, Spry1 and 2 are consequently downregulated by other means than epigenetic silencing and expression of dominant-negative Spry2 induced anchorage-independent growth and tumor formation in vivo<sup>160</sup>. Furthermore, Spry2 but not Spry1 was identified to be downregulated in hepatocellular carcinoma (HCC)<sup>159, 184</sup>. It was shown that this was not due to LOH and promoter hypermethylation<sup>159</sup>. Using an in vivo model, expression of dominant negative Spry2 in combination with activated  $\Delta N90$ - $\beta$ -catenin lead to HCC tumor formation in 50% of mice, featuring highly proliferative cells, upregulated pErk levels (no effect on pAkt) and induction of cell-cycle specific genes such as cyclinB1, D1 and E1<sup>184</sup>. In lung-derived non-small cell lung cancer (NSCLC) overexpression of Spry2 reduced tumor multiplicity and diameter in urethane-induced lung tumor development in mice<sup>185</sup>. In melanoma cells, Spry2 was downregulated in melanocytes and wt B-Raf melanoma cells, compared to high levels in dominant active B-Raf<sup>N599E</sup>-expressing cells<sup>186</sup>. Induced levels of Spry2 were also found in mice expressing dominant active K-Ras<sup>G12D156</sup>. Since ectopic expression of Spry4 failed to inhibit constitutive active Ras<sup>L61</sup>-mediated MAPK activation<sup>107</sup>, these data suggest that Spry proteins counteract RTK-Ras-MAPK-mediated signaling upstream of Ras and that during carcinogenesis Spry proteins

only need to be downregulated in cells featuring unaltered Ras-induced signaling cascades, whereas high levels of Spry are tolerated when activating mutations occur at the level or downstream the inhibiting mode of action of Spry.

### **3 Aims of the study**

A considerable body of evidence indicates that alterations in receptor tyrosine kinase (RTK)-mediated signaling contribute to cancer development and progression. Accordingly, RTK-induced intracellular signaling cascades have to be tightly regulated via positive and negative feedback mechanisms to ensure homeostasis of cells and tissues. The recently discovered family of Sprouty proteins was shown to regulate RTK-activated signaling in an autoregulatory feedback loop manner. The main mode of action of Spry proteins was described to inhibit MAPK activation in response to RTK/Ras/Erk-mediated signaling. Different studies described an inhibitory effect of Spry proteins especially during lung development. Consequently, loss of Spry lead to aberrant RTK-mediated signaling and lung branching morphogenesis.

Therefore, we chose non-small cell lung cancer (NSCLC) as our tumor model system to investigate the deregulation of Spry expression compared to non-malignant lung and to elucidate the consequences of exogenous Spry expression on the malignant phenotype of NSCLC. Further, we attempted to investigate those growth factor-mediated signaling cascades inducing Spry expression in tumor and non-malignant cells. At last we studied Spry expression during cell cycle in normal cells. Since all Sprouty proteins were postulated to be induced, activated and functional in a similar manner, we further tried to elaborate Spry family member-specific differences throughout this study.

## 4 Materials and Methods

### 4.1 Competent bacteria

A single colony of XL1blue or DH5 $\alpha$  bacteria taken from a selective LB plate (15g agar/1l LB medium - 10g NaCl, 10g Trypton from Casein, 5g yeast-extract, 1l ddH<sub>2</sub>O) was inoculated in 2.5ml LB medium, o/n at 37°C, under constant shaking. The o/n culture was sub-cultured 1:100 in 250ml LB medium with 20mM MgSO<sub>4</sub> and incubated at 37°C, under constant shaking, until its optical density at 600nm (OD<sub>600</sub>) reached 0.4-0.6. The bacteria were pelleted by centrifugation at 4500g, 5', 4°C. Medium was removed and the pellet was re-suspended in 100ml chilled TFB1 buffer (30mM CH<sub>3</sub>COOK, 10mM CaCl<sub>2</sub>, 50mM MnCl<sub>2</sub>, 100mM RbCl, 15% glycerol, in ddH<sub>2</sub>O, adjust to pH 5.8 with 1M CH<sub>3</sub>COOH, filter-sterilize (0.45 $\mu$ M) and stored at room temperature (RT)) and incubated for 5' on ice.

For the remaining steps, the cells were always kept on ice, and all pipets, tubes and flasks had to be chilled. The bacteria were pelleted by centrifugation at 4500g, 5', 4°C, re-suspended in 10ml TFB2 buffer (10mM MOPS, 75mM CaCl<sub>2</sub>, 10mM RbCl, 15% glycerol, adjust to pH 6.5 with 1M KOH, filter-sterilize (0.45 $\mu$ M) and stored at RT) and incubated for 15-60' on ice. Afterwards, the aliquots were immediately stored on -80°C.

### 4.2 Transformation by heat shock

Competent XL1blue or DH5 $\alpha$  bacterial cells were thawed on ice. 50 $\mu$ l were added to 1-10 $\mu$ l DNA plasmid solution and incubated for 30' on ice. Afterwards, a 90'' heat shock on 42°C was performed, 500 $\mu$ l LB medium were added and the bacteria were incubated constantly shaking for 1<sup>h</sup> on 37°C. The bacteria were pelleted by centrifugation at 2500g, 3' and the supernatant (SN) was discarded. The pellet was re-suspended in LB medium and plated o/n on selective LB plates (additionally containing either [100 $\mu$ g/ml] Ampicillin, Kanamycin, or [25 $\mu$ g/ml] Chloramphenicol, respectively).

### 4.3 Polymerase Chain Reaction (PCR)-based techniques

PCR was used to amplify specific regions of DNA adding artificial overhangs used for cloning or to introduce mutations by site-directed mutagenesis.

PCR used for cloning: PCR mix: 1µl template DNA (10pg-200ng), 0.4µM sense primer, 0.4µM anti sense primer, 1x AccuPrime™ Pfx mix, 0.4mM deoxy-nucleotide tri-phosphates (dNTPs), 0.5mM MgSO<sub>4</sub>, 1.25U AccuPrime™ Pfx DNA polymerase (Invitrogen), final volume 50µl ddH<sub>2</sub>O – cycle conditions: 1 cycle 5' 94°C, 25 cycles 1' 94°C, 45'' 58°C, 1' 68°C, 1cycle 10' 68°C, ∞ 4°C.

The DNA fragment was either recovered following Agarose gel electrophoresis or desalted before restriction digested and cloned into the respective pre-cut vector.

Site-directed mutagenesis: PCR mix: 100ng template DNA, 0.4µM sense primer 0.4µM anti sense primer, 1x Phusion HF Buffer, 0.4mM dNTPs, 2U Phusion Hot Start DNA polymerase (Finnzymes), final volume 50µl ddH<sub>2</sub>O – cycle conditions 1 cycle 30'' 98°C, 25 cycles 10'' 98°C, 30'' 60°C, 30''/1kb 72°C, 1cycle 10' 72°C, ∞ 4°C.

10µl 10xA buffer, 39µl ddH<sub>2</sub>O and 1µl DpnI (Roche) were added and the mixture digested o/n at 37°C. On the next day, transformation by heat shock was performed into competent bacteria and the cells were plated onto selective LB plates.

Restriction fragment length polymorphism (RFLP)-Analysis of K-Ras<sup>G12</sup> mutations: The artificial RFLP was performed as described<sup>187</sup>. Shortly, genomic DNA was isolated in a buffer containing 10mM Tris-HCl pH 8, 1mM EDTA, 1%SDS, 200µg/ml Proteinase K (Roche) using Precellys 24 Lyser/Homogenisator (Bertin Technologies, Saint-Quentin-en-Yvelines Cedex, France) and incubated overnight at 56°C. After phenol/ chloroform extraction, DNA was precipitated and stored at -20°C. Exon 1 of K-Ras was amplified (30 PCR cycles) using the following primers 5'-ACTGAATATAAACTTGTGGTCCATGGAGCT-3' and 5'-TTACCCATATTGTTGGATCATATTC-3' introducing an artificial BstXI enzyme restriction site. In case of K-Ras<sup>wt</sup> a second BstXI site was generated. Following restriction digestion using BstXI (Roche), DNA was separated via non-denaturing polyacrylamide gel electrophoresis (PAGE) using 19:1-acrylamide:bisacrylamide for polymerization and 1xTBE (0.09M Tris-borate, 0.002M EDTA) as running buffer.

Reverse Transcription PCR: Using Taq DNA Polymerase (Promega) and selective oligonucleotide-primers expression levels of transcripts in tumor tissues were determined by semiquantitative reverse transcription PCR procedure. Dynamics of PCR amplification were evaluated at different PCR cycle numbers and the respective controls were included.

## 4.4 Restriction digestion and cloning

Restriction digestion: Plasmid restriction digestions were performed following the conditions of the manufacturer company (Roche, New England Biolabs). The respective 10x buffers were used and diluted 1:10 in the final reaction. According to the amount of applied DNA the reaction volume differed between 10-50 $\mu$ l. All other reagents have to be adapted to the final volume and the mixture incubated at the indicated temperature.

Agarose gel electrophoresis: Agarose electrophoresis was used to check the accuracy and correct size of plasmids and PCR fragments. Therefore, restriction digested plasmids or PCR products were mixed with 6x loading buffer (0.25% bromphenolblue, 40% sucrose) and separated via agarose gel electrophoresis using 1xTAE as running buffer (0.04M Tris-acetate, 1mM EDTA), respectively. Afterwards, the gel was stained in a 0.25 $\mu$ g/ml ethidium bromide solution and DNA fragments were visualized under the UV screen.

Gel DNA recovery: Under the UV screen (see Agarose gel electrophoresis) the DNA fragments were cut out of the gel and purified according to the supplier's protocol (Zymoclean Gel DNA Recovery Kit, #D4002).

Desalting DNA: Mini Quick Spin columns (Roche) were used to desalt DNA fragments after restriction digestion and gel recovery or to remove oligonucleotides after PCR reaction. Before use, the columns Sephadex G50 matrix was re-suspended by inverting. The cap and the bottom tip were removed and the column was centrifuged for 3', 1000g to pack the column and to remove residual buffer. Finally, the sample was added to the column bed. The column was centrifuged for 3', 1000g and the plasmid-containing eluate was collected in a tube.

Cloning: Pre-cut vector and insert were ligated according to the manufacture's protocol (Roche Rapid DNA Ligation Kit, #11635379001). After the ligation step, the newly cloned plasmid was transformed by heat shock and plated on selective LB plates.



## 4.5 StetI, MIDI, MAXI and CsCl plasmid DNA purification

In all cases, isolation of the correct plasmid was checked by restriction digestion using restriction endonucleases (Roche, New England Biolabs) and the amount ( $\mu\text{g}/\mu\text{l}$ ) determined via  $\text{OD}_{260}$   $\eta$ -drop measurement.

StetI Prep: A single clone (see Transformation) was inoculated in 3ml selective LB medium o/n at 37°C under constant shaking. The bacteria were pelleted by centrifugation 10000g for 3' and the SN was decanted. The pellet was re-suspended in chilled 110 $\mu\text{l}$  StetI-buffer (8% Sucrose, 0,5% Triton X-100, 50mM Tris, pH 8, 50mM EDTA and freshly added 0.05% Lysozyme (Roche)) and the bacteria lysed by incubation on 95°C, 1'. The bacterial debris was pelleted by centrifugation (10000g, 10', 4°C) and removed with an autoclaved toothpick, previously tipped in chilled RNase solution (10mM Tris, 15mM NaCl, 5% Ribonuclease A (Sigma), adjusted to pH 7.55, heated for 15' at 100°C and stored at -20°C). The DNA in the SN was precipitated by adding 110 $\mu\text{l}$  of isopropanol, followed by rigorous vortexing and centrifugation (15', 10000g, 4°C). The SN was decanted and the pellet washed twice using chilled 70% ethanol. After each washing step the DNA was collected by centrifugation (15', 10000g, 4°C). Finally, the pellet was dried under the fume hood and the purified DNA resuspended in ddH<sub>2</sub>O. The DNA solution was stored at -20°C.

MIDI, MAXI Prep: A single clone was inoculated in 100ml (MIDI) or 500ml (MAXI) selective LB medium, respectively, o/n at 37°C under constant shaking and the plasmid DNA isolated according to the supplier's protocol (Promega PureYield plasmid MIDI prep system #A2492, QIAGEN Plasmid Maxi Kit #12162).

CsCl-Prep: A single clone was cultured o/n in 500ml selective LB medium. The cells were pelleted via centrifugation (5000rpm, 5'). The pellet was resuspended in 18ml resuspension buffer (50mM glucose, 25mM Tris/HCl pH8, 10mM EDTA pH8.0) and 2ml Lysozyme (Roche) solution [10mg/ml] were added. Then, 40ml freshly prepared lysis solution (0.2M NaOH, 1% SDS) were added, mixed thoroughly and incubated for 5'-10' at RT. Then, 20ml ice-cold neutralization solution (60ml 5M potassium acetate, 11.5ml glacial acid, 28.5ml ddH<sub>2</sub>O - the resulting solution is 3M with respect to potassium and 5M to acetate) were added and immediately mixed by shaking, before incubating for 10' on ice. The lysate was centrifuged for 15', 4000rpm, 4°C and the collected SN filtered. 0.6 volume of isopropanol were added, mixed well and incubated for 10' at RT. The nucleic acids was recovered by

centrifugation (8000rpm, 15', RT) and the pellet washed with chilled 70% ethanol. The plasmid DNA was resuspended in 5ml ddH<sub>2</sub>O, 5g CsCl added and incubated for 10' in a 30°C water bath. Next, 0.8ml ethidium bromide (AppliChem) stock solution (10mg/ml in ddH<sub>2</sub>O)/10ml CsCl-plasmid DNA solution was added, mixed and centrifuged for 5', 1500rpm, RT. The SN was collected carefully, filled bubble-free into Beckman tubes (polyallomer quick-seal centrifuge tubes, #362248) and sealed. A density-gradient ultracentrifugation step was performed for 20<sup>h</sup>, 45000rpm, RT using a Beckmann VTi 65.2 rotor. On the next day, the DNA was recovered using an 18G needle and filled up to 6ml with ddH<sub>2</sub>O. The ethidium bromide residual was removed by repeating steps of extraction using 2ml isoamyl alcohol. The upper, aqueous phase was collected and the plasmid DNA precipitated by adding 1/10 volume 3M NaOAc, pH5.2 and 2-2.5 volume ethanol abs. for 1<sup>h</sup> at -20°C. Again, the DNA was recovered by centrifugation (15', 4°C, 13000rpm) and washed using chilled 70% ethanol. Finally, the plasmid DNA was resuspended in 0.5-2ml ddH<sub>2</sub>O.

#### 4.6 Cell culture

All cell lines used are of human origin and were cultured in the respective medium containing 10% fetal calf serum (FCS) at 37°C in a humidified incubator with 5% or 7.5% CO<sub>2</sub>. Every second to third day medium was replaced. When the cells had reached 90% confluency they were split using trypsin/EDTA (0.1% trypsin (BD), 0.01% EDTA, 0.001% phenol red).

Cell line	Site	Stage	Type	Medium	Source / Alias
WI 38	lung		fibroblasts	DMEM	ATCC - CCL75
A-427	lung		AdenoCa	DMEM	ATCC - HTB53
A-549	lung		AdenoCa	RPMI	ATCC - CCL185
Calu-3	lung	IV	AdenoCa	DMEM	ATCC - HTB55
Calu-6	lung		AdenoCa	DMEM	ATCC - HTB56
E14	lung	III	AdenoCa	DMEM	ICR / VL-1
SK-LU-1	lung	III	AdenoCa	DMEM	ATCC - HTB57
HZA	lung	III	Large cell	RPMI	ICR / VL-2
LPHE	lung	II	Large cell	RPMI	ICR / VL-4
AHWG	lung	II	Squamous	RPMI	ICR / VL-10
JHWE	lung	I	Squamous	RPMI	ICR / VL-3
LSWW	lymph node	III	Squamous	RPMI	ICR / VL-6

MBSJ	lymph node	IV	Squamous	RPMI	ICR / VL-8
MCKW	lymph node	III	Squamous	RPMI	ICR / VL-5
MSPG	lymph node	IV	Squamous	RPMI	ICR / VL-7
ZYGF	lung	II	Squamous	RPMI	ICR / VL-9
HEK 293	kidney		embryonic	DMEM	ATCC – CRL1573*
CRE8	kidney			DMEM	HEK 293-derived

## 4.7 Construction of adenoviruses

The construction of adenoviral vectors was based on Cre-lox recombination between a  $\Psi$ 5 donor virus and a pADlox vector-containing target insert<sup>188</sup>.

### 4.7.1 Preparation of $\Psi$ 5 donor virus DNA

Logarithmically growing HEK 293 (between passage 35-40) cells were cultured on a  $\phi$ 15cm plate and infected with 1-2 $\mu$ l  $\Psi$ 5 donor virus until the cells started to lyse. The cells including the SN were harvested and centrifuged for 5', 1500rpm. The SN was reduced to 5-8ml and the cells lysed by repeating cycles of freeze ( $N_{2(l)}$ ) and thaw (37°C).

The virus-containing SN was distributed on 15-20 logarithmically growing HEK 293  $\phi$ 15cm plates until the cells started to lyse. The cells were scraped off and collected in polypropylene tubes via centrifugation (5', 1500rpm) and the SN discarded. The pellet was resuspended in 8ml sterile 10mM Tris, pH8 and the cells lysed by repeating cycles of freeze and thaw. After centrifugation, 4.4g CsCl were added to the virus-containing SN and centrifuged for 18-24h, 32000rpm, 10°C in a Beckmann centrifuge. The  $\Psi$ 5 donor virus was recovered using an 18G needle and aliquots were stored at -20°C. Note: one aliquot should be diluted 1:1 in 2x storage buffer (10mM Tris pH8, 100mM NaCl, 0.1% BSA, 50% glycerol) and can be used to propagate  $\Psi$ 5 donor virus in HEK 293 cells.

A second aliquot was subjected to Proteinase K digestion in a buffer containing 10mM Tris, pH8, 1mM EDTA, 1%SDS, 200 $\mu$ g/ml Proteinase K (Roche) at 56°C o/n. After phenol/chloroform (pH 7-8) extraction, DNA was precipitated by adding 1/10 volume 3M NaOAc, pH5.2 and 2.5 volumes EtOH abs at -20°C o/n. The virus DNA was recovered by centrifugation (30', 13000rpm, 4°C) and washed with 70% ethanol. The pellet was dried under the fume hood and resuspended in ddH<sub>2</sub>O. The concentration ( $\mu$ g/ $\mu$ l) was determined by measuring the absorbance at 260nm. Aliquots were stored at -20°C.

#### 4.7.2 Preparation of the target recombinant virus

3 $\mu$ g of gene-shuttled pADlox plasmid DNA were co-transfected with 1 $\mu$ g  $\Psi$ 5 DNA (see *Transfection*) into Cre8 cells (ratio pAdlox shuttle plasmid: $\Psi$ 5 virus = 3:1). Therefore, the day before transfection, 10<sup>5</sup> cells were plated in a tissue culture plate ( $\phi$  6cm). Per plate 200 $\mu$ l serum-free medium and 6 $\mu$ l FuGENE 6 Reagent (Roche) were mixed and incubated for 5' at room temperature (RT). Meanwhile, 3 $\mu$ g SfiI-digested pADlox-DNA and 1 $\mu$ g  $\Psi$ 5 DNA were placed in a separate tube, and the FuGene mixture was added and incubated for 15'-45' at RT. Then the reagent solution was added dropwise to 80% confluent cells, cultured in medium (10%FCS), distributing it around the well and returned overnight (o/n) into the incubator. The medium was changed on the next day.

When the cells started to lyse, they were scraped off and collected by centrifugation (3', 1500rpm). The SN was reduced to about 2ml and the virus was extracted by four to five cycles of freeze and thaw. The sample was centrifuged again for 3', 1500rpm before new Cre8 cells were re-infected with less amount of virus-containing SN than before.

After about five re-infections, fifteen to twenty tissue culture plates ( $\phi$ 15cm) of HEK 293 cells were infected with an adequate amount of virus (derived from the last Cre8 infection). Before the cells started to lyse, they were scrapped off, collected and pelleted by centrifugation (5', 1500rpm). The SN was removed and the cells re-suspended in 8ml of 10mM Tris, pH8. If not used immediately, the pellet was stored at -20°C.

Then the pellet was again lysed by cycles of freeze and thaw as before. After centrifugation (5', 1500rpm) the virus containing SN was collected and 4g CsCl added, followed by density-gradient ultracentrifugation (18-24<sup>h</sup>, 32000rpm, 10°C) in a Beckmann centrifuge. The purified virus was collected from the gradient using an 18G needle, diluted 1:1 in 2x Storage buffer and stored in small aliquots on -20°C.

#### 4.8 Clonogenic assay, Growth curve, Scratch assay

Cells were infected by adenoviruses - multiplicity of infection (MOI) 50 - and cultured in their respective medium containing 10%FCS. Two days post-infection the virus was washed away and the cells were subsequently cultured in adenovirus-free medium.

Clonogenic Assay: 1-2x10<sup>3</sup> cells were cultured in a 6-well plate in the respective medium (10%FCS) until multicellular clones had formed. The medium was removed and the cells washed using 1xPBS (137mM NaCl, 2.7mM KCl, 4.3mM Na<sub>2</sub>HPO<sub>4</sub>, 1.4mM KH<sub>2</sub>PO<sub>4</sub>). Then

the cells were fixed in Giemsa solution (Merck) by incubating 10' at RT. Afterwards, Giemsa solution was removed, the remaining fixation agent removed by rinsing several times with ddH<sub>2</sub>O and dried under the fume hood. A photograph was taken to document the distribution and amount of stained clones.

Growth curve: Equal amounts of cells ( $1-5 \times 10^4$ ) were plated and counted in duplicates every 2-3 days, 1:1 diluted in 0.4% trypan blue solution (Sigma), whereas medium change was performed for the other plates.

Scratch assay:  $2 \times 10^5$  cells were plated in a 6-well plate and cultured until they reached total confluence. A scratch was set with a 200 $\mu$ l plastic tip into the cell monolayer. The gap's closure was documented by photomicrographs and the closure velocity ( $\mu$ m/h) calculated using MetaMorph 6.1, Universal Imaging Corp.

## 4.9 Flow cytometry

Cells were harvested (shock frozen in N<sub>2(l)</sub> and stored at -80°C until use) and resuspended in 100 $\mu$ l 1xPBS. Then, 150 $\mu$ l chilled trypsin solution (20.4mM Na-citrate, 0.6% NP-40, 3mM Tris, 0.02% trypsin (BD), pH7.6) were added, mixed carefully and incubated for 10', RT. Afterwards, 125 $\mu$ l trypsin inhibitor solution (20.4mM Na-citrate, 0.6% NP-40, 3mM Tris, 0.3% trypsin inhibitor (Sigma), 0.06% RNase A (Sigma), pH7.6) was added, mixed by inverting and incubated for 10', RT. Finally, propidium iodide-containing solution (1xPBS, 0.02% propidium iodide (Sigma) was added and incubated for 10', RT under light protection. The cell cycle-specific distribution was measured by flow cytometry (BD FACSCalibur) and illustrated using ModFit software.

## 4.10 Generation of Spry-specific antibodies

Single colonies of either glutathione S-transferase (pGEX vector)-tagged NH<sub>2</sub>-terminal 150 amino acids of human Spry2, NH<sub>2</sub>-terminal 200 amino acids of human Spry1 and NH<sub>2</sub> terminal 220 amino acids of human Spry4 were inoculated in 50-100ml selective LB medium o/n at 37°C under constant shaking. On the next morning, the culture was diluted 1:10 with selective LB medium and incubated for 1<sup>h</sup> at 37°C under constant shaking. Then, isopropyl- $\beta$ -D-thiogalactopyranoside (Applichem) was added to a final concentration of 100 $\mu$ M and

further inoculated for 2-3<sup>h</sup> as before. Afterwards, the cells were harvested (10', 5000rpm, 4°C) and resuspended in 50ml 1xPBS. A spatula tip of Lysozyme (Roche) was added and the mixture incubated for 30' on ice. Afterwards, TritonX-100 (Fluka) was added to a final concentration of 0.5% and sonicated (Bandelin Sonopuls) 5 times for 30'' at 70% on ice. The debris was pelleted by centrifugation (10', 8000rpm, 4°C, SS-34 rotor). The SN was collected and Glutathione Sepharose 4B (GE Healthcare) beads (before use, 400µl beads solution was rinsed 3 times with 1xPBS) added. The mixture was incubated head over head at 4°C o/n to couple the proteins to Sepharose beads. On the next day, the solution was applied to a Poly-Prep chromatography column (BioRad, #731-1550) and the beads column matrix washed with 10ml TNN buffer (50mM Tris pH7.5, 250mM NaCl, 5mM EDTA, 50mM NaF, 0.5% NP-40) and 50ml 1xPBS. The beads were transferred to an Eppendorf tube, 500µl 5U Thrombin-containing 1xPBS added and incubated o/n, head over head at 4°C to release the coupled Spry protein fragments from the beads matrix. On the next day, the solution was applied to another Poly-Prep chromatography column and the Spry protein antigen (AG)-containing eluate collected. Further, the beads were additionally washed with 500µl 1xPBS and a second eluate collected. The protein concentration was estimated by PAGE (using 37.5:1 acrylamide:bisacrylamide for polymerization), followed by coomassie staining (0.25% Coomassie Brilliant Blue G250, 10% glacial acid, 30% methanol) in comparison to 0.2, 1 and 5µg/µl BSA standards.

600µg of Spry AG were used to raise polyclonal anti-Spry-specific rabbit serum, respectively (Eurogentec, 4102 Seraing, Belgium).

The remaining Spry AG solutions were dialyzed o/n in Coupling buffer (0.1M NaHCO<sub>3</sub> pH8, 0.5M NaCl) at 4°C using a dialysis membrane (Pierce, Slide-A-Lyzer 3.5kDa, #66110) according to the manufacturer's protocol. On the next day the AG solution was bled off and filled up to 10ml with Coupling buffer (5ml of were used for antibody purification and the remaining half stored at -20°C until use). 0.5g CNBr Sepharose4B (GE Healthcare) was activated using 1l 1mM HCl on a suction filter by vacuum filtration and added to 5ml dialyzed AG solution. After an incubation time for at least 2<sup>h</sup> head over head at RT, the AG-coupled matrix beads were collected by centrifugation (5', 1500rpm) and washed twice with Coupling buffer. Afterwards, 10ml blocking buffer (0.1M Tris pH 8) was added to the beads and incubated head over head for at least 1<sup>h</sup> at RT. Again, the matrix was recovered by centrifugation and washed with 3 cycles of washing buffer A (0.1M CH<sub>3</sub>COONa pH 4, 0.5M NaCl) and B (0.1M Tris pH 8, 0.5M NaCl). After each washing step, the matrix was collected by centrifugation and finally poured into a Poly-Prep chromatography column.

The crude Spry polyclonal antibody-containing serum was diluted in 2 volume 1xPBS/0.2% Tween, added to the AG matrix prepared before and eluted 3x for matrix-AG-antibody coupling. Afterwards, the Sepharose beads were washed 3x with 12ml 1xPBS/0.2% Tween each. Before elution, several Eppendorf tubes were filled with 750 $\mu$ l neutralizing 1M K<sub>2</sub>HPO<sub>4</sub>. Finally, the antibody was eluted using 5ml 0.2M glycine pH2.2 to final volumes of 1ml into the 1M K<sub>2</sub>HPO<sub>4</sub>-containing Eppendorf tubes and the antibody-positive fractions (checked using BioRad Protein Assay Dye Reagent) collected. Note: To avoid cross-reactivity, antibodies against Spry1, 2 and 4 were depleted by cycling each of the 3 crude antisera over columns containing GST and the other Spry proteins, respectively, followed by affinity purification.

#### 4.11 Immunoblotting

Cells were scraped off the culture plate, centrifuged (1000g, 3') shock frozen in N<sub>2(l)</sub> and stored at -80°C until use. For protein lysis the pellet was resuspended in chilled TGH buffer (50mM Hepes pH7.6, 150mM NaCl, 1.5mM MgCl<sub>2</sub>, 5mM NaF, 1mM EGTA, 1% TritonX-100, 10% glycerol, Complete (Roche), 0.5mM Na-vanadate, 1 $\mu$ M PMSF), incubated for 10' on ice and exposed for 2' to a sonication water bath. After centrifugation, the SN was collected and stored at -80°C upon use. The protein concentration was determined by spectrophotometry using Micro BCATM Protein Assay Reagent Kit (Pierce) compared to BSA standards. Equal amounts of proteins were subjected to PAGE (using 37.5:1-acrylamide:bisacrylamide for polymerization) followed by tank blotting onto nitrocellulose membrane. Accordingly, the membrane was probed with respective primary protein-specific, followed by species-specific secondary-horseradish peroxidase (HRP)-conjugated antibodies. The antibody-complexes were visualized by HRP-mediated light emission onto x-ray film using detection buffer (200mM pCoumaric acid, 1.25mM Luminol, 0.009% H<sub>2</sub>O<sub>2</sub> in 0.1M Tris pH8.8) and the Western blot signals were quantified using Image Quant software (Molecular Dynamics).

#### 4.12 Immunoprecipitation

Cells were lysed in TNN buffer additionally containing Complete (Roche), 0.5mM Na-vanadate and 1 $\mu$ M PMSF for 10' on ice and the SN collected after centrifugation (30', 13000, 4°C). 25 $\mu$ l Protein A Sepharose CL-4B (GE Healthcare) slurry solution (before use, beads

were rinsed 3x in 1xPBS, collected by centrifugation (1000g, 3') and resuspended in 0.5 volume 1xPBS to generate a 50% slurry) was added and incubated for 1<sup>h</sup> head over head at RT. Afterwards, the SN was collected by centrifugation (1000g, 3') and incubated from 1<sup>h</sup> onwards head over head at RT with a specific antibody. Subsequently, 30µl 50% Sepharose slurry was added and the mixture incubated o/n head over head at 4°C. On the next day, the matrix was collected by centrifugation (1000g, 3') and washed 5x with TNN buffer. Finally, the proteins were eluted and lysed by incubating the matrix 5', 95°C in 1x sample loading buffer (250mM Tris pH6.8, 10% glycerine, 1.25% 2-Mercaptoethanol, 2.3% SDS, bromphenolblue) and collecting the SN after centrifugation. Proteins were separated by PAGE and visualized as described in *Immunoblotting*.

#### 4.13 Northern blotting and <sup>32</sup>P-labeling

Cells were harvested, shock frozen in N<sub>2</sub>(l) and stored at -80°C until use. For mRNA extraction, the pellet was resuspended in RNA lysis-buffer (100mM KCl, 10mM Tris pH7.5, 0.5% NP-40), additionally adding 25mM EDTA, ribonucleoside vanadyl and RNase inhibitor (Fermentas) and incubated for 10-30' on ice. The mRNA-containing SN was collected by centrifugation (10', 13000rpm, 4°C) and the following components added 2.8M Urea, 0.4%SDS, 0.14M NaCl, 4mM EDTA, 4mM Tris pH7.5, 1M LiCl. The mixture was extracted twice with 400µl phenol:chloroform:isoamyl alcohol (49.5:49.5:1) and RNA precipitated by adding 0.6 volume of isopropanol. The RNA was recovered by centrifugation (30', 13000rpm, 4°C), washed with 70% ethanol and dried under the fume hood. Finally, the RNA was re-suspended in 1mM DTT, RNase inhibitor-containing ddH<sub>2</sub>O, incubated for 5-15' at 68°C, and stored at -80°C until use. Note: All aqueous solutions were prepared using Diethylpyrocarbonat-pre-treated ddH<sub>2</sub>O.

Equal amounts of RNA were mixed with RNA loading buffer (50% formamide, 5.9% formaldehyde, 6.7% glycerol, bromphenolblue in 1xMOPS (200mM MOPS, 50mM NaOAc, 10mM EDTA) and separated by agarose gel electrophoresis using 1xMOPS, 1.85% formaldehyde as running buffer. Afterwards, the RNA was blotted onto nylon membrane using 10x SSC (1.5M NaCl, 0.15M sodium citrate) as transfer buffer by capillary force. The ribosomal RNAs were stained using methylen-blue solution (0.04% methylene blue in 0.5M NaOAc, pH5.2) to check that no degradation has occurred. Finally, the membrane was autocrosslinked with 120mJ for 10'' in a Stratgene Crosslinker. If not used immediately, the membrane was stored in a foil at -20°C.



5-50ng of a purified DNA fragment was used for  $^{32}\text{P}$ -labeling (Rediprime<sup>TM</sup> Random Prime Labelling System,  $^{32}\text{P}$ -Nucleotides [ $\alpha$ - $^{32}\text{P}$ ] dCTP RedivueTip<sup>TM</sup>, RT3000-250 $\mu\text{Ci}$ , both Amersham Biosciences) in hybridization buffer (5xSSPE (0.9M NaCl, 50mM  $\text{NaH}_2\text{PO}_4$ , 5mM EDTA, pH8), 5xDenhardt (0.1% BSA, 0.1% Polyvinylpyrrolidone, 0.1% Ficoll), 0.1M  $\text{NaH}_2\text{PO}_4$ , pH6.5, 50% formamide, 10mM EDTA, pH8, 1% N-Lauroylsarcosine) additionally containing 0.1mg/ml tRNA. After o/n incubation at 42°C using the  $^{32}\text{P}$ -specific probe, the membrane was washed 3 times for at least 20' in cycles using wash solution I (2x SSC, 0.5% SDS) and wash solution II (0.1xSSC, 0.5% SDS) at 55°C. The specific  $^{32}\text{P}$ -mediated mRNA signals were emitted on a storage phosphor screen (Amersham Biosciences) and detected via phosphorimager scan. Additionally, the mRNA bands were detected by x-ray film at -80°C. Northern blot signals were quantified using Image Quant software (Molecular Dynamics).

#### 4.14 Statistics

Correlation analyses regarding Spry expression normalized to respective housekeeping controls obtained by Northern- and Immunoblot were set up by linear regression and two-sided Mann-Whitney *U*-test using GraphPad Prism software. Regressions, or mean differences were considered as significant at  $P \leq 0.05$ , respectively.

#### 4.15 Construction of a human lung cDNA library

Total RNA was extracted as described in *Northern blotting*. Isolation of the poly(A)<sup>+</sup> mRNA fraction (Promega PolyAtract mRNA Isolation System IV, Promega #Z5310) and cDNA library synthesis (HybriZap-2.1 XR cDNA Synthesis Kit - Stratagene #235614, HybriZap-2.1 XR Library Construction Kit - Stratagene #235612) were performed according to the manufacturer's protocol.

#### 4.16 Yeast quick trafo

YRG-2 yeast was re-cultured on an YPAD agar plate o/n at 30°C. On the next day the yeast was scraped off and dissolved in 1ml ddH<sub>2</sub>O. The mixture was centrifuged for 30'' top speed, the SN decanted and the following components added to the pellet to a final volume of 360 $\mu\text{l}$ : 240 $\mu\text{l}$  50% (w/v) polyethylenglycol 3500 (Sigma), 36 $\mu\text{l}$  1M LiOAc, 50 $\mu\text{l}$  Salmon Sperm Carrier DNA [2mg/ml], 5 $\mu\text{l}$  pBD-Gal4-hSpry2 [0.1-1 $\mu\text{g}$ ] and 29 $\mu\text{l}$  ddH<sub>2</sub>O. The

transformation mixture was incubated 40-60' in a 42°C water bath. Afterwards the mixture was centrifuged at top speed for 30'', the pellet resuspended in 1ml ddH<sub>2</sub>O and 10µl plated on a selective SD-1 plate (6.7g BD-Difco yeast nitrogen base without amino acids, 182.2g D-sorbitol, add ddH<sub>2</sub>O to 860ml, adjust to pH 5.8, add 62mg amino acids mixture –Histidine (His), -Leucine, -Tryptophane (Trp) (Bio 101 Systems # 4530-112), 200mg L-Adenine hemisulfate (Sigma #A9126), 200mg His HCl Monohydrate (Sigma #H8125), 1000mg L-Leucine (Sigma #L8000) and 15-20g agar, autoclave, add 40ml 50% D-glucose stock solution). pBD-Gal4-hSpry2-containing yeast clones were grown for 3-4 days in a 30°C incubator.

#### 4.17 LacZ Assay

His and LacZ reporter gene are both integrated into the YRG-2 yeast chromosome and are only expressed after direct interaction between two chimeras - bait protein fused to the reporter-binding domain and a specific library protein fused to the reporter-activating domain - to induce transcription. Since there can be a leaky His expression throughout the screen, the induction of LacZ reporter gene is the final step to identify positive clones.

A positive pBD-Gal4-hSpry2 yeast clone was scraped-off a SD-1 plate, re-streaked onto an YPAD plate (20g BD-Difco peptone, 10g yeast extract, add ddH<sub>2</sub>O to 960ml, adjust to pH 5.8, add 40mg L-Adenine hemisulfate, 15-20g agar, autoclave and add D-glucose to 2% (v/v) from a D-50% glucose stock solution which has been autoclaved or filter-sterilized) and incubate at least o/n at 30°C (for some clones it takes 1 ½ days). On the next day, the yeast was re-streaked onto a Whatman 1 filter paper and subjected to 4-6 rounds of freeze (N<sub>2(l)</sub>) and thaw (RT). Afterwards, 5.5µl β-mercaptoethanol and 34µl [20mg/ml] X-Gal (Fisher Biotech #BP1615-1) in DMSO was added freshly to 1.6ml Z-buffer (per liter: 16.1g Na<sub>2</sub>HPO<sub>4</sub>·7H<sub>2</sub>O, 16.1g NaH<sub>2</sub>PO<sub>4</sub>·H<sub>2</sub>O, 0.75g KCl, 0.246g MgSO<sub>4</sub>·7H<sub>2</sub>O, adjust to pH7, autoclave or filter sterilize, store at 4°C) and dropped on another Whatman 1 filter paper (for Ø70mm use 2ml), laid the yeast-containing filter paper face pointing up on top and incubated under a fume hood. Positive control yeast transformed with pBD-wt and pAD-wt vector should exhibit LacZ-β-galactosidase-mediated blue staining after ~90' and negative control yeast transformed with pLamin C and either pBD-mut, or pAD-mut, should not stain blue until 8<sup>h</sup> of exposure, respectively.

**Description of the Control Plasmids**

Control plasmid	Insert description <sup>a</sup>	Vector	Genotype	Function
pGAL4	Wild-type, full-length GAL4	pRS415	LEU2, Amp <sup>r</sup>	Positive control
pBD-WT	Wild-type fragment C of lambda cl repressor (aa 132–236)	pBD-GAL4 Cam	TRP1, Cam <sup>r</sup>	Interaction control
pAD-WT	Wild-type fragment C of lambda cl repressor (aa 132–236)	pAD-GAL4-2.1	LEU2, Amp <sup>r</sup>	Interaction control
pBD-MUT	E233K mutant fragment of lambda cl repressor (aa 132–236)	pBD-GAL4 Cam	TRP1, Cam <sup>r</sup>	Interaction control
pAD-MUT	E233K mutant fragment of lambda cl repressor (aa 132–236)	pAD-GAL4-2.1	LEU2, Amp <sup>r</sup>	Interaction control
pLamin C	Human lamin C (aa 67–230)	pBD-GAL4	TRP1, Amp <sup>r</sup>	Negative control

<sup>a</sup> aa, Amino acid.

**Figure 9**      *Control plasmids for LacZ assay*

## 5 Results

### 5.1 Manuscript 1: Down-Regulation of Sprouty2 in Non-Small Cell Lung Cancer Contributes to Tumor Malignancy via Extracellular Signal-Regulated Kinase Pathway-Dependent and -Independent Mechanisms

Hedwig Sutterlüty<sup>1\*</sup>, Christoph-Erik Mayer<sup>1\*</sup>, Ulrike Setinek<sup>2</sup>, Johannes Attems<sup>2</sup>, Slav Ovtcharov<sup>1</sup>, Mario Mikula<sup>1</sup>, Wolfgang Mikulits<sup>1</sup>, Michael Micksche<sup>1</sup>, and Walter Berger<sup>1</sup>

<sup>1</sup>*Institute of Cancer Research, Department of Medicine I, Medical University Vienna and*

<sup>2</sup>*Institute for Pathology and Bacteriology, Otto Wagner Hospital Baumgartner Höhe, Vienna, Austria*

\* equally contributed

published in Mol Cancer Res 2007;5(5). May 2007<sup>112</sup>.

# Down-Regulation of Sprouty2 in Non-Small Cell Lung Cancer Contributes to Tumor Malignancy via Extracellular Signal-Regulated Kinase Pathway-Dependent and -Independent Mechanisms

Hedwig Sutterlüty,<sup>1</sup> Christoph-Erik Mayer,<sup>1</sup> Ulrike Setinek,<sup>2</sup> Johannes Attems,<sup>2</sup> Slav Ovtcharov,<sup>1</sup> Mario Mikula,<sup>1</sup> Wolfgang Mikulits,<sup>1</sup> Michael Micksche,<sup>1</sup> and Walter Berger<sup>1</sup>

<sup>1</sup>Institute of Cancer Research, Department of Medicine I, Medical University Vienna and <sup>2</sup>Institute for Pathology and Bacteriology, Otto Wagner Hospital Baumgartner Höhe, Vienna, Austria

## Abstract

**Sprouty (Spry) proteins function as inhibitors of receptor tyrosine kinase signaling mainly by interfering with the Ras/Raf/mitogen-activated protein kinase cascade, a pathway known to be frequently deregulated in human non-small cell lung cancer (NSCLC). In this study, we show a consistently lowered Spry2 expression in NSCLC when compared with the corresponding normal lung epithelium. Based on these findings, we investigated the influence of Spry2 expression on the malignant phenotype of NSCLC cells. Ectopic expression of Spry2 antagonized mitogen-activated protein kinase activity and inhibited cell migration in cell lines homozygous for K-Ras wild type, whereas in NSCLC cells expressing mutated K-Ras, Spry2 failed to diminish extracellular signal-regulated kinase (ERK) phosphorylation. Nonetheless, Spry2 significantly reduced cell proliferation in all investigated cell lines and blocked tumor formation in mice. Accordingly, a Spry2 mutant unable to inhibit ERK phosphorylation reduced cell proliferation significantly but less pronounced compared with the wild-type protein. Therefore, we conclude that Spry2 interferes with ERK phosphorylation and another yet unidentified pathway. Our results suggest that Spry2 plays a role as tumor suppressor in NSCLC by antagonizing receptor tyrosine kinase-induced signaling at different levels, indicating feasibility for the usage of Spry in targeted gene therapy of NSCLC. (Mol Cancer Res 2007;5(5):509–20)**

## Introduction

Lung cancer is the leading cancer-related death in the industrial world. Lung tumors are classified in small cell and non small cell lung cancer (SCLC and NSCLC), the latter representing over 75% of all lung tumors. NSCLC are further subdivided into squamous cell carcinoma (SCC), adenocarcinoma, and large cell carcinoma (LCC). All types of lung tumors are associated with poor prognosis, and further progress in treatment strategies is believed to be dependent on a more extensive knowledge on critical pathways involved in tumor development and progression (1).

One of the characteristics frequently linked to human cancer is the deregulation of signal transduction via receptor tyrosine kinases (RTK). RTKs play an important role in the control of fundamental processes, including cell proliferation, migration, metabolism, survival, and differentiation. Due to amplifications and/or mutations of genes involved in signal transmission, these cellular processes turn insensitive to external regulatory signals (2). Several reports describe high frequency of alterations causing hyperactivation of RTK-regulated pathways in NSCLC. For example, the proto-oncogene K-Ras is mutated in 20% to 25% of the lung tumors (3), and mutations in the epidermal growth factor receptor are found in 10% of all NSCLC (4). In addition, overexpression of fibroblast growth factor (FGF)/FGF receptor family members are frequently found in NSCLC cell lines (5). Besides mutations in signal-transmitting genes, enhanced RTK signaling in tumors can be based on deletions or mutations of genes coding for proteins counteracting RTK-mediated signal transduction, thus often representing tumor suppressors (e.g., phosphatase and tensin homologue deleted on chromosome 10; ref. 6).

Recently, a new antagonist of RTK signaling has been identified in *Drosophila*, which was termed Sprouty (*dSpry*), because disruption of this gene led to irregular and excessive branching events in tracheal development. This phenotype is almost identical to the one observed by overexpression of the branchless receptor (an FGF orthologue in *Drosophila*; ref. 7). Subsequent studies have exemplified that Spry proteins, which comprise a family of four members in mammals, have a conserved function as modulators of RTK signaling mainly by interfering with the Ras/mitogen-activated protein kinase (MAPK) cascade in divergent species (8, 9). Additionally, mammalian Sprys were found to play a conserved function during organogenesis by adjusting growth factor induced

Received 8/25/06; revised 2/27/07; accepted 3/12/07.

**Grant support:** Herzfelder'sche Familienstiftung, Hochschuljubiläumsstiftung der Stadt Wien grant H-1224/2003, Medizinisch-wissenschaftlicher Fonds des Bürgermeisters der Bundeshauptstadt Wien grant 2483, and FWF grant P17630-B12.

The costs of publication of this article were defrayed in part by the payment of page charges. This article must therefore be hereby marked *advertisement* in accordance with 18 U.S.C. Section 1734 solely to indicate this fact.

**Note:** H. Sutterlüty and C-E. Mayer contributed equally to the main findings of the study.

**Requests for reprints:** Hedwig Sutterlüty, Institute of Cancer Research, Medical University Vienna, Borschkegasse 8a, 1090 Vienna, Austria. Phone: 43-1-427765244; Fax: 43-1-427765196. E-mail: hedwig.sutterluty@meduniwien.ac.at  
Copyright © 2007 American Association for Cancer Research.  
doi:10.1158/1541-7786.MCR-06-0273

remodeling processes particular of branching tissues (10, 11). Multiple reports have shown that impaired Spry functions during embryogenesis cause malformation of specific organs (12-16), which can be rescued by reducing the respective growth factor doses. In line with these data, overexpression of different Spry members was reported to suppress sprouting events during lung development (17, 18) and angiogenesis (11, 19). *In vitro*, Spry proteins inhibit cell proliferation (20) and migration (21-23) by negatively interfering with RTK-mediated MAPK activation induced by various growth factors (summarized in ref. 8). However, whereas in *Drosophila* dSpry protein generally interferes with RTK signaling (24), in mammals, expression of Spry rather enhances MAPK activation in response to epidermal growth factor (25, 26). Multiple proteins involved in RTK-mediated signal transduction like Grb2, Raf1, c-Cbl, Shp2, and GAP1 were shown to interact with Spry proteins (27). Based on these findings, several mechanisms suggesting a Spry function via interfering with Ras activation, receptor degradation, and/or Raf kinase induction have been anticipated, but the exact molecular determinants underlying growth factor specific signal transduction inhibition by Spry proteins are still unclear.

The complexity of this regulatory network is further increased by the fact that Spry proteins themselves are subjected to regulation by RTK-induced signals at multiple levels (28, 29). Levels and activity of Spry proteins are induced in response to diverse growth factors. Expression patterns during embryonic development coincide with known sites of growth factor activity (especially of the FGF family), suggesting involvement in negative feedback loops (30, 31). In tissue culture, Spry protein expression levels are responsive to growth factor induced signaling. In addition to the transcriptional up-regulation, it has been shown that a growth factor dependent phosphorylation on Tyr<sup>55</sup> in a conserved NH<sub>2</sub>-terminal region of Spry2 contributes to the inhibitory activity on the MAPK pathway (28, 32). This phosphorylation event also influences localization of the protein and its interaction with c-Cbl and Grb2 (33-35).

Because activation of diverse RTK-mediated signals is known to play major roles in development and progression of NSCLC, and because Spry2 is found to be expressed in normal rodent lung epithelium (36, 37), we hypothesized that Spry2 function might be deregulated in lung cancer. In this study, we show that Spry2 expression is frequently decreased in NSCLC compared with normal bronchial epithelium. Furthermore, we compared the consequences of ectopic Spry2 expression in NSCLC cell lines harboring wild-type (K-Ras<sup>wt</sup>) or mutated (K-Ras<sup>G12mut</sup>) K-Ras. Thus, we show that Spry2 down-regulation in NSCLC can contribute to tumor malignancy by interfering with K-Ras mediated extracellular signal-regulated kinase (ERK) phosphorylation and another Ras-independent pathway yet to be identified.

## Results

### *Spry2* Expression Is Reduced in NSCLC Tissue

As an initial experiment, we compared Spry1 and Spry2 mRNA expression of normal and malignant tissues by performing reverse transcription-PCR analysis of matched

cDNA pairs from human lung tumors and the corresponding bronchial epithelia. As shown in Fig. 1A, Spry2 mRNA was expressed in all tumor samples but was distinctly down-regulated compared with the respective normal lung tissues in four of five cases analyzed. The only sample showing no down-regulation of Spry2 in the tumor was derived from SCLC. In contrast, Spry1 mRNA was generally expressed at higher levels in the tumor compared with the normal lung tissue. Therefore, we conclude that Spry2 but not Spry1 mRNA is consistently down-regulated in NSCLC.

To confirm our observations on protein levels, immunohistochemistry was done. Antibodies recognizing Spry1 and Spry2 were generated and purified. Using immunoblotting, the quality of the antibodies was tested and compared with a commercially available antibody (Fig. 1B). Before analyzing tumor tissue, normal adult lung tissues of control patients with nonmalignant diseases ( $n = 4$ ) were stained using Spry1 and Spry2 antibodies. As representatively shown in Fig. 1C (Spry1) and Fig. 1D (Spry2), both Spry proteins were strongly expressed in the epithelium of the bronchus, whereas staining was weak in fibroblasts.

To evaluate staining intensities of the malignant tissues with respect to the ones observed in corresponding normal epithelial cells, preferentially, samples from the tumor boundary that included also unaffected healthy tissue were used. In all cases analyzed, normal bronchial epithelium and tumor tissue stained positively for Spry1 and Spry2, whereas in the control slide, in which the primary antibody had been omitted, staining was completely negative (Fig. 1E). Consistent with the expression data obtained by reverse transcription-PCR (Fig. 1A), Spry1 expression was up-regulated in 6 of 10 tumor samples analyzed. Two of the other four samples showed a comparable intensity in staining of the tumor and the adjacent normal epithelium (Fig. 1F). Only 2 of 10 samples revealed down-regulated Spry1 protein levels in the tumor sections. Therefore, we conclude that Spry1 is not commonly down-regulated in NSCLC.

Hence, immunohistochemical staining of Spry2 was done in 25 tissue sections from surgical NSCLC specimens (11 adenocarcinoma, 11 SCC, and 2 LCC). Nineteen of 25 tumor sections stained with a commercially available antibody (Spry) contained also normal bronchial epithelium and thus could be evaluated. In no case was Spry2 expression in the epithelium weaker than in the tumor. In 7 of 19 (37%) cases, Spry2 expression was comparable or only weakly reduced in the tumor sections (score 3), whereas 12 of 19 (63%) tumors displayed a distinctly weaker Spry2 staining compared with the adjacent normal epithelium. Twenty-one percent of the tumors were scored as 1 (Fig. 1G and H), and 42% were scored as 2 (Fig. 1I). To validate the expression analysis, the sections were re-stained with a second Spry2 antibody raised against the NH<sub>2</sub>-terminal region of hSpry2 (Fig. 1J-L). Staining of the tumor samples with the Spry2 antibody from a second source confirmed that Spry2 is down-regulated in tumor tissues of NSCLC patients.

With regard to histology, 4 adenocarcinoma and 3 SCC scored as 3; 3 adenocarcinoma, 4 SCC, and 2 LCC scored as 2; and 2 adenocarcinoma and 2 SCC had almost completely lost Spry2 expression (score 1). On average, less Spry2 was detected in SCC compared with adenocarcinoma, although the difference was not significant. Regarding tumor stage, no significant

differences were found in Spry2 expression. However, it has to be mentioned that only material from patient stage I to IIIb were available for analysis. Additionally, the few ( $n = 3$ ) tumor samples staged as T<sub>4</sub> had clearly reduced Spry2 expression (score 1 and 2). With regard to differentiation, no effect on Spry2 expression level was detectable (mean: G<sub>1</sub>, 2.2; G<sub>2</sub>, 2.3; G<sub>3</sub>, 2.0).

#### NSCLC Cell Lines with High Levels of Spry2 Expression Harbor Mutations in K-Ras

Spry2 expression levels of 15 NSCLC cell lines were determined by Northern and Western blot analyses. mRNA and protein levels of Spry2 correlated significantly in the investigated cell lines (linear regression,  $P < 0.001$ ; compare Fig. 2A and B). Furthermore, we observed that all cell lines derived from metastases (VL-5 to VL-8 and Calu-3) showed particularly low Spry2 expression. In parallel to Spry2, MAPK activity

in NSCLC cells was measured using an antibody recognizing phosphorylation of ERK (pERK). No correlation was found between the basic levels of pERK and Spry2 expression in NSCLC cell lines (Fig. 2A).

Because Spry expression is reported to be activated by growth factor-induced signals as part of a negative feedback loop, we analyzed the NSCLC-derived cell lines with respect to K-Ras mutations by artificial RFLP (38). Our mutation analysis focused on alterations in codon 12 of the K-Ras oncogene because in NSCLC, more than 80% of the Ras mutations affect this codon (3). As shown in Fig. 2C, 5 of 15 investigated cell lines were mutated at K-Ras codon 12. In addition, Calu-6 is known to harbor a K-Ras mutation at codon 61 (39). K-Ras mutations were found only in cell lines established from adenocarcinoma and LCC, whereas all investigated SCC-derived cell lines were K-Ras<sup>wt</sup>. High levels of Spry2

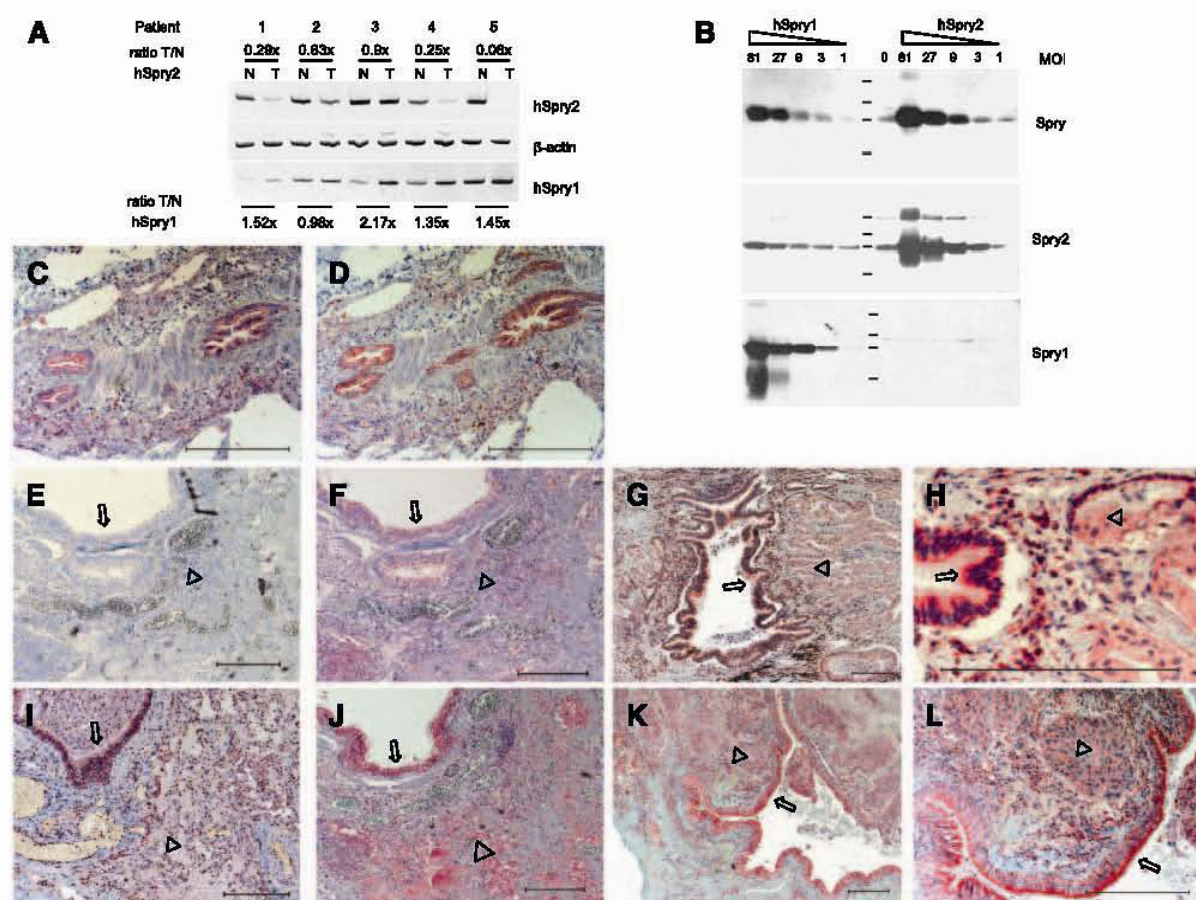


**FIGURE 1.** Analysis of Spry expression in NSCLC tissues. **A.** Spry1 and Spry2 mRNA expressions were analyzed by reverse transcription-PCR using total RNA from tumor (T) and corresponding normal lung (N) tissues.  $\beta$ -Actin was used as internal standard for normalization. The indicated expression ratios (T/N) were calculated after densitometric analysis of the respective pairs using Image Quant 5.0. **B.** Cells (VL-1) were infected with decreasing amounts of adenoviruses expressing either hSpry1 (left) or hSpry2 (right) and analyzed by Western blot using antibodies against Spry (Upstate Biotechnology) and Spry2 and Spry1 (both raised in our laboratory), as indicated. **C** and **D.** Paraffin-embedded sections of normal lung tissue were stained for Spry1 (**C**) and Spry2 (**D**; red) counterstained with hemalaun (nuclei in blue). NSCLC were stained using either Spry1 (**F**), Spry (**G-I**), or Spry2 (**J-L**) antibodies and evaluated as described in Materials and Methods. Adenocarcinoma with intermediate Spry2 expression (scored as 2) was stained using a primary antibody recognizing Spry1 (**F**), Spry (**I**), or Spry2 (**J**). As a control, the primary antibody was omitted (**E**). A representative adenocarcinoma (**G** and **H**) and SCC (**K** and **L**) showing weak Spry2 expression (scored as 1) and adjacent normal bronchial epithelium with strong Spry2 expression. Selected tumor regions (arrowheads) and normal bronchial epithelium (arrows) are emphasized. Bar, 500  $\mu$ m.

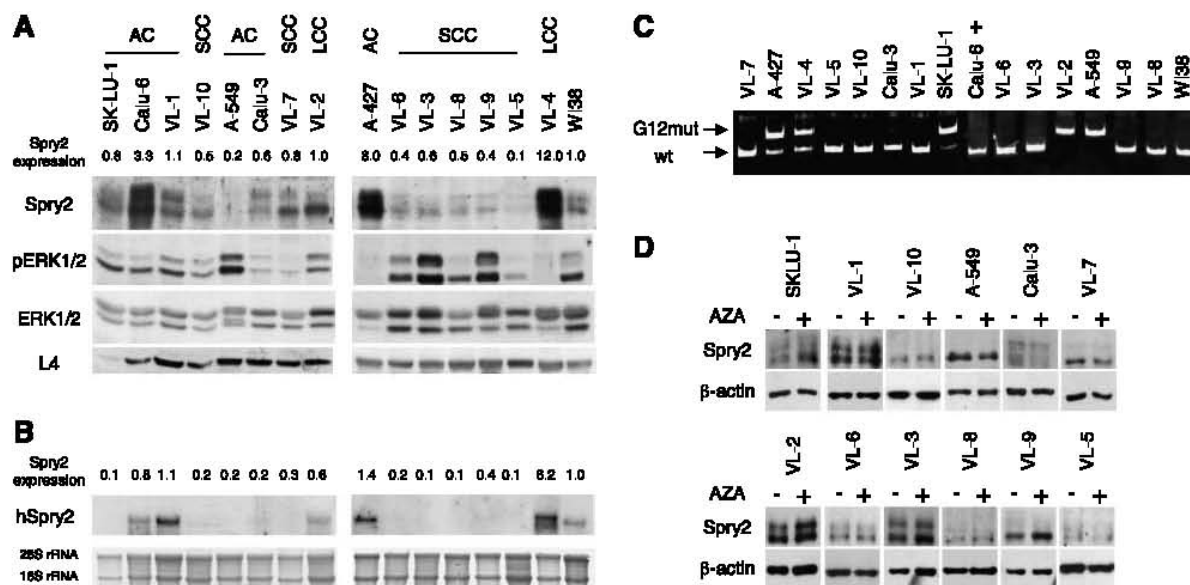


**FIGURE 2.** Characterization of NSCLC cell lines. **A.** Using Western blot, endogenous expression of Spry2 was analyzed in 15 NSCLC cell lines and in human embryonic lung fibroblasts WI38. Equal amounts of protein (150  $\mu$ g as determined by protein concentration measurement using bovine serum albumin as a standard) were loaded in each lane. Note that none of the common loading controls reflected the protein amounts, but, with the exception in the SK-LU-1 cells, ribosomal protein L4 did. Therefore, protein concentration determination was verified by staining a second SDS-PAGE gel with Coomassie Blue. The resulting Western blots were sequentially probed with the indicated antibodies. Levels of Spry2 protein were quantified by densitometry analysis and normalized to WI38 as indicated. AC, adenocarcinoma. **B.** Northern blots were used to determine Spry2 mRNA levels in NSCLC-derived cell lines. After densitometric analysis, the Spry2 expression levels were indicated as ratio to 18S rRNA. **C.** Mutation analysis of K-Ras in NSCLC cell lines was done by PCR, inserting an artificial RFLP (*Bst*XI) discriminating wild-type and mutated codon 12 (*G12mut*). Note that Calu-6 is mutated at codon 61 (+) as described in ref. 39. **D.** Western blots of selected cell lines were done to detect Spry2 expression with (+) or without (-) 5-azacytidine (AZA) treatment (10  $\mu$ M for 3 d).

expression were exclusively detected in cell lines identified as K-Ras mutated (Calu-6, A-427, and VL-4; Fig. 2A and C). However, not all of the K-Ras-mutated cell lines showed high Spry2 expression levels.

To address whether epigenetic inactivation of the promoter is responsible for the down-regulation of Spry2 in NSCLC, all tumor cell lines with reduced Spry2 expression were treated with the demethylating agent 5-azacytidine. As seen in Fig. 2D, only 3 of 12 cell lines (SKLU-1, VL-2, and VL-9) contained slightly elevated Spry2 expression levels after treatment with 5-azacytidine. These data indicate that only in few cases is hypermethylation of the Spry2 promoter involved in reducing Spry2 expression in lung cancer.

#### *Inhibition of MAPK Activation by Spry2 Expression Is Only Observed in Cell Lines with Homozygous Wild-type K-Ras Alleles*

The adenoviral system was used to analyze the function of ectopic Spry2 expression on MAPK activation in selected NSCLC cell lines. For these experiments, we selected normal embryonic lung fibroblasts (WI38), two NSCLC cell lines homozygous for K-Ras<sup>wt</sup> and three cell lines harboring K-Ras<sup>G12mut</sup>, susceptible for adenoviral infection and distinguishable in expression levels of Spry2 protein (see Fig. 2). First, logarithmically growing cells were infected with control or Spry2-expressing adenoviruses, and 48 h after infection, cells were harvested to investigate the influence of Spry2 on Ras/MAPK activity. Immunodetection of pERK proteins revealed that ectopic Spry2 expression reduced MAPK activity in all cell

lines with K-Ras<sup>wt</sup> (Fig. 3A, left). In contrast, Spry2 failed to inhibit or even enhanced ERK phosphorylation in cell lines expressing K-Ras<sup>G12mut</sup> (Fig. 3A, right). To ensure that inhibition of ERK phosphorylation by Spry2 is restricted to cell lines homozygous for K-Ras<sup>wt</sup>, we repeated the experiments including FGF2. Therefore, cells were infected with the respective adenoviruses and cultured in reduced serum levels (2%) supplemented with FGF2 (20 ng/mL) for 2 days. Resembling logarithmically growing cells, no inhibition of ERK phosphorylation by Spry2 was observed in cell lines harboring K-Ras<sup>G12mut</sup> (Fig. 3A). Next, we studied the influence of Spry2 on ERK phosphorylation following serum stimulation in those cell lines harboring a constitutively active K-Ras (A-549, VL-4, and VL-2). As a control, we included WI38 cells. Cells were serum starved and infected with control or Spry2-expressing adenoviruses. After 2 days, cells were stimulated with 20% serum for 5, 10, 15, or 20 min. Cells were lysed in SDS sample buffer and analyzed by Western blot using the respective antibodies. In all the cell lines expressing K-Ras<sup>G12mut</sup>, ectopic Spry2 expression failed to inhibit ERK phosphorylation, whereas in the WI38 control, MAPK activation was reduced by ectopic Spry2 expression (Fig. 3B).

#### *Constitutively Activated K-Ras Overrides the Antagonizing Function of Spry2 on Cell Migration*

Next, we tested the influence of Spry2 on cell migration, a known RTK-mediated process, by using scratch assays. Velocity of migration was measured in selected NSCLC cell



lines harboring K-Ras<sup>wt</sup> or K-Ras<sup>G12mut</sup>. The migration study with VL-1 was impossible because this cell line underwent apoptosis in response to cell density. As shown in Fig. 4, Spry2 expression had a pronounced effect on cell migration in K-Ras<sup>wt</sup> WI38 and VL-8 cells (Fig. 4A). In both cell lines, ectopic Spry2 expression potently (2- to 3- fold) prolonged the time to close the gap compared with uninfected cells (data not shown) or cells infected with a control virus (Fig. 4A and B). In comparison, in the three cell lines expressing K-Ras<sup>G12mut</sup> (Fig. 4A), the Spry2-induced reduction in migration velocity was very modest (Fig. 4B). On average, Spry2 decelerated the migration velocity in all three cell lines harboring K-Ras<sup>G12mut</sup> just 1.2- to 1.3 fold, arguing again for the dependency of Spry2 function on a switchable K-Ras<sup>wt</sup> protein.

#### Spry2 Expression Inhibits Cell Proliferation *In vivo* and *In vitro* also in Cells Expressing a Constitutively Active K-Ras

Cell proliferation is another biological process induced by RTK activation. Therefore, we investigated the influence of Spry2 on cell proliferation by generating growth curves and

performing clonogenic assays using cell lines homozygous for K-Ras<sup>wt</sup> (Fig. 5A) or harboring a K-Ras<sup>G12mut</sup> (Fig. 5B). Although infection with control virus had no effect (data of uninfected cells are not shown), ectopic hSpry2 expression significantly reduced NSCLC cell proliferation. This growth-inhibitory function of Spry2 was, in contrast to its ability to fine tune ERK activation and to interfere with cell migration, not restricted to cell lines homozygous for K-Ras<sup>wt</sup> (Fig. 5A).

Because cell proliferation in all tested cell lines was inhibited by Spry2 expression, we next examined the ability of Spry2 to interfere with tumor formation *in vivo* (Fig. 5C). In former experiments, A-549 formed reproducibly tumors of comparable size (6 of 6 mice). In addition, A-549 is a well-characterized cell line known to express K-Ras<sup>G12mut</sup> and was therefore chosen for s.c. injection into severe combined immunodeficient mice. Each mouse was injected with 10<sup>6</sup> cells infected either with Spry2-expressing (right flank) or control virus (left flank). A-549 cells infected with the control virus rapidly formed tumors, whereas cells infected with the Spry2-expressing virus completely failed to do so (Fig. 5C), which was also verified after the mice were

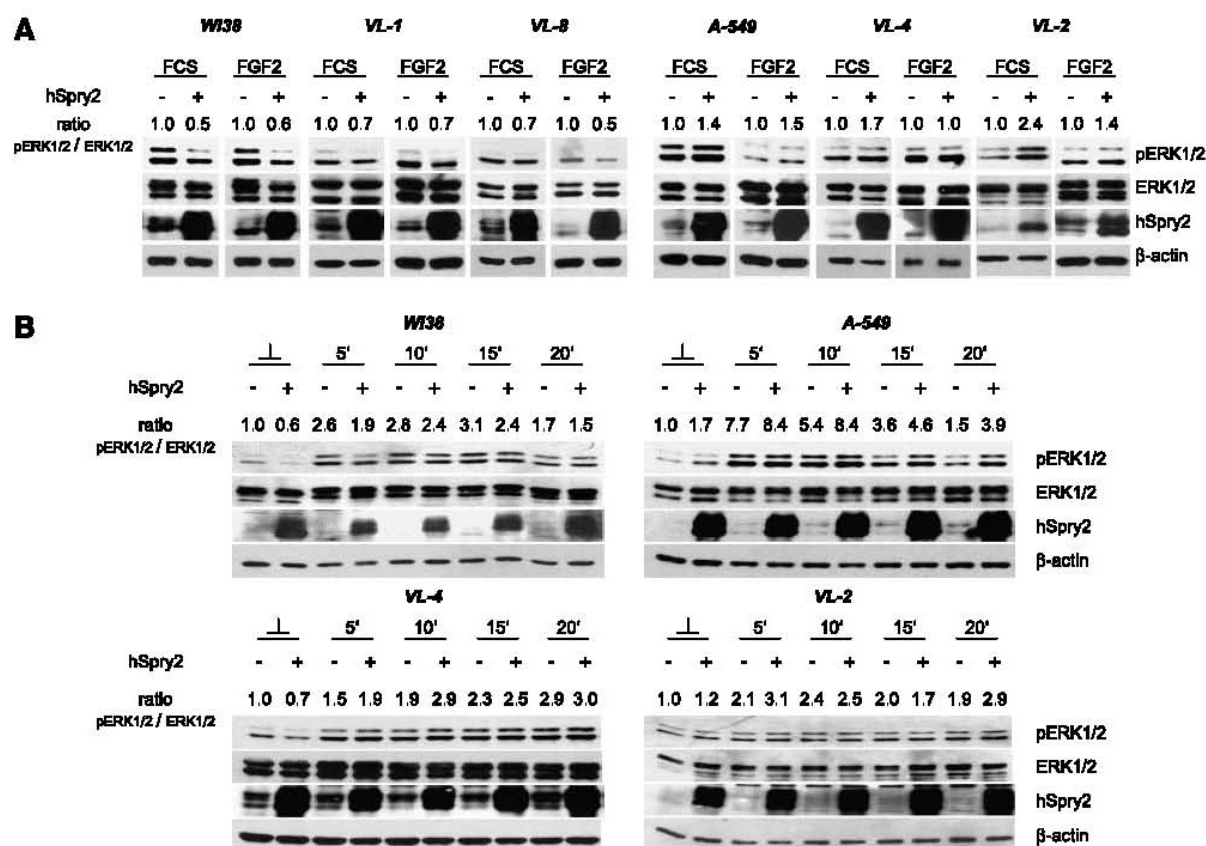


**FIGURE 3.** Effect of ectopic Spry2 expression on MAPK activity in selected cell lines. **A.** Logarithmically growing cells (FCS) as well as cells cultured in reduced serum (2%) supplemented with 20 ng/mL FGF2 (FGF2) were infected with control and Spry2 adenoviruses and analyzed by Western blot 48 h after infection using the indicated antibodies. The indicated ratios of pERK/ERK were calculated after densitometric analysis of the respective pairs using Image Quant 5.0. Ratios of hSpry2-infected cells are given relatively to those controls. **B.** Cells were serum starved and infected with control and Spry2 adenoviruses, respectively. Two days after serum withdrawal, the cells were stimulated with 20% FCS and analyzed. Representative Western blots showing the influence of Spry2 expression on ERK phosphorylation in WI38 in comparison with the selected cell lines harboring K-Ras<sup>G12mut</sup> (A-549, VL-4, and VL-2).

sacrificed at day 32 after injection. These data confirm that cell proliferation is inhibited by Spry2 also in cells with constantly active K-Ras and show that Spry2 interferes with tumor formation *in vivo*.

*Expression of a Spry2 Mutant Defective in Antagonizing ERK Activity Inhibits Cell Proliferation Less Potently but Still Significantly*

To inhibit Ras/MAPK activation, Spry2 has to be activated by phosphorylation of Tyr<sup>55</sup> (Y55; ref. 27). Hence, a mutation of Spry2 protein changing this tyrosine to a phenylalanine (Spry2<sup>Y55F</sup>) was shown to be defective in inhibiting RTK-mediated ERK phosphorylation. To confirm these data in lung cells, cells harboring either K-Ras<sup>wt</sup> (WI38, Fig. 6A) or K-Ras<sup>G12mut</sup> (A-549, Fig. 6B) were infected with a control

virus or adenoviruses expressing Spry2<sup>Y55F</sup> or Spry2<sup>wt</sup> protein. As shown in Fig. 6A, we confirmed that Spry2 mutated at Tyr<sup>55</sup> had lost the ability to reduce ERK phosphorylation. Phosphorylation of AKT (pAKT) and ribosomal protein S6, which are signal molecules within the phosphatidylinositol 3-kinase pathway, are neither reduced by Spry2<sup>wt</sup> protein nor by the mutant Spry2<sup>Y55F</sup> protein (Fig. 6A and B). As expected for a mutant defective in influencing MAPK activation, Spry2<sup>Y55F</sup> protein was less effective in inhibiting proliferation of normal lung fibroblasts (Fig. 6C) than the Spry2<sup>wt</sup> protein. The average doubling time in WI38 cells expressing Spry2<sup>Y55F</sup> was about 130 h compared with almost 240 h in WI38 cells infected with virus expressing Spry2<sup>wt</sup>. Nonetheless, overexpression of mutated Spry2<sup>Y55F</sup> protein clearly reduced cell proliferation in WI38 when compared with cells infected with

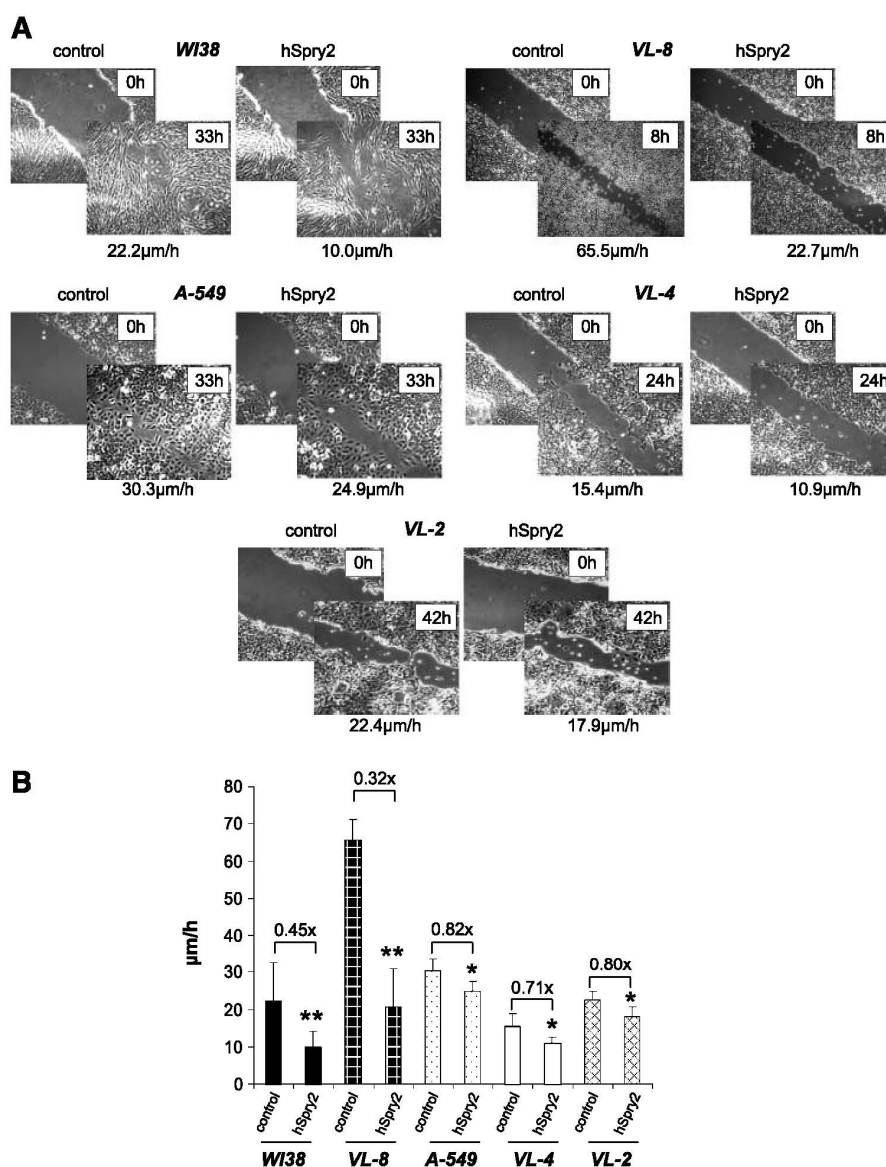


**FIGURE 4.** Influence of Spry2 expression on cell migration. **A.** Cells homozygous for K-Ras<sup>wt</sup> (WI38 and VL-8) were compared with cell lines expressing K-Ras<sup>G12mut</sup> (A-549, VL-4, and VL-2) in a scratch assay (see Materials and Methods). Mean migration velocities are indicated. **B.** Summary of the data from three to five experiments. Columns, means of the different migration velocities; bars, SD. \*,  $P < 0.05$ ; \*\*,  $P \leq 0.01$  (Mann-Whitney  $U$  test).

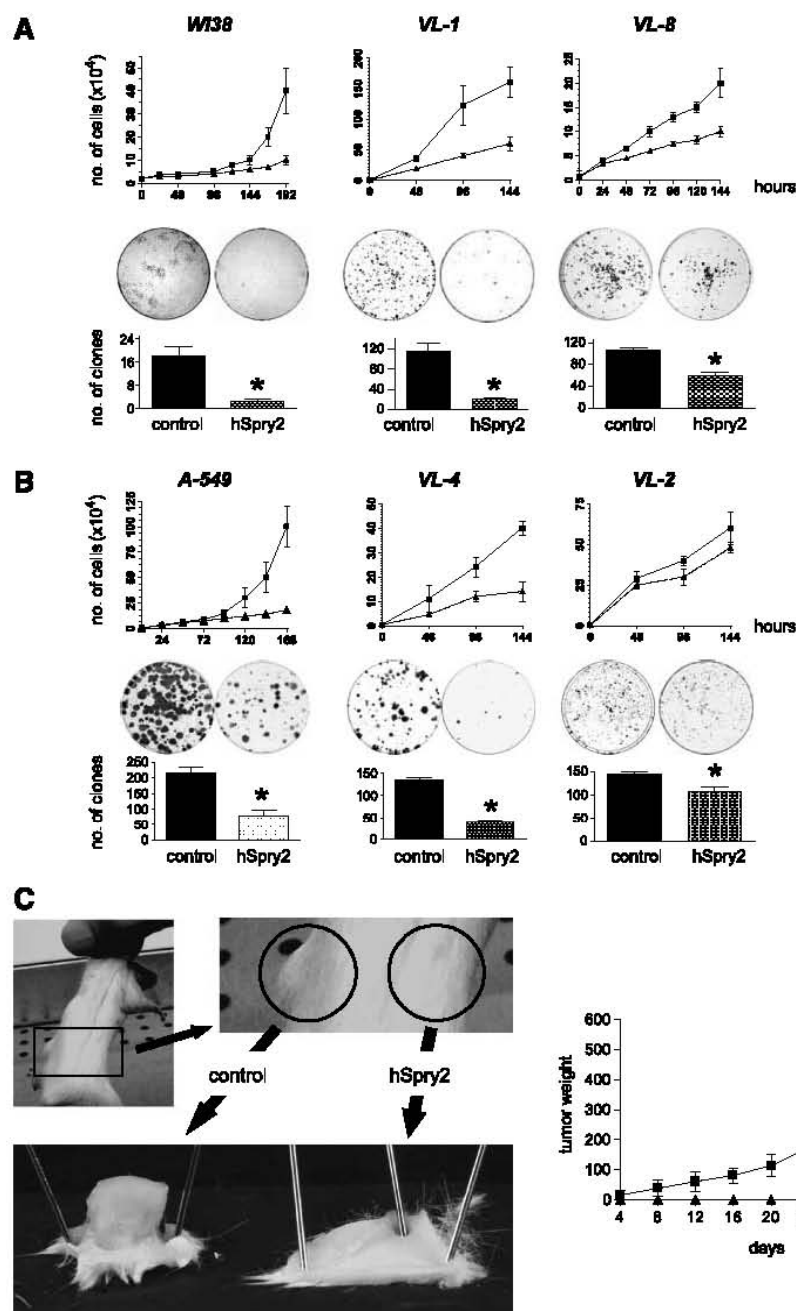


**FIGURE 5.** Effect of Spry2 on cell proliferation *in vitro* and *in vivo*. Proliferation of cell lines expressing either K-Ras<sup>wt</sup> (**A**) or K-Ras<sup>G12mut</sup> (**B**) was determined using growth curve analyses (top) and clonogenic assays (bottom). All growth curves were done at least thrice. For clonogenic assays, representative plates are shown. Columns, means of at least five experiments; bars, SD. \*,  $P < 0.01$  (Mann-Whitney  $U$  test). Note that VL-2 is less susceptible to the adenoviruses (compare Fig. 3A); thus, after few cell divisions, Spry2 overexpression is lost. Therefore, growth inhibition is obvious within the first 96 h, but afterwards, cell doubling time is comparable. **C.** Tumor formation of A-549 cells infected with control or Spry2 adenoviruses was analyzed in immunocompromised SCID/BALB/c mice (left). The calculated tumor weight represents a mean value of six mice from two independent experiments (right). —■—, control virus; —▲—, Spry2 virus.

the control virus (minimal doubling time around 50 h), enforcing the former data that Spry2 inhibits cell proliferation not only by interfering with MAPK activation (compare Fig. 5). In addition, cells with K-Ras<sup>G12mut</sup> (A-549) doubled slower when infected with either Spry2<sup>wt</sup> or Spry2<sup>Y55F</sup> (Fig. 6D). Furthermore, we observed that inhibition of cell proliferation in A-549 cells expressing either Spry2<sup>Y55F</sup> or Spry2<sup>wt</sup> protein was equal effective during the first 72 h. At later time points, the growth reduction was, like in WI38, more

pronounced with Spry2<sup>wt</sup> protein, suggesting that activation of Spry2 by phosphorylation at Y55 induces an additional inhibitory function also in cell lines expressing K-Ras<sup>G12mut</sup> (Fig. 6D).

## Discussion

Autonomous cell growth independent of external signals is a characteristic feature of human cancers. Therefore, changes affecting genes involved in signal transduction are among the

most frequent alterations in tumors. In this study, we report that expression of the MAPK inhibitory protein Spry2 is down-regulated in NSCLC, whereas another Spry family member, Spry1, tends to be up-regulated in this tumor type. In accordance with these data, also in hepatoma, Spry2 but not Spry1 expression was shown to be down-regulated in the malignant cells (40). In breast cancer, both Spry1 and Spry2 expression levels are frequently repressed (41), and in prostate cancer, decreases in Spry1 and Spry4 levels contribute to malignant transformation (42, 43). These data indicate that Spry proteins are commonly down-regulated in cancer, but dependent on tumor types, different members of the family are affected.

Several mechanisms may account for the reduced Spry2 expression in NSCLC cells. In agreement with published data describing Spry2 expression in rodents (17, 36), in human nonmalignant adult lungs, Spry2 was primarily expressed in the bronchial epithelium. During malignant progression, many epithelial tumors are supposed to undergo a transition endowing the cancer cell with typical mesenchymal properties to facilitate invasion and metastasis. Spry2 down-regulation in tumors might thus be connected to this dedifferentiation process. Accordingly, cell lines derived from NSCLC metastases tended to be low in Spry2 expression. In addition, in prostate cancer, an inverse correlation between Spry expression and tumor grade

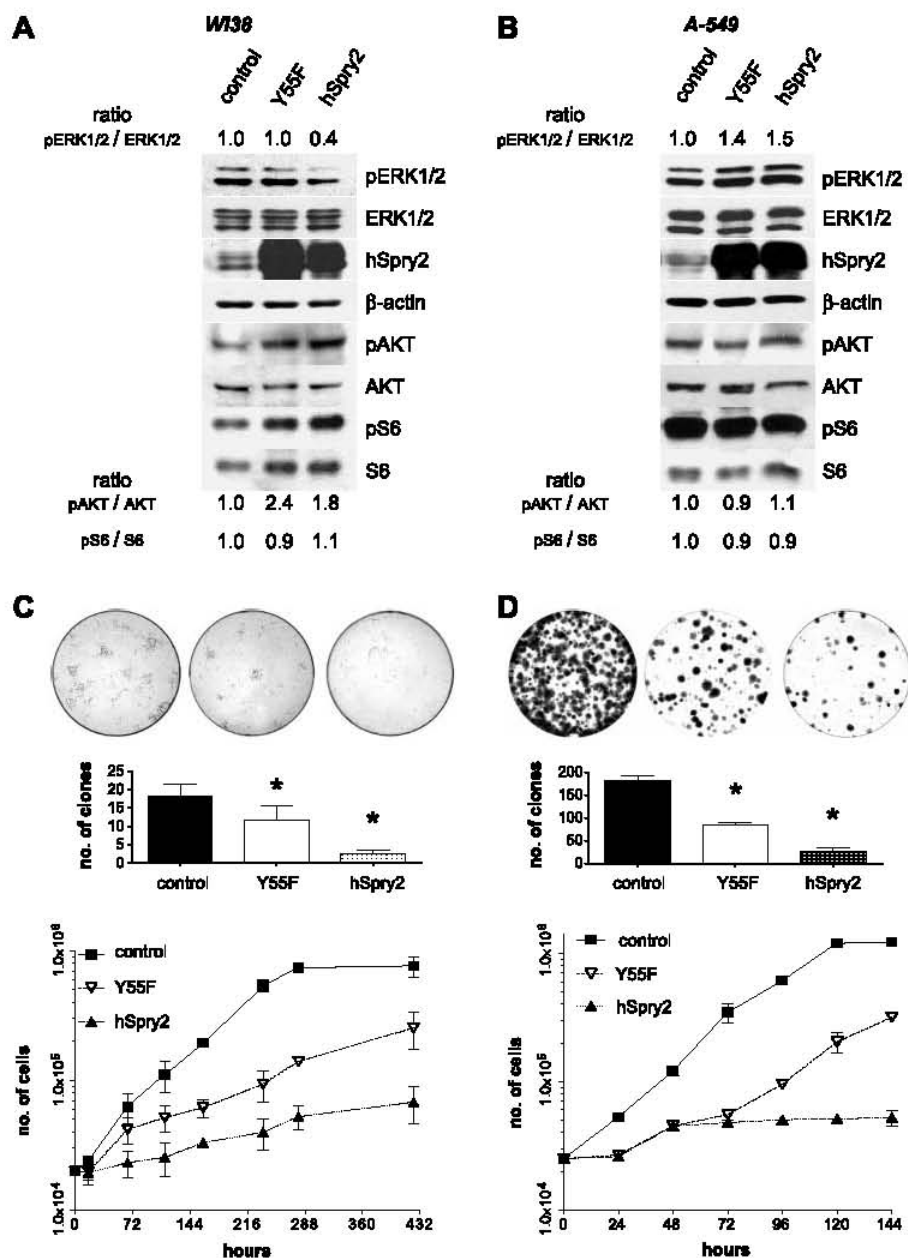


**FIGURE 6.** Effects of mutant Spry2<sup>Y55F</sup> compared with Spry2<sup>wt</sup>. Logarithmically growing WI38 cells (**A**) and A-549 (**B**) cells were infected with the indicated adenoviruses and analyzed by immunoblotting with the indicated antibodies. The indicated ratios of pERK, pAKT, and pS6 to the respective total proteins (ERK, AKT, and S6) were calculated after densitometric analysis of the respective pairs using Image Quant 5.0. Proliferation of WI38 (**C**) and A-549 (**D**) cells infected with control, Spry2<sup>wt</sup>, and Spry2<sup>Y55F</sup> adenoviruses was measured by clonogenic assays and growth curve analyses (compare Fig. 5). The clonogenic assays (*top*) were done six times. Representative plates are shown. Columns, mean numbers of clones formed from 500 cells plated; bars, SD. Colony formation between cells infected with the respective adenoviruses differed significantly in both cell lines. \*,  $P < 0.01$  (Mann-Whitney  $U$  test). Growth curve analyses (*bottom*) were done thrice. Points, means; bars, SD.

was reported (44). In this tissue, low Spry expressions correlated with enhanced methylation of the Spry2 and Spry4 promoters, respectively (43, 44), whereas in NSCLC, only 3 of 12 cell lines exhibited slightly enhanced Spry2 expression following treatment with demethylating agents. Accordingly, in breast cancer and hepatocellular carcinoma, methylation of the Spry2 promoter was unchanged (40, 41). Besides epigenetic silencing, additionally, selection for lower gene doses might be involved in Spry2 repression. In prostate, McKie et al. observed frequently loss of heterozygosity in microsatellite markers flanking the *Spry2* gene locus. (44), whereas in hepatocellular carcinoma, no loss of heterozygosity was observed in this region (40). Using comparative genomic hybridization, Luk et al. showed that in 21% of NSCLC cases, the chromosomal region 13q31 harboring the *Spry2* gene is underrepresented (45). Some of the NSCLC-derived cell lines investigated in this study have 13q31 underrepresented.<sup>3</sup> For example, A-549, VL-8, and VL-10 are among the cell lines that have a lowered 13q31 gene dosage and express low levels of Spry2 (data not shown). Furthermore, Spry expression is suggested to be regulated as part of an autoregulatory feedback loop (27). In agreement with this hypothesis, we observed that only NSCLC cell lines harboring mutated K-Ras express high levels of Spry2. This may explain why, with respect to histologic subtypes, Spry2 levels tend to be higher in adenocarcinoma-derived than in SCC-derived cell lines. K-Ras mutations are more frequent in adenocarcinoma compared with SCC (3). Nevertheless, the mechanisms responsible for down-regulation of Spry2 in NSCLC cancer are not completely elucidated, and ongoing studies in our laboratory will focus on this issue.

To investigate the contribution of Spry2 down-regulation to the malignant phenotype of NSCLC cells, we expressed the protein by an adenoviral approach. Ectopic expression of Spry2 caused inhibition of ERK phosphorylation and decelerated tumor formation, proliferation, and cell migration. However, Spry2-mediated repression of ERK activity was exclusively observed in cells containing only K-Ras<sup>wt</sup>. In agreement with these data, additionally, Gross et al. showed that Spry2 inhibits Raf binding activity of H-Ras<sup>wt</sup> but not of a H-Ras<sup>R12</sup> mutant in NIH3T3 cells (20). These observations indicate that constitutively active Ras can circumvent Spry2 function in the MAPK pathway regulation. Because initial attempts to immunoprecipitate Spry2 with K-Ras have been unsuccessful (data not shown), we speculate that Spry2 interferes with ERK phosphorylation upstream of K-Ras.

Accordingly, attenuation of cell migration by Spry2 was significantly more potent in NSCLC cell lines expressing only K-Ras<sup>wt</sup> compared with cell lines harboring K-Ras<sup>G12mut</sup>. Previous reports show that Spry and Spry-like Spred proteins inhibit cell migration by interfering with Rac-1 activation or by direct interaction with RhoA, respectively (21, 46, 47). Because both RhoA (through GAP120 and GAP190 interaction) and Rac-1 (via phosphatidylinositol 3-kinase) were shown to be activated by Ras (48), it is possible that Spry2 inhibits cell

migration via the same mechanism responsible for inhibition of ERK phosphorylation. Nonetheless, we cannot exclude that Spry2 interferes with mechanisms directly regulating Rac1 and/or RhoA, which could be circumvented by activated Ras.

In contrast to cell migration, cell proliferation was reduced by Spry2 in all tested NSCLC cell lines. These data argue for a Spry2 function in cell proliferation independent of Ras/ERK activation. In agreement with this conclusion, a Spry2 mutant (Spry2<sup>Y55F</sup>) that was reported to be diminished with respect to MAPK inhibition (28, 32) also significantly attenuated proliferation. Nevertheless, the effect of Spry2<sup>Y55F</sup> was lower compared with the Spry2<sup>wt</sup> protein, indicating a cumulating contribution of MAPK-mediated signals. In A-549, harboring K-Ras<sup>G12mut</sup>, Spry2<sup>Y55F</sup> was also less effective compared with the Spry2<sup>wt</sup> protein. Because in the K-Ras<sup>G12mut</sup> background, the difference between Spry2<sup>wt</sup> and Spry2<sup>Y55F</sup> became visible only from 72 h onwards (Fig. 6D), we hypothesize that activated Ras, with a reported half-life of around 30 h (49), is lost due to protein degradation, and that Spry2<sup>wt</sup> but not Spry2<sup>Y55F</sup> might interfere with the activation also of newly synthesized, dominant-active K-Ras. The mechanisms as to how Spry2 achieves inhibition of cell proliferation without affecting ERK phosphorylation are to be clarified. A recent study suggests that Spry2 inhibits proliferation via a mechanism connected to the coinciding elevation of phosphatase and tensin homologue deleted on chromosome 10 (PTEN) expression (50). However, neither AKT nor S6 phosphorylation were reduced by ectopic Spry2. In contrast, pAKT was rather elevated in response to Spry2 overexpression. Similar results were reported by de Alvaro et al. (51). Therefore, we conclude, in accordance with several other reports (8), that also in NSCLC cells Spry2 expression does not inhibit the phosphatidylinositol 3-kinase pathway. The most prominent Ras-independent signal cascades induced through RTK signaling involve generation of the second messengers phosphoinositol triphosphate and diacylglycerol by phospholipase-C (2). Accordingly, studies in *Xenopus* clearly showed that Spry exerts parts of its inhibitory functions via influencing Ca<sup>2+</sup> efflux (52), known to be activated by phospholipase-C (2). In addition, it was shown that phospholipase-C can activate Spry2 expression, suggesting the presence of an alternative autoregulatory feedback loop (53). Studies investigating the influence of Spry2 on Ras-independent signaling are initiated in our laboratory.

In summary, our data show that Spry2 expression is almost generally repressed in NSCLC, and that this alteration contributes to the malignant phenotype by enhancing RTK-mediated processes like cell migration and proliferation. In addition, we show that Spry2 inhibits RTK-mediated signals both upstream of Ras but also by mechanisms independent of the Ras/MAPK signaling axis. Our observations implicate that Spry2 represents a tumor suppressor in NSCLC and suggest Spry2 re-expression as a promising therapeutic strategy against lung tumors even with mutated K-Ras.

## Materials and Methods

### Patient Material and Cell Lines

For reverse transcription-PCR analysis, a panel of cDNA samples synthesized from four NSCLC and one SCLC (patient 3)

<sup>3</sup> C. Pirker, personal communication.

and the corresponding normal tissue from individual patients (BD Biosciences) was used. Concerning the histologic subtypes, patient 1 was diagnosed with LCC, and patients 2, 4, and 5 represent SCC.

Immunohistochemistry was done using tissue sections derived from 25 lung cancer patients who underwent surgical resection due to proven NSCLC at the Otto Wagner Hospital. The pathologic stage of each tumor was classified according to the WHO classifications. All patients had given informed consent. Eleven of 25 tumor samples were derived from clinical stage I patients; 4 of 25 samples were from stage II patients; 6 of 25 samples were from stage IIIa patients; and 3 of 25 samples were from stage IIIb patients. One patient could not be classified. Eleven tumors each were identified as adenocarcinoma and SCC, whereas three tumors were LCC. Surgical specimens of four patients with pneumothorax were used as nonmalignant controls.

Ten of 15 NSCLC cell lines analyzed were established at our institute as described (5): surgical specimens from one histologic confirmed adenocarcinoma (VL-1), seven SSC (VL-3 and VL-5 to VL-10), and two LCC (VL-2 and VL-4) were used at passage numbers between 15 and 30. Six of 10 cell lines (VL-1 to VL-4, VL-9, and VL-10) were derived from primary tumors, and four (VL-5 to VL-8) were derived from lymph node metastases. Additionally, five of the adenocarcinoma cell lines (A-427, A-549, Calu-3, Calu-6, and SK-LU-1) and the normal embryonic lung fibroblasts (WI38 at passage 16) were purchased from the American Type Culture Collection.

#### Antibodies

Polyclonal rabbit serum to Spry2 was raised against glutathione *S*-transferase tagged NH<sub>2</sub>-terminal 150 amino acids of human Spry2. Rabbit sera against Spry1 were generated using glutathione *S*-transferase tagged NH<sub>2</sub>-terminal 200 amino acids of human Spry1. According to the manufacturer's protocol, purified glutathione *S*-transferase, NH<sub>2</sub>-terminal 150 amino acids of human Spry2, and NH<sub>2</sub>-terminal 200 amino acids of human Spry1 were coupled to CNBr-activated Sepharose (GE Healthcare). The antibodies were affinity purified from rabbit serum by incubation with a glutathione *S*-transferase affinity column, followed by Spry2 and Spry1 protein affinity columns, respectively. To also deplete hSpry1-specific antibodies, the crude Spry2 antiserum was cycled twice over hSpry1 protein coupled to beads before affinity purification against hSpry2. Antibodies against pERK, pAKT, AKT, pS6, and S6 were purchased from Cell Signaling; Spry and total ERK1/2 were from Upstate; and  $\beta$ -actin was from Santa Cruz Biotechnology.

#### Immunohistochemistry

Immunohistochemistry was done as described previously (54) using Fast Red as a chromogen (Ventana) and hemalaun as counterstain. The intensity of immunohistochemical staining was assessed semiquantitatively by two authors (H.S. and C.E.M.). In all cases, both malignant and normal epithelial cells stained positive, the latter consistently showing strong staining intensity. We therefore scored overall staining intensities of malignant cells with respect to the ones observed in

corresponding normal epithelial cells: 3, strong positive staining resembling or slightly below that of the normal epithelium; 2, clearly below the normal epithelium but still with distinct immunoreactions; 1, weak to very weak staining.

#### Reverse Transcription-PCR

Expression levels of Spry2 transcripts in tumor tissues were determined by semiquantitative reverse transcription-PCR procedure as described previously (55), using  $\beta$ -actin as house-keeping gene. Dynamics of PCR amplification was evaluated at different PCR cycle numbers. For data presentation, 30 cycles for Spry1 and Spry2 and 25 cycles for  $\beta$ -actin were used. Several controls were included in each experiment. Oligonucleotides are as follows: Spry2, 5'-ATGGAGGCCAGAGCT-CAGAGTG-3' and 5'-GTTCAGAGGAGCTGCTGCTGG-3'; Spry1, 5'-GAGAGCATGGTGGAAATATGG-3' and 5'-GAGT-TAGACCTTGGCAACAG-3';  $\beta$ -actin, 5'-GTGGGGCGCAGG-CACCA-3' and 5'-CTCCTTAATGTCACGCACGATTC-3'.

#### RFLP Analysis of K-Ras Mutations in Codon 12

The artificial RFLP was done as described by Nishikawa et al. (38). Briefly, genomic DNA was extracted using QiaAMPBlood kit (Qiagen GmbH), and exon 1 of K-Ras was amplified by PCR. By using the forward primer 5'-ACTGAA-TATAAACTTGTGGTCCATGGAGCT-3' and the reverse primer 5'-TTTACCAIATTTGGATCAIATTC-3', an artificial *Bst*XI restriction enzyme site was introduced. In the case of K-Ras<sup>wt</sup>, a second *Bst*XI site, including the first two nucleotides (GG) of codon 12, is generated. After restriction digest with *Bst*XI (Roche), the fragment size was analyzed using PAGE gel electrophoresis and staining with ethidium bromide.

#### Recombinant Adenovirus Generation and Cell Infection

The coding sequence of human Spry2 was amplified by PCR using Pfx Polymerase (Invitrogen) with upstream primer 5'-TAGCGAATTCGGATCCATGGAGGCCAGAGCTCAGAG-3' (Spry2-s) and downstream primer 5'-TAGCGAATTCCTCGAGCTATGTTGGTTTTTCAAAGT-3' (Spry2-as) to add appropriate cloning sites. The Spry2<sup>Y55F</sup> mutation was introduced by PCR using primers 5'-AATGAATTCACAGAGGGCCT-3' and 5'-TGTAATTCATGGTGGTTCG-3' in combination with Spry2-s and Spry2-as primers. The PCR-amplified DNA fragments were cloned via *Bam*HI/*Eco*RI into a pADlox plasmid to generate pADlox-Spry2<sup>wt</sup> and pADlox-Spry2<sup>Y55F</sup>, and correct cloning was confirmed by sequencing. Recombinant viruses were produced as described (56) by cotransfection of adenoviral DNA and pADlox-Spry2<sup>wt</sup> and pADlox-Spry2<sup>Y55F</sup> plasmid DNA, respectively. Empty (pADlox) and control (pADlox-LacZ) viruses were generated using the same procedure. For infection, viruses were diluted in serum-free medium. If not indicated otherwise, adenoviruses were generally used at a multiplicity of infection of 50.

#### RNA Extraction and Northern Blotting

RNA preparation and Northern blotting procedures followed published methods (57). The 948-bp Spry2 coding sequence was used as a probe for labeling with High Prime Labeling kit (Roche).

### Immunoblotting

Protein isolation and immunoblotting were done as described (5). Western blot signals were quantified using Image Quant software (Molecular Dynamics).

### Scratch Assay

Cells were infected with the respective adenoviruses, and after 24 h,  $2 \times 10^5$  cells were seeded into a six-well plate and allowed to grow to 90% confluency. An "X"-shaped scratch was set into the cell monolayers with a sterile pipette tip. Wounded monolayers were then washed thrice to remove cell debris, and comparable proportions of three scratches per experimental group were selected and marked. At the indicated times, still images were taken under a Leica TE100 microscope equipped with a CCD camera, and the gap width was measured using Metamorph 6.1 software (Universal Imaging Corp.) to calculate migration velocity ( $\mu\text{m}/\text{h}$ ).

### Growth Curves

Twenty-four hours after infection,  $10^4$  cells were seeded into Petri dishes and re-incubated in the appropriate medium containing 10% FCS. Two plates each were counted at different time points (dependent on the cell line) using a Bürker-Türk cell-counting chamber. Every experiment was done at least twice in duplicates.

### Clonogenic Assay

Twenty-four hours after infection, 500 cells each were seeded into six-well plates in sextuplicates. Two to 3 weeks later, the cells were stained and fixed with GIEMSA solution (Merck), and colonies were counted.

### Tumor Formation in Severe Combined Immunodeficient Mice

Two days after infection with control and Spry2-expressing adenoviruses,  $1 \times 10^6$  A-549 cells were re-suspended in 100  $\mu\text{L}$  PBS and injected s.c. into immunocompromised SCID/BALB/c recipient mice. The tumor size was periodically determined using a Vernier caliper, and the tumor weight was calculated from tumor size according to the formula: diameter  $\times$  diameter  $\times$  length / 2. Thirty-two days after cell injection, the respective areas were surgically removed and fixed in 4% formaldehyde solution. All experiments were done according to the Austrian guidelines for animal care and protection.

### References

- Janssen-Heijnen ML, Coebergh JW. The changing epidemiology of lung cancer in Europe. *Lung Cancer* 2003;41:245–58.
- Schlessinger J. Cell signaling by receptor tyrosine kinases. *Cell* 2000;103:211–25.
- Mascaux C, Iannino N, Martin B, et al. The role of RAS oncogene in survival of patients with lung cancer: a systematic review of the literature with meta-analysis. *Br J Cancer* 2005;92:131–9.
- Johnson BE, Janne PA. Epidermal growth factor receptor mutations in patients with non-small cell lung cancer. *Cancer Res* 2005;65:7525–9.
- Berger W, Setinek U, Mohr T, et al. Evidence for a role of FGF-2 and FGF receptors in the proliferation of non-small cell lung cancer cells. *Int J Cancer* 1999;83:415–23.
- Tang JM, He QY, Guo RX, Chang XJ. Phosphorylated Akt overexpression and loss of PTEN expression in non-small cell lung cancer confers poor prognosis. *Lung Cancer* 2006;51:181–91.

- Hacohen N, Kramer S, Sutherland D, Hiromi Y, Krasnow MA. Sprouty encodes a novel antagonist of FGF signaling that patterns apical branching of the *Drosophila* airways. *Cell* 1998;92:253–63.
- Mason JM, Morrison DJ, Albert Basson M, Licht JD. Sprouty proteins: multifaceted negative-feedback regulators of receptor tyrosine kinase signaling. *Trends Cell Biol* 2006;16:45–54.
- Kim HJ, Bar-Sagi D. Modulation of signalling by Sprouty: a developing story. *Nat Rev Mol Cell Biol* 2004;5:441–50.
- Tefft JD, Lee M, Smith S, et al. Conserved function of mSpry-2, a murine homolog of *Drosophila* sprouty, which negatively modulates respiratory organogenesis. *Curr Biol* 1999;9:219–22.
- Impagnatiello MA, Weitzer S, Gannon G, et al. Mammalian sprouty-1 and -2 are membrane-anchored phosphoprotein inhibitors of growth factor signaling in endothelial cells. *J Cell Biol* 2001;152:1087–98.
- Basson MA, Akbulut S, Watson-Johnson J, et al. Sprouty1 is a critical regulator of GDNF/RET-mediated kidney induction. *Dev Cell* 2005;8:229–39.
- Gross I, Morrison DJ, Hyink DP, et al. The receptor tyrosine kinase regulator Sprouty1 is a target of the tumor suppressor WT1 and important for kidney development. *J Biol Chem* 2003;278:41420–30.
- Chi L, Zhang S, Lin Y, et al. Sprouty proteins regulate ureteric branching by coordinating reciprocal epithelial Wnt11, mesenchymal Gdnf and stromal Fgf7 signalling during kidney development. *Development* 2004;131:3345–56.
- Taketomi T, Yoshiga D, Taniguchi K, et al. Loss of mammalian Sprouty2 leads to enteric neuronal hyperplasia and esophageal achalasia. *Nat Neurosci* 2005;8:855–7.
- Shim K, Minowada G, Coling DE, Martin GR. Sprouty2, a mouse deafness gene, regulates cell fate decisions in the auditory sensory epithelium by antagonizing FGF signaling. *Dev Cell* 2005;8:553–64.
- Mailleux AA, Tefft D, Ndiaye D, et al. Evidence that SPROUTY2 functions as an inhibitor of mouse embryonic lung growth and morphogenesis. *Mech Dev* 2001;102:81–94.
- Perl AK, Hokuto I, Impagnatiello MA, Christofori G, Whitsett JA. Temporal effects of Sprouty on lung morphogenesis. *Dev Biol* 2003;258:154–68.
- Lee SH, Schloss DJ, Jarvis L, Krasnow MA, Swain JL. Inhibition of angiogenesis by a mouse sprouty protein. *J Biol Chem* 2001;276:4128–33.
- Gross I, Bassit B, Benezra M, Licht JD. Mammalian sprouty proteins inhibit cell growth and differentiation by preventing ras activation. *J Biol Chem* 2001;276:46460–8.
- Yizgaw Y, Cartin L, Pierre S, Scholich K, Patel TB. The C terminus of sprouty is important for modulation of cellular migration and proliferation. *J Biol Chem* 2001;276:22742–7.
- Lee CC, Putnam AJ, Miranti CK, et al. Overexpression of sprouty 2 inhibits HGF/SF-mediated cell growth, invasion, migration, and cytokinesis. *Oncogene* 2004;23:5193–202.
- Zhang C, Chaturvedi D, Jaggar L, et al. Regulation of vascular smooth muscle cell proliferation and migration by human sprouty 2. *Arterioscler Thromb Vasc Biol* 2005;25:533–8.
- Casci T, Vinos J, Freeman M. Sprouty, an intracellular inhibitor of Ras signaling. *Cell* 1999;96:655–65.
- Lim J, Wong ES, Ong SII, et al. Sprouty proteins are targeted to membrane ruffles upon growth factor receptor tyrosine kinase activation. Identification of a novel translocation domain. *J Biol Chem* 2000;275:32837–45.
- Egan JE, Hall AB, Yatsula BA, Bar-Sagi D. The bimodal regulation of epidermal growth factor signaling by human Sprouty proteins. *Proc Natl Acad Sci U S A* 2002;99:6041–6.
- Mason JM, Morrison DJ, Basson MA, Licht JD. Sprouty proteins: multifaceted negative-feedback regulators of receptor tyrosine kinase signaling. *Trends Cell Biol* 2006;16:45–54.
- Sasaki A, Taketomi T, Wakioka T, Kato R, Yoshimura A. Identification of a dominant negative mutant of Sprouty that potentiates fibroblast growth factor- but not epidermal growth factor-induced ERK activation. *J Biol Chem* 2001;276:36804–8.
- Ozaki K, Kadamoto R, Asato K, et al. ERK pathway positively regulates the expression of Sprouty genes. *Biochem Biophys Res Commun* 2001;285:1084–8.
- de Maximy AA, Nakatake Y, Moncada S, et al. Cloning and expression pattern of a mouse homologue of *Drosophila* sprouty in the mouse embryo. *Mech Dev* 1999;81:213–6.
- Minowada G, Jarvis LA, Chi CL, et al. Vertebrate Sprouty genes are induced by FGF signaling and can cause chondrodysplasia when overexpressed. *Development* 1999;126:4465–75.
- Mason JM, Morrison DJ, Bassit B, et al. Tyrosine phosphorylation of

Sprouty proteins regulates their ability to inhibit growth factor signaling: a dual feedback loop. *Mol Biol Cell* 2004;15:2176–88.

33. Fong CW, Leong HF, Wong ES, et al. Tyrosine phosphorylation of Sprouty2 enhances its interaction with c-Cbl and is crucial for its function. *J Biol Chem* 2003;278:33456–64.

34. Rubin C, Litvak V, Medvedovsky H, et al. Sprouty fine-tunes EGF signaling through interlinked positive and negative feedback loops. *Curr Biol* 2003;13:297–307.

35. Hanafusa H, Torii S, Yasunaga T, Nishida E. Sprouty1 and Sprouty2 provide a control mechanism for the Ras/MAPK signalling pathway. *Nat Cell Biol* 2002;4:850–8.

36. Hashimoto S, Nakano H, Singh G, Katyal S. Expression of Sprouty and Sprouty2 in developing rat lung. *Mech Dev* 2002;119 Suppl 1:S303–9.

37. Zhang S, Lin Y, Itaranta P, Yagi A, Vainio S. Expression of Sprouty genes 1, 2 and 4 during mouse organogenesis. *Mech Dev* 2001;109:367–70.

38. Nishikawa T, Maemura K, Hirata I, et al. A simple method of detecting K-ras point mutations in stool samples for colorectal cancer screening using one-step polymerase chain reaction/restriction fragment length polymorphism analysis. *Clin Chim Acta* 2002;318:107–12.

39. Lehman TA, Bennett WP, Metcalf RA, et al. p53 mutations, ras mutations, and p53-heat shock 70 protein complexes in human lung carcinoma cell lines. *Cancer Res* 1991;51:4090–6.

40. Fong CW, Chua MS, McKie AB, et al. Sprouty 2, an inhibitor of mitogen-activated protein kinase signaling, is down-regulated in hepatocellular carcinoma. *Cancer Res* 2006;66:2048–58.

41. Lo TL, Yusoff P, Fong CW, et al. The ras/mitogen-activated protein kinase pathway inhibitor and likely tumor suppressor proteins, sprouty 1 and sprouty 2 are deregulated in breast cancer. *Cancer Res* 2004;64:6127–36.

42. Kwabi-Addo B, Wang J, Erdem H, et al. The expression of Sprouty1, an inhibitor of fibroblast growth factor signal transduction, is decreased in human prostate cancer. *Cancer Res* 2004;64:4728–35.

43. Wang J, Thompson B, Ren C, Ittmann M, Kwabi-Addo B. Sprouty4, a suppressor of tumor cell motility, is down regulated by DNA methylation in human prostate cancer. *Prostate* 2005;66:613–24.

44. McKie AB, Douglas DA, Olijslagers S, et al. Epigenetic inactivation of the human sprouty2 (hSPRY2) homologue in prostate cancer. *Oncogene* 2005;24:2166–74.

45. Luk C, Tsao MS, Bayani J, Shepherd F, Squire JA. Molecular cytogenetic analysis of non-small cell lung carcinoma by spectral karyotyping and comparative genomic hybridization. *Cancer Genet Cytogenet* 2001;125:87–99.

46. Miyoshi K, Wakioka T, Nishinakamura H, et al. The Sprouty-related protein, Sprouty, inhibits cell motility, metastasis, and Rho-mediated actin reorganization. *Oncogene* 2004;23:5567–76.

47. Poppleton HM, Edwin F, Jaggar L, et al. Sprouty regulates cell migration by inhibiting the activation of Rac1 GTPase. *Biochem Biophys Res Commun* 2004;323:98–103.

48. Scita G, Tenca P, Frittoli E, et al. Signaling from Ras to Rac and beyond: not just a matter of GEFs. *EMBO J* 2000;19:2393–8.

49. Tsai FM, Shyu RY, Jiang SY. RIG1 inhibits the Ras/mitogen-activated protein kinase pathway by suppressing the activation of Ras. *Cell Signal* 2006;18:349–58.

50. Edwin F, Singh R, Endersby R, Baker SJ, Patel TB. The tumor suppressor PTEN is necessary for human Sprouty 2-mediated inhibition of cell proliferation. *J Biol Chem* 2006;281:4816–22.

51. de Alvaro C, Martinez N, Rojas JM, Lorenzo M. Sprouty-2 overexpression in C2C12 cells confers myogenic differentiation properties in the presence of FGF2. *Mol Biol Cell* 2005;16:4454–61.

52. Nutt SL, Dingwell KS, Holt CE, Amaya E. *Xenopus* Sprouty2 inhibits FGF-mediated gastrulation movements but does not affect mesoderm induction and patterning. *Genes Dev* 2001;15:1152–66.

53. Abe M, Naski MC. Regulation of sprouty expression by PLCgamma and calcium-dependent signals. *Biochem Biophys Res Commun* 2004;323:1040–7.

54. Berger W, Setinek U, Hollaus P, et al. Multidrug resistance markers P-glycoprotein, multidrug resistance protein 1, and lung resistance protein in non-small cell lung cancer: prognostic implications. *J Cancer Res Clin Oncol* 2005;131:355–63.

55. Berger W, Elbling L, Micksche M. Expression of the major vault protein LRP in human non-small-cell lung cancer cells: activation by short-term exposure to antineoplastic drugs. *Int J Cancer* 2000;88:293–300.

56. Sutterluty H, Chatelain E, Marti A, et al. p45SKP2 promotes p27Kip1 degradation and induces S phase in quiescent cells. *Nat Cell Biol* 1999;1:207–14.

57. Sutterluty H, Bartl S, Doetzlhofer A, et al. Growth-regulated antisense transcription of the mouse thymidine kinase gene. *Nucleic Acids Res* 1998;26:4989–95.



## 5.2 Manuscript 2: Ras signaling has a clearly distinguishable impact on Sprouty1, 2 and 4 expressions

Christoph-Erik Mayer, Barbara Haigl, Florian Jantscher, Gerald Siegwart, Walter Berger and Hedwig Sutterlüty

*Institute of Cancer Research, Department of Medicine I, Medical University of Vienna, Austria*

submitted to BBA-Molecular Cell Research

### **Abstract**

Sprouty (Spry) proteins are intracellular inhibitors of RTK-signaling. Since their expression coincides with growth factor activity, an autoregulatory-feedback loop was postulated as general mechanism for controlling Spry family members' expression. Here, we report that activating mutants of Ras proteins induced Spry2 and to a lesser extent Spry4 protein levels. In contrast, Spry1 expression was not affected by activation of Ras. Correspondingly, only Spry2 and Spry4 expressions were significantly elevated in cell lines harboring oncogenic K-Ras mutations. Despite the observed elevation of Spry4 by Ras, induction of Spry4 levels could only be achieved by serum addition. These data demonstrate that Spry4 is influenced by activation of Ras, but there are additional factors involved in its regulation. The central role of Ras in controlling Spry2 expression was emphasized by our results illustrating that in cells harboring mutant Ras, growth factors were unable to induce Spry2 protein levels. In cell lines expressing wildtype Ras, elevation of Spry2 expression was always connected to MAPK activation. Corroborating, using Ras mutants specifically binding Raf or PI3K, we show that Spry2 expression is solely induced by MAPK pathway. Therefore we conclude that Ras signaling has a clearly distinguishable impact on the expression of different Spry family members.

## Introduction

Deregulated cell proliferation is one of the defining features of all cancers. Hence, the critical balance between proliferation and growth on one hand and cell death and differentiation on the other hand is always disturbed. One of the pathways frequently mutated or deregulated in cancer involves receptor tyrosine kinase (RTK)-mediated signaling which plays an essential role in governing extracellular growth, proliferation and differentiation signals<sup>189</sup>. In non-transformed cells this signaling network is precisely coordinated and integrated at any time. This is achieved by the implementation of several negative feedback loops which attenuate and terminate the cellular stimulation induced by RTK-derived signals<sup>14</sup>.

One of these negative feedback loops includes the members of the Sprouty (Spry) protein family. Therefore Spry proteins are considered to play a role as tumor suppressors in several cancers. Consequently, various isoforms of Spry proteins have been found deregulated in tumors. A decrease in Spry1, Spry2 and Spry4 levels contributes to malignant transformation in prostate<sup>181-183</sup>. In breast cancer Spry1 and Spry2 are repressed<sup>160</sup>, and Spry2 expression levels are frequently downregulated in hepatocellular carcinoma<sup>159</sup> as well as in non-small cell lung cancer (NSCLC)<sup>112</sup>.

Spry was discovered as antagonist of RTK-mediated signaling in *Drosophila*<sup>113</sup>. Subsequent studies demonstrate that Spry proteins are involved in regulatory pathways counteracting growth factor-induced processes in several organisms including xenopus<sup>115</sup>, chicken<sup>116, 117</sup>, zebrafish<sup>118</sup>, mouse<sup>120</sup> and humans<sup>122</sup>. Also mammalian Spry proteins function mainly as inhibitors of RTK-mediated processes, and their expression was shown to repress lung branching morphogenesis<sup>122, 135</sup>, angiogenesis<sup>106, 107</sup>, as well as cell growth<sup>109-112</sup> and migration<sup>107, 110-112</sup>. Correspondingly, the phenotypes observed in Spry knock-out mice are comparable to phenotypes observed when growth factors are overexpressed during embryonic development<sup>141, 142, 149, 150</sup>.

In agreement with the postulated feedback loop, Spry proteins are expressed mainly at sites of excessive FGF signaling during organogenesis<sup>116, 117, 134-136</sup>. Using different cell culture models several groups reported that Spry expression is induced in response to FGF2, EGF, PDGF, VEGF and HGF/SF<sup>106, 109, 111, 152, 153</sup>. In addition, loss of the GAP protein neurofibromin (NF-1) and expression of the oncogenic Raf1-CAAX caused an increase of Spry2 and Spry4 mRNA<sup>155</sup>. In accordance with these data, transgenic mice expressing the constitutive active K-Ras<sup>G12D</sup> mutant show increased expression of Spry2 in the lung epithelium<sup>156</sup>.

In this study we investigated the impact of Ras-induced signaling on Spry expression in human lung-derived cells. The presented data emphasize the influence of Ras signaling on Spry2 and Spry4 expression. The results demonstrate that mainly mitogen-activated protein kinase (MAPK) pathway activation is responsible for Spry2 induction.

## Results

### Expression of activated Ras induces Spry2 and Spry4 expressions.

As an initial experiment, we tested the influence of Ras on Spry1, 2 and 4 expressions. Serum-starved as well as logarithmically growing WI38 cells were infected with adenoviruses expressing the constitutive active mutants of all three Ras family members. Using antibodies specifically recognizing either Spry1, Spry2 or Spry4, protein levels were measured by immunoblotting. Antibody-specificity was achieved by affinity chromatography (see Figure 10).

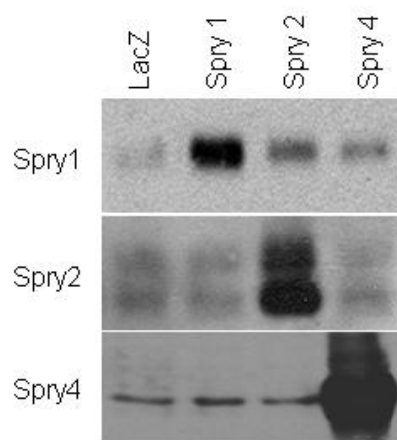


**Figure 10** *Specificity of the used Spry antibodies.*

*Logarithmically growing cells were infected using adenoviruses expressing Spry1, Spry2, Spry4 and as a control LacZ, respectively. Cells were harvested after 2 days and equal amounts of protein were separated via SDS-PAGE, transferred onto nitrocellulose membrane and immunoblot was performed using the indicated antibodies.*

In addition the dominant negative forms of the three Ras proteins and the LacZ protein as control were included. The obtained results show that logarithmically growing and serum-deprived cells expressing either dominant negative H-Ras<sup>S17N</sup>, K-Ras<sup>S17N</sup> or N-Ras<sup>S17N</sup>

reduced the expression of the Spry proteins analyzed (Figure 11). In serum starved cells, only Spry2 and Spry4, but not Spry1 protein levels were elevated by N-Ras<sup>Q61R</sup>, K-Ras<sup>G12V</sup> and H-Ras<sup>G12V</sup> expression. Concerning the extent of the induction, Spry2 and Spry4 proteins differed. While activated Ras induced Spry2 levels about 8-fold, Spry4 protein was only 2- to 3-fold elevated. These data demonstrate that all three activated Ras family members elevate Spry2 expression and to a less pronounced extent also Spry4 expression, while Spry1 expression is not activated by Ras (Figure 11).

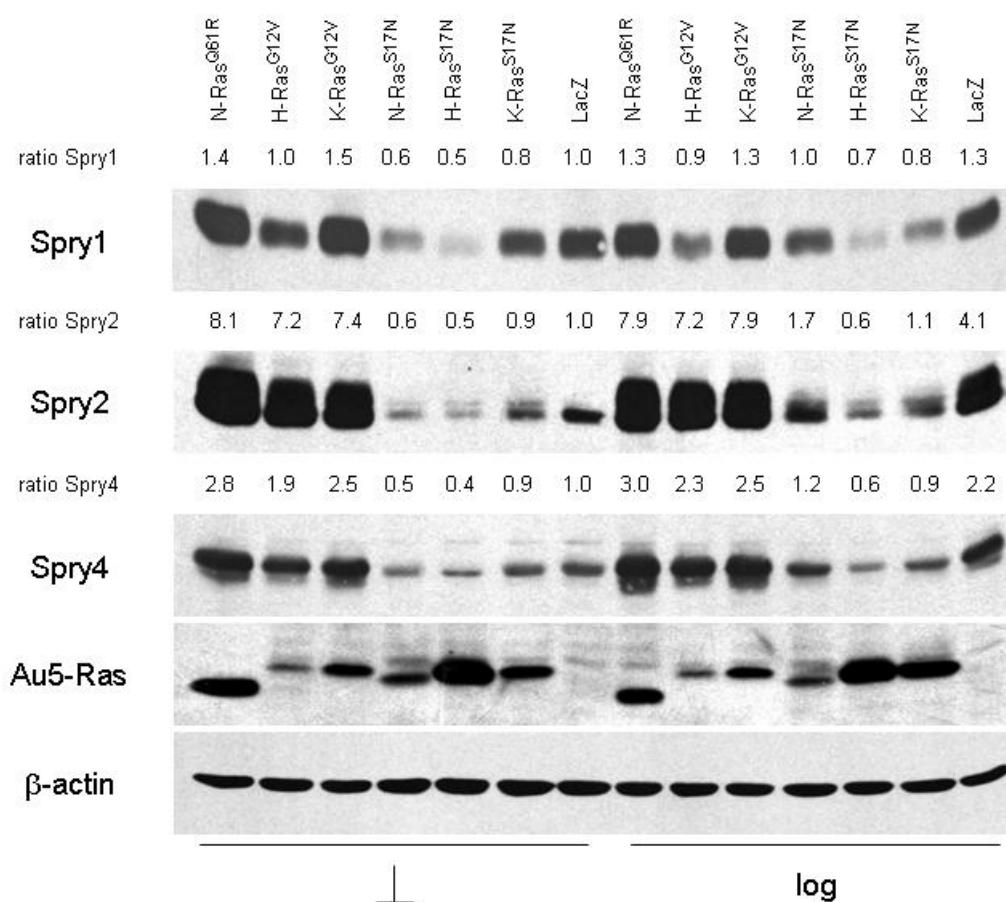


**Figure 11** Induction of Spry1, 2 and 4 expressions by oncogenic Ras.

Serum-deprived and logarithmically growing WI38 cells were infected using adenoviruses expressing different oncogenic Ras proteins. LacZ and the respective dominant-negative Ras<sup>S17N</sup> adenoviruses were included in the experiment. Cells were harvested after 3 days and equal amounts of protein were separated via SDS-PAGE, transferred onto nitrocellulose membrane and immunoblot was performed using the indicated antibodies. A representative immunoblot is shown. Protein levels were quantified by densitometry analyses and normalized to β-actin and serum-starved LacZ-infected cells. ⊥, serum-deprived; log, logarithmically growing cells.

NSCLC-derived tumors harboring dominant K-Ras mutations express higher levels of Spry2 and Spry4.

Based on these results, we analyzed if Spry protein expression correlates with constitutive active K-Ras mutations in different cell lines. Therefore Spry1, Spry2 and Spry4 expression levels were determined in 15 serum-depleted NSCLC-derived cell lines, 6 of which harbor a K-Ras mutation<sup>112</sup>. For normalization serum-arrested normal human lung fibroblasts WI38 were chosen. All of the cell lines expressed the Spry proteins but the levels differed considerably. As shown in Figure 2, Spry1 protein levels in K-Ras mutated cell lines were only marginally but not significantly elevated compared to K-Ras wt tumor cell lines (2-fold), while both, Spry2 and Spry4 levels were clearly and significantly up-regulated in the cell lines harboring activating K-Ras mutations. This difference was more pronounced in case of Spry2 (9-fold) than on Spry4 levels (6-fold). These data indicate a central role of Ras only in the regulation of Spry2 and Spry4, while Spry1 expression was again not elevated by endogenous oncogenic Ras mutations (Figure 12). Therefore Spry1 was omitted in the subsequent experiments.

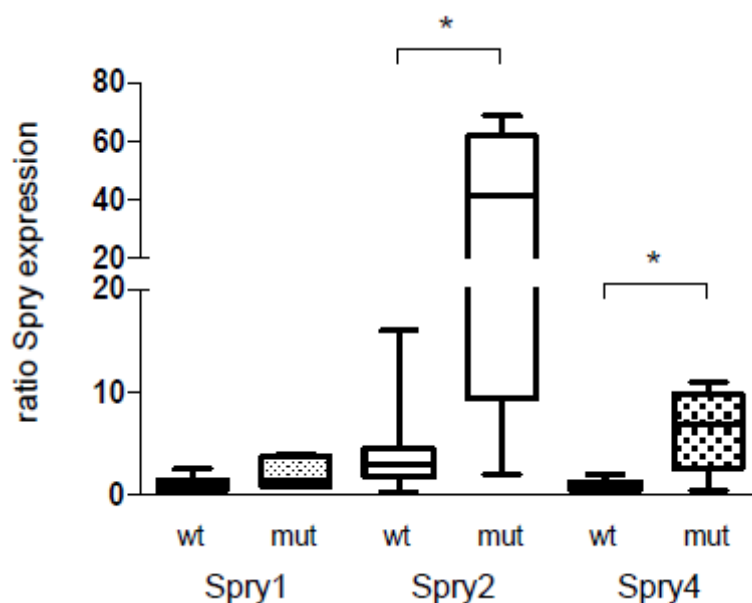


**Figure 12** Spry1, 2 and 4 expressions in NSCLC-derived tumor cell lines.

Endogenous Spry protein expression was analyzed in 15 NSCLC-derived tumor cell lines. All cells were serum-deprived for 2 days before harvesting. Equal amounts of protein were used for immunoblotting. After densitometric analysis the protein levels were normalized to  $\beta$ -actin. WI38 cells were arbitrarily set as 1. The results are presented as box and whiskers diagram and statistical analyses were performed using Mann-Whitney U test. \*  $P < 0.05$ .

### Spry2 induction in response to growth factors is K-Ras dependent.

Several reports describe a growth factor-dependent induction of Spry expression (summarized in<sup>136</sup>). To investigate if growth factor-induced Spry activation is solely dependent on Ras activation, we compared how addition of growth factors influences Spry2 and Spry4 expression in NSCLC cell lines harboring either wild-type K-Ras or a constitutive activated K-Ras<sup>G12</sup> mutation. Both tumor cell lines were serum-deprived for 48 hours before growth factors – mainly of the FGF family – were added. Induction of ERK was measured 5 minutes after addition of the indicated factors and expression analyses were performed 5 hours later. In both cell lines, Spry4 protein levels were not altered by any of the growth factors added (Figure 13A, C). Also Spry2 protein levels were not induced by addition of growth factors in A-549 cells harboring a K-Ras<sup>G12</sup> mutation indicating that serum-deprivation failed to downregulate Spry2 expression. Addition of FCS caused an obvious protein shift suggesting protein modifications such as phosphorylation by a Ras-independent mechanism (Figure 13B). Irrespectively of the K-Ras mutation in A549, ERK was still activated by FCS and EGF (Figure 13B).

In contrast, in the K-Ras wt cell line VL-3 FCS as well as EGF caused 2- to 3-fold elevation of Spry2 levels in comparison to serum-deprived cells (Figure 13C). This upregulation of Spry2 protein was accompanied by induced activity of the MAPK pathway in response to FCS and EGF as monitored by measuring phosphorylated ERK levels 5 minutes after growth factor addition (Figure 13D). All other growth factors used (FGF2, FGF5, KGF, FGF9, FGF10, FGF18, PDGF and IGF) neither activated Spry2 expression (Figure 13C) nor strongly induced the MAPK pathway (Figure 13D). On the basis of these data we conclude that growth factor-induced Spry2, in contrast to Spry4, expression is dependent on activation of K-Ras.

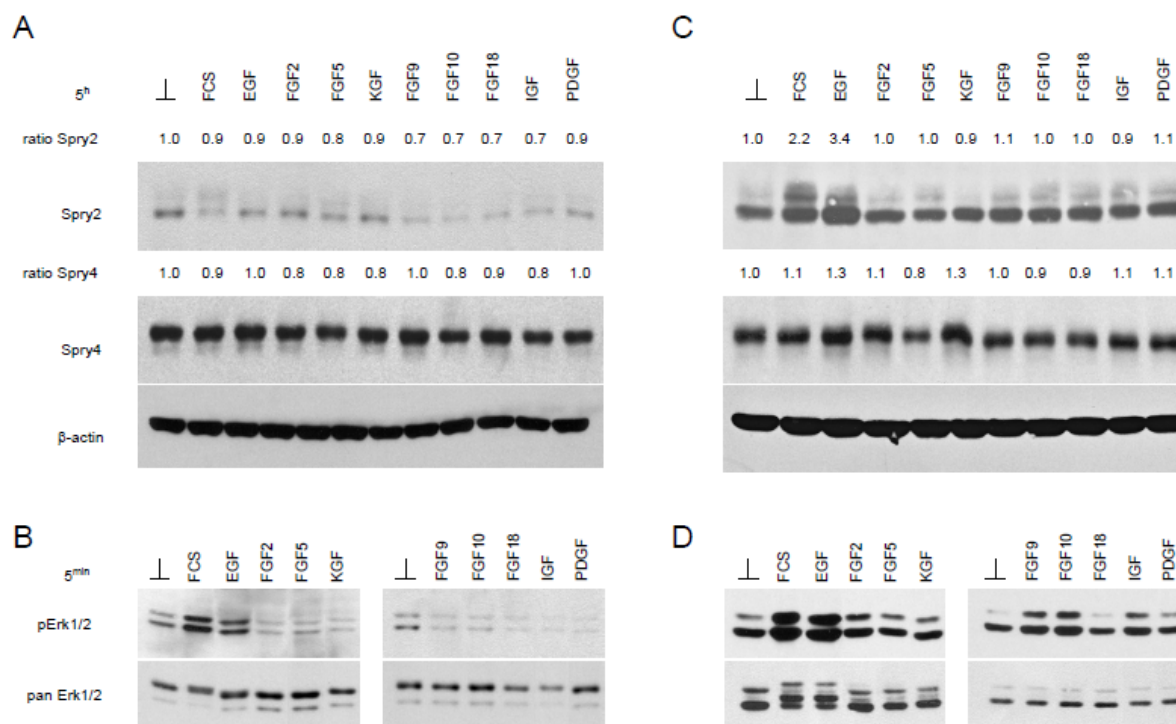


**Figure 13** *Spry2 and 4 expressions in response to growth factors in NSCLC-derived tumor cells.*

**A, B)** *K-Ras mutated A-549 and C, D)* *K-Ras wild-type VL-3 cells were serum-deprived for 2 days. Before harvesting the cells, the indicated growth factors were added for 5 minutes B, D) and 5 hours A, C). Equal amounts were analyzed by Western Blot using the indicated antibodies. The ratios of Spry expression were calculated after densitometric analysis and normalized to  $\beta$ -actin and the respective serum-deprived cells.*

Growth factor-mediated upregulation of Spry2 expression in normal human fibroblasts correlates with MAPK activation.

Next, we analyzed the influence of different growth factors on the expression of Spry2 and Spry4 in primary human fibroblasts (WI38 cells). Therefore WI38 cells were serum-deprived for 72 hours and subsequently various growth factors were added. Using immunoblot and Northern blot analyses we investigated Spry2 and Spry4 expression levels 5 hours after growth factor addition. Spry2 protein levels were induced in response to FCS, EGF, FGF2 and FGF9, whereas FGF5, KGF, FGF10, FGF18, PDGF and IGF failed to induce Spry2 expression. Spry4 protein was clearly induced after stimulation with FCS. The only growth factor which moderately increased Spry4 protein levels was EGF (Figure 14A). To explore if upregulation of Spry proteins is due to an induction of Spry mRNAs, serum-deprived WI38 cells treated with FCS, EGF, FGF2 and FGF9 were compared to untreated or IGF-treated cells using Northern blot (Figure 14B). Induction of Spry2 and Spry4 at mRNA levels

reflected the results observed at the protein levels, but to a less pronounced extent. To test the influence of the external signals on the cellular response in WI38, activation of MAPK and PI3K pathway were tested by monitoring phosphorylation of ERK and rPS6 5 minutes and 20 minutes after growth factor addition, respectively. This analysis of RTK-mediated signaling pathways revealed that the same growth factors - FCS, EGF, FGF2 and FGF9 - were able to strongly induce MAPK and PI3K pathways 5 minutes after their addition. Phosphorylation of rPS6 was additionally observed after stimulating the cells with IGF (Figure 14C), but exclusive activation of PI3K failed to induce the Spry protein expressions. These results show that Spry2 induction correlates strongly with MAPK activation, while Spry4 induction requires additional or different signals.



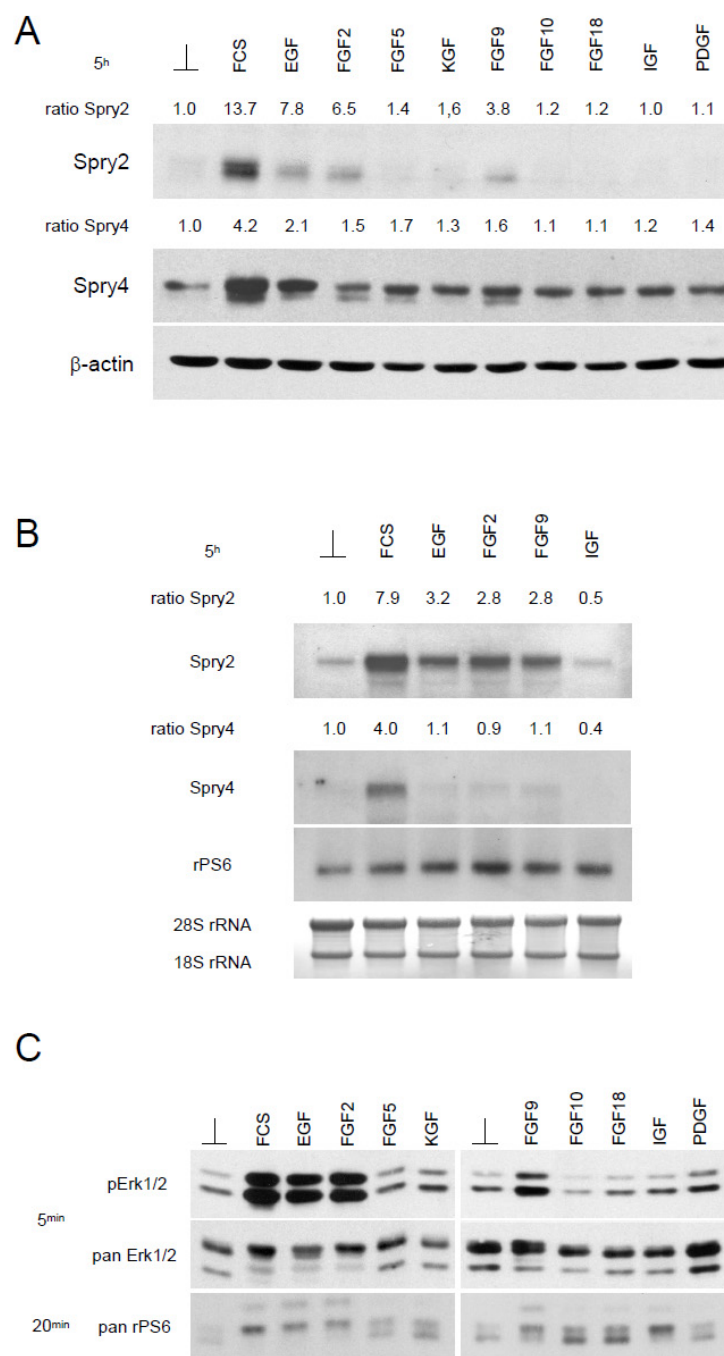


**Figure 14** Growth factor-mediated induction of Spry protein and mRNA expression in human WI38 fibroblasts.

Normal human WI38 fibroblasts were serum-deprived for 3 days before the indicated growth factors were added for **A, B**) 5 hours, **C**) (upper 2 panels) 5 minutes or **C**) (lower panel) 20 minutes. Protein-lysates were prepared for Immunoblot (a) using the indicated antibodies. mRNA was analyzed via Northern Blot (b) using <sup>32</sup>P-labeled full-length Spry2, Spry4 and rPS6 as probes. The ratios of Spry expression were calculated after densitometric analysis normalized to either **A**) β-actin or **B**) rPS6. Serum-deprived cells were set as 1, respectively.

K-Ras induces Spry2 expression via the Raf-induced pathway.

To prove that the MAPK pathway is indeed responsible for K-Ras-mediated activation of Spry2, we introduced constitutive active K-Ras versions carrying mutations in the effector loop in such ways as to exclusively bind Raf (K-Ras<sup>G12V,T35S</sup>) or PI3K (K-Ras<sup>G12V,Y40C</sup>), respectively. Starved WI38 cells were infected with viruses expressing K-Ras<sup>G12V</sup>, K-Ras<sup>G12V,T35S</sup>, or K-Ras<sup>G12V,Y40C</sup>, respectively. 48 hours post-infection the cells were harvested and analyzed concerning their effects on MAPK and PI3K pathway by measuring ERK phosphorylation and p110<sup>PI3K</sup> binding to Ras, respectively. In accordance with the literature, the K-Ras<sup>G12V</sup> activated both pathways, while K-Ras<sup>G12V,T35S</sup> failed to bind p110<sup>PI3K</sup> and K-Ras<sup>G12V,Y40C</sup> was unable to activate ERK (Figure 5A). Additionally, viruses expressing dominant negative K-Ras<sup>S17N</sup> and LacZ were included. Next, the influence of the K-Ras mutations on Spry2 and Spry4 expression was analyzed in serum-deprived (Figure 5B, left column) and logarithmically growing (Figure 5B, right column) pairs of WI38 cells. Corroborating with the induction assays shown in Figure 4, Spry2 was exclusively induced when the K-Ras variants were able to activate ERK phosphorylation, while the PI3K pathway again failed to induce Spry2 expression. Spry4 was induced by the K-Ras mutants known to activate MAPK pathway, but in addition the K-Ras K-Ras<sup>G12V,Y40C</sup> caused a moderate elevation of the Spry4 protein levels. Again Spry4 induction was less pronounced compared to Spry2.

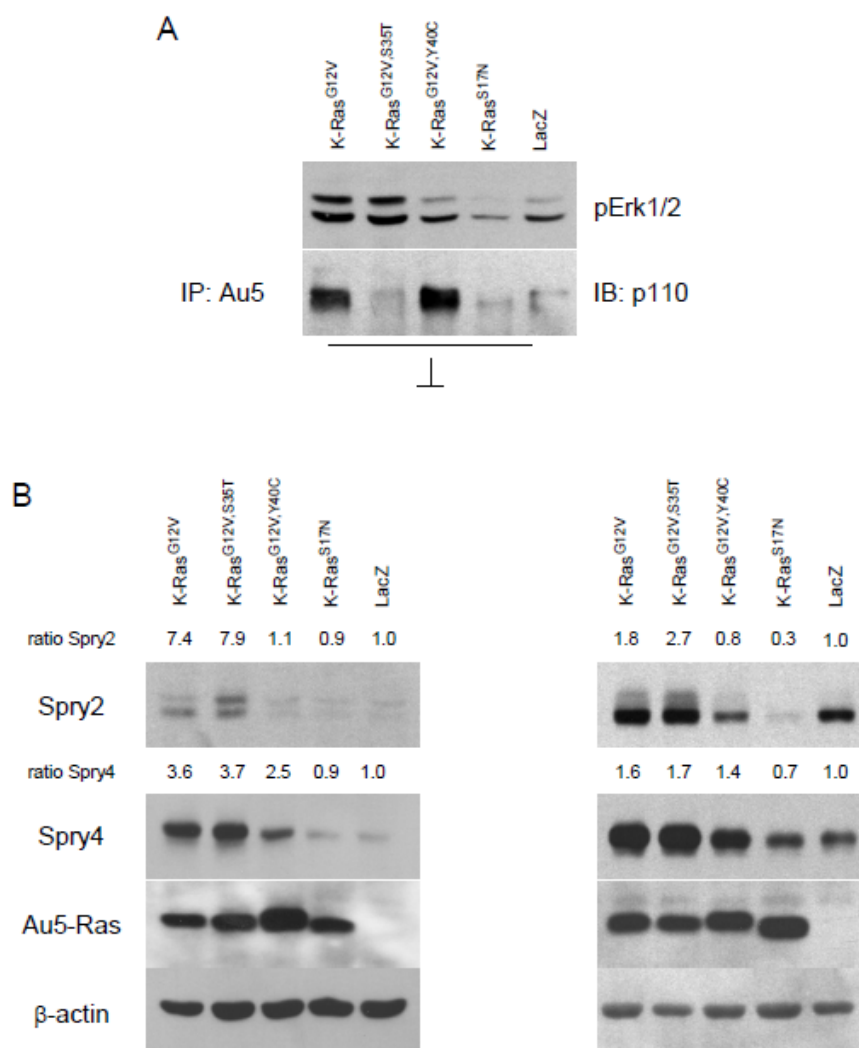


**Figure 15** The influence of K-Ras effector loop mutations on Spry2 and 4 expressions.

**A)** Serum deprived WI38 cells were infected with adenoviruses expressing the indicated Ras mutations. **A)** (upper panel) Activation of Ras/MAPK was measured via immunoblot using phospho ERK-specific antibody and **A)** (lower panel) binding of Ras to PI3K was determined via AU5 immunoprecipitation and subsequent immunoblotting using p110<sup>PI3K</sup> antibodies. In parallel, Spry2 and 4 expressions were determined in **B)** (left panel) serum-deprived and logarithmically **B)** (right panel) growing WI38 cells infected with the indicated adenoviruses via immunoblotting using specific antibodies. The ratios of Spry2 and 4 were calculated via densitometry analyses and normalized to  $\beta$ -actin and LacZ-infected cells, respectively.

## Discussion

Precise regulation of signaling is critical for the coordination of cell proliferation, differentiation and survival. To avoid inappropriate cellular responses several inhibitory mechanisms operate to constrain unwanted activating events. Such regulators are the Sprouty family members, which were shown to be intracellular inhibitors of Ras-MAPK activation. In accordance to the postulated model of a negative feedback loop, Spry proteins were mainly found expressed at sites of excessive growth factor signaling (summarized in<sup>104, 136</sup>).

In this report, we assessed Spry1, Spry2 and Spry4 expressions as a direct consequence of RTK/Ras-mediated signaling with a focus on family member-specific differences.

Our data strongly suggest that Spry1 is not under the control of Ras-mediated signaling. The Spry1 protein levels are not elevated in the presence of serum. An observation which is in accordance with former studies<sup>106, 151, 152</sup>, describing even a decrease of Spry1 mRNA levels in response to growth factor induction. Additionally, ectopic expression of all three oncogenic Ras family members (H-Ras<sup>G12V</sup>, N-Ras<sup>Q61R</sup> and K-Ras<sup>G12V</sup>) failed to induce Spry1 protein levels in logarithmically growing and in serum-deprived cells. Corroborating, Spry1 expression in NSCLC-derived cell lines carrying a K-Ras mutation was not elevated when compared to lung tumor cell lines expressing wt K-Ras. Therefore we conclude that Spry1 is mainly regulated by Ras-independent mechanisms. One such mechanism involves the transcription factor WT-1 during kidney development, as published by Gross et al<sup>151</sup>. Nonetheless we can not completely exclude that endogenous Ras may play a minor role in the regulation of Spry1 expression, since the dominant-negative Ras<sup>S17N</sup> variants reduced Spry1 levels in logarithmically and serum-starved cells. In the context of the other results we assume that dominant negative Ras variants influence Spry1 levels by other mechanisms than by directly interfering with Ras.

In contrast, Spry2 and Spry4 protein levels are clearly influenced by Ras signaling. Expressions of both proteins were induced by the ectopic expression of any of the three oncogenic Ras family members. Correspondingly, NSCLC-derived cell lines carrying a mutated K-Ras express significantly much higher Spry2 and Spry4 protein levels than cell lines derived from tumors harboring wt K-Ras. These data demonstrate that regulation of Spry2 and Spry4 expression is directly or indirectly dependent on Ras activation. In line with these data, Shaw et al. show in a recent report using mice expressing an oncogenic Ras<sup>G12D</sup> variant in fetal lungs that Spry2 and Spry4 are increased after the knock in of the Ras variant<sup>156</sup>. In their report the elevation of Spry2 and Spry4 protein was comparably high,

while we observed that the up-regulation of Spry2 as a consequence of Ras activation was more pronounced than the induction of Spry4 protein levels. We assume that the observed differences might be a consequence of the used systems. Shaw et al. generated their data in mice and it is possible that there is a slight difference between the regulation of Spry proteins in human and in mouse. Accordingly, in another report, expression of activated Raf-1 resulted in a stronger upregulation of Spry2 compared to Spry4 mRNA using human BJ fibroblasts<sup>155</sup>. Additionally, induction of Spry2 expression proved to be sensitive to a wider range of growth factor signals than Spry4. Additionally, we observed that all growth factors able to induce ERK-phosphorylation caused an elevation of Spry2 protein levels. Spry2 activation in response to growth factor was observed at mRNA level even if the extent was less pronounced. Therefore we conclude that mechanisms at the mRNA level are involved in growth factor-mediated upregulation of Spry2 expression. Furthermore, these results demonstrate that growth factor-induced Spry2 expression is dependent on the MAPK pathway. Accordingly, former studies<sup>152, 153</sup> demonstrated that growth factor (EGF, FGF2 and PDGF)-induced Spry2 expression could be diminished by inhibitors of MEK-1. Similar to their results showing that an inhibitor of PI3K pathway failed to reduce Spry2 expression, IGF was able to induce PI3K pathway already after 20 min, but did not augment Spry2 protein levels. Since in cell lines harboring activated K-Ras, Spry2 levels - irrespective of the growth factors' effect on ERK phosphorylation - are no more inducible, we conclude that growth factors activate Spry2 expression via activation of Ras. To verify our conclusions we used K-Ras mutations which specifically bind Raf to activate MAPK pathway or the p110 subunit of PI3K, respectively. These data emphasize that Ras-induced Spry2 expression is only mediated by Raf/ERK signals, whereas the PI3K effector pathway has no impact on Spry2.

In contrast to the important role of ERK activation for Spry2 regulation, its impact on Spry4 is less distinct. Like Spry2, Spry4 was induced by ectopic expression of a Ras mutant activating the RAS/Raf/ERK cascade, but Spry4 was also slightly induced by a PI3K-specific Ras mutant. A more complex regulation of Spry4 is also emphasized by the results obtained after stimulation of the cells with growth factors. Spry4 protein induction was only clearly detectable when serum was used for stimulation. Therefore we conclude that different or additional signals than ERK and PI3K activation are required for elevation of Spry4 protein. In response to growth factor addition only EGF caused a modest twofold elevation of Spry4. This is in contrast to former reports which describe an induction of Spry4 mRNA in response to EGF, FGF and PDGF<sup>152, 153</sup>. Since we also applied Northern blots, we can exclude the possibility that mRNA levels are differently regulated than protein levels. The main difference

between our study and the other two reports is that we starved the cells for 3 days to synchronize them in G0/G1 phase, while Ozaki et al. serum deprived their Swiss 3T3 cells only for 48 hours in medium containing insulin and transferrin and Sasaki et al. added the growth factors to non-serum-deprived cells<sup>152, 153</sup>. This would argue that the deepness of the arrest decides if a certain growth factor is sufficient to induce Spry4 protein, again suggesting that elevation of Spry4 requires further stimuli than the one supplied by addition of a single growth factor. A more complex regulation of Spry4 was also indicated by published data showing that Wnt signaling is able to induce Spry4 expression<sup>148, 157</sup>. Therefore we suggest that multiple signaling pathways are able to regulate the time and extent of Spry4 expression.

Summarizing, in this work we demonstrate that the mechanisms responsible for regulation of the different Spry proteins are clearly distinguishable. While the impact of Ras-dependent signaling on Spry2 and Spry4 expressions are clearly obvious and significant, additional factors are involved in regulating Spry4 expression. Downstream of Ras, induction of Spry2 is exclusively mediated by MAPK pathway. In contrast, Spry1 expression is mainly controlled by non-Ras-influenced mechanisms.

## Materials and Methods

### *Patient Material and Cell Lines*

10/15 analyzed NSCLC cell lines were established at our institute: Surgical specimen from one histological confirmed AC (VL-1), 7 SSC (VL-3 and VL-5 - VL-10) and 2 LCC (VL-2 and VL-4) were used at passage numbers between 15 and 30. 6/10 cell lines (VL-1 to VL-4, VL-9 and VL-10) were derived from primary tumors and 4 (VL5 –VL8) from lymph node metastases. Additionally, 5 of the adenocarcinoma cell lines (A-427, A-549, Calu-3, Calu-6 and SK-LU-1) and the normal embryonic lung fibroblasts (WI38 at passage 16) were purchased from ATCC (Rockville, MD). 6/15 cell lines harbor a mutated K-Ras (VL-2, VL-4, A-427, A-549, Calu6, SK-LU-1). For a detailed description of the mutation analyses see<sup>112</sup>.

### *Antibodies*

The antisera against hSpry1, hSpry2 and hSpry4 were produced as described<sup>112</sup>. hSpry4 was raised against glutathione S-transferase–tagged NH2-terminal 220 amino acids of human Spry4. To avoid cross-reactivity, antibodies against the other Sprys were depleted by cycling

each of the 3 crude antisera over columns containing GST and the other Spry proteins, respectively, followed by affinity purification. Antibodies against pERK1/2, S6, p110PI3K were purchased from Cell Signaling (MA 01923, USA); total ERK1/2 (Acris Antibodies, 32120 Hiddenhausen, Germany),  $\beta$ -actin (Novus Biologicals, CO 80160, USA), AU5 (Bethyl Laboratories TX 77356, USA).

### *Immunoblotting*

Protein isolation and Immunoblotting were performed as described in <sup>190</sup>. For protein lysis TGH buffer (50mM Hepes pH7.6, 150mM NaCl, 1.5mM MgCl<sub>2</sub>, 5mM NaF, 1mM EGTA, 1% TritonX-100, 10% glycerol) was used. Western blot signals were quantified using Image Quant software (Molecular Dynamics).

### *Recombinant Adenovirus Generation and Cell Infection*

Using the AU5-tagged constructs kindly provided by Dr. Rojas (Instituto de Salud Carlos III, Madrid, Spain) we amplified the coding sequences of human H-, K- and N-Ras wt and K-Ras<sup>G12V</sup> using the following primers: at the 5 prime end for all Ras forms the primer 5-ATGCGGATCCATGACCGACTTCTACCTAAAGAGATCT-3 against the AU5 tag and at the 3 prime end 5-ATGCGAATTCTCAGGAGAGCACACACTT-3 for H-Ras, 5-ATGCGT CGACTTACATAATTACACACTTTGT-3 for K-Ras4b and 5-ATGCGAATTCTACATCAC CACACATGGCAA-3 for N-Ras were used and cloned into the pADlox vector, respectively. All mutations were introduced by PCR site-directed mutagenesis using the primers 5-GTGGG CGCAGTAGGTGTGGGCAAGAGTGCG-3 and 5-CCCACACCTACTGCGCCACCACC ACCAG-3 for H-Ras<sup>G12V</sup>, 5-GATACAGTC GGACGAGAAGAGTACAGTGCC-3 and 5-AC TGTACTCTTCTCGTCCAGCTGTATCGAC-3 for N-Ras<sup>Q61R</sup>, 5-AAGAACGCGTTGACGA TACAGCTAATT-3 and 5-CAACGCGTTCTTGCCCTACG CCACCAGC-3 for K-Ras<sup>S17N</sup>, 5-AAGAACGCGTTGACCATCCAGCTGATC-3 and 5- CAACGCGTTCTTGCCACACCCG CCGGC-3 for H-Ras<sup>S17N</sup>, 5-AAAAACGCGTTGACAATCCAGCTAATC-3 and 5-CAACGC GTTTTTCCCAACACCACCTGC-3 for N-Ras<sup>S17N</sup>, 5-CTCTATGCTAGGATCATATTCGT C-3 and 5-TCGACGAATATGATCCTAGCATAGAGGATTCCTACAGG-3 for K-Ras<sup>S35T</sup> and 5-CTTCCTGCAGGAATCCTCTATGGTTGGATC-3 and 5-CCTGCAGGAAGCAAGT AGTAATTGAT-3 for K-Ras<sup>Y40C</sup>. All constructs were verified by restriction digestion and sequencing.

Recombinant viruses were produced as described<sup>190</sup> by cotransfection of adenoviral DNA and the respective pADlox plasmids. If not indicated otherwise, adenoviruses were generally used at a multiplicity of infection of 50.

#### *Growth factors*

All growth factors used were applied in a final concentration of 10ng/ml. FGF-2, FGF-5, KGF, FGF10, FGF18 and IGF-1 were purchased from Strathmann Biotec AG (22459 Hamburg, Germany), EGF from Sigma (MO 63103, USA), FGF9 from R&D Systems (MN 55413, USA) and PDGF-AA was purchased from Chemicon International (CA 92590, USA).

#### *RNA Extraction and Northern Blotting*

RNA preparation and Northern blotting procedures followed published methods<sup>191</sup>. For radioactive labeling the Rediprime Random Prime Labelling Kit (GE Healthcare, 75184 Uppsala, Sweden) was used. As probes we used the coding sequence of hSpry2, hSpry4 and ribosomal protein S6 (rPS6).

#### *Immunoprecipitation*

Immunoprecipitation was performed as described in<sup>190</sup>.

### **Acknowledgements**

We are thankful to Ilse Fröhlich for skilful technical assistance as well as Christine Pirker for proofreading the manuscript. Michael Micksche we thank for his general support. This study was supported by Herzfelder'sche Familienstiftung, Fonds der Stadt Wien für Innovative Interdisziplinäre Krebsforschung, project number K-7/07 and the Medizinisch-wissenschaftlicher Fonds des Bürgermeisters der Bundeshauptstadt Wien grant 2483.



## 5.3 Unpublished data

### 5.3.1 Cell cycle-specific regulation of Spry proteins

#### Spry expression during cell cycle in WI38 cells

Our further studies focused on the exact temporal expression profiles of Spry proteins during cell cycle progression of normal embryonic WI38 fibroblasts on mRNA and protein levels. Therefore, the cells were arrested in G0 by serum deprivation for 3 days in serum-free DMEM medium. Cell cycle block release was accomplished in medium containing 20% serum. At different time points after induction, cells were harvested and analyzed by flow cytometry, Northern- and Immunoblot. In parallel, logarithmically growing cells were investigated.

According to the obtained results, selective time points were chosen to investigate Spry mRNA and protein levels during G0 (0 hours), early induction in G1 (4<sup>h</sup>), shortly before G1/S phase transition (22<sup>h</sup>), late S phase (28<sup>h</sup>) and S/G2-M transition (32<sup>h</sup>). At 42<sup>h</sup>, cell cycle in WI38 was already completed and re-entered G1 phase. Cell cycle progression was controlled via flow cytometry analysis (Figure 16a) and protein staining of cell cycle-specific CyclinD1 (induced during G1 phase), CyclinA (highest during S/ G2 phase) and B (highest during G2-M phase), respectively via immunoblot (Figure 16b). Our data demonstrated that hSpry1 was highest in G0 cells and strongly downregulated after serum induction on mRNA and protein levels throughout the cell cycle (Figure 16b, c). Linear regression analysis revealed that mRNA and protein Spry1 are co-regulated significantly ( $P < 0.01$ ). Spry2 mRNA and protein levels were downregulated during G0/G1 cell cycle arrest compared to logarithmically growing cells. Spry2 expression peaked in early G1 (measured 4<sup>h</sup> after induction) of the cell cycle, but was again repressed at the G1/S transition at 22<sup>h</sup> after serum induction. This downregulation was followed by a constant slope of the protein levels in S and G2 phase. After mitosis when cells proceed in the next G1 phase Spry2 was re-expressed. Linear regression analysis ( $P < 0.05$ ) showed that Spry2 mRNA and protein levels are co-expressed during cell cycle, whereas the extent of induction (normalized to serum-arrested G0/G1 cells) was more pronounced on protein than on mRNA levels (Figure 16b, c). At last, Spry4 mRNA and protein expression were both induced by serum addition early in G1. While Spry4 protein levels were still increased until G1/S transition and then maintained at a nearly constant plateau level, mRNA was found downregulated afterwards throughout the cell cycle. Therefore we conclude that all Spry members analyzed differed clearly in their expression patterns on mRNA and protein levels depending on the cell cycle stage. In the case of Spry1

and 2, mRNA levels represented very well the amount of protein expression suggesting that their expression is mainly regulated on the level of transcription. Spry4 mRNA and protein levels on the other hand were not co-regulated, with constant high protein levels through late G1, S and G2-M phase (Figure 16b, c), suggesting that the amount of Spry4 protein in the cells is mainly influenced by translation and/or post-translational stabilization.

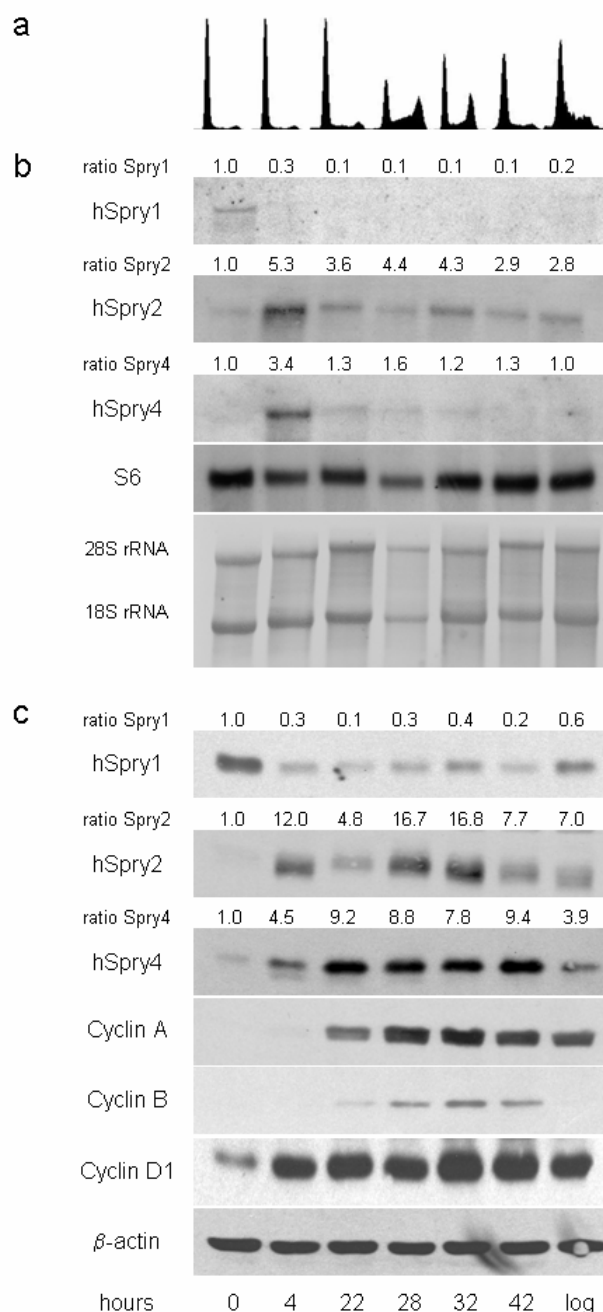


**Figure 16** *Spry expression during cell cycle.*

*WI38 cells were harvested at the indicated time points after serum addition to G0 cell cycle-arrested cells. (a) WI38 cells were lysed and stained using propidium iodide, followed by flow cytometry analysis to determine cell cycle distribution of WI38. (b) Northern blot was used to*

determine *Spry* mRNA levels.  $^{32}\text{P}$ -labeling was performed using full-length *hSpry1*, *hSpry2*, *hSpry4* and *rpS6* (housekeeping gene) cDNAs as probes, respectively. The methylene blue stain after capillary transfer was added as further loading control. Ratio of *Spry* expression levels were calculated normalized to *rpS6* and starved cells were set arbitrarily as 1, respectively. (c) Immunoblot was used to determine *Spry* protein levels during specific phases of the cell cycle. Equal amounts were separated by PAGE, blotted onto nitrocellulose membrane and probed using the indicated antibodies. The ratio *Spry* expression levels were calculated normalized to  $\beta$ -actin and starved cells were set arbitrarily as 1, respectively.

#### Spry expression between G0 and G1/S transition

Next, we investigated the period between early G1 (4<sup>h</sup>) and G1/S transition (around 22<sup>h</sup> after serum addition). WI38 cells were serum-deprived and induced as described before, but harvested at several time points between G0 and S-phase and analyzed by immunoblot. Flow cytometry analysis was used to verify G1/G0 arrest in serum-deprived cells, and cell cycle release after serum addition for 24<sup>h</sup> (Figure 17a).

In accordance with the data described before in Figure 16, *Spry1* was shortly downregulated after serum induction and remained low during the remaining G1 phase. *Spry4* expression peaked after 6<sup>h</sup> and was maintained at the same high level between 6<sup>h</sup>-24<sup>h</sup>. Accordingly, we could also show that *Spry2* truly exhibits a biphasic expression pattern during G1 phase. In corroboration with our initial results, at the G0/G1 transition *Spry2* protein levels increase constantly until 8<sup>h</sup> after induction, then the protein expression is downregulated when entering S phase (Figure 17b).

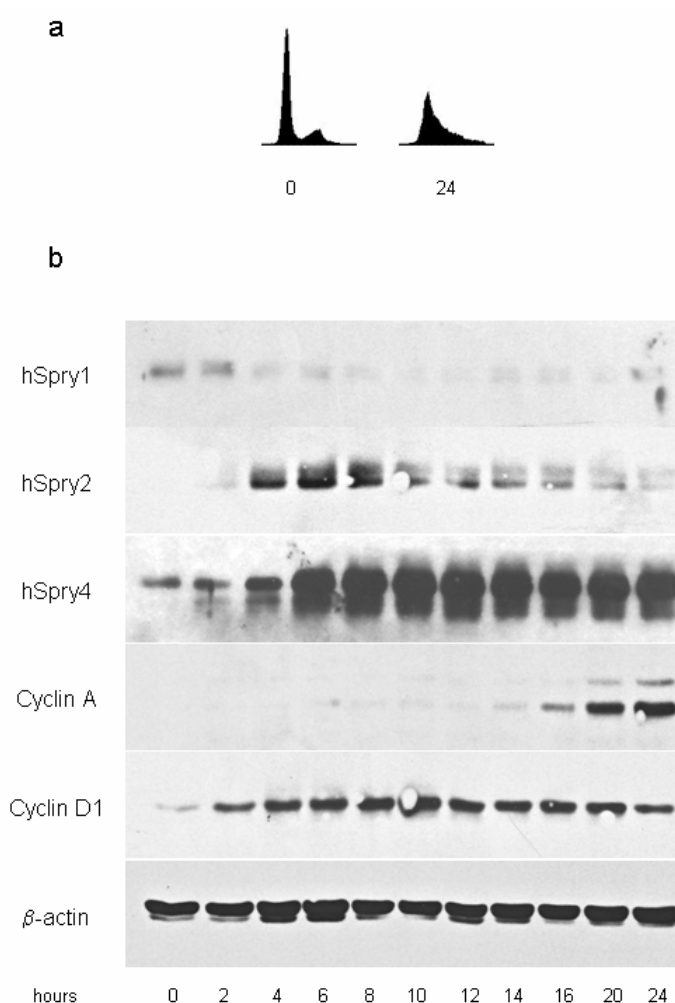


**Figure 17** *Spry protein expression between G0 and S phase.*

*WI38 cells were harvested at the indicated time points after serum addition to G0 cell cycle-arrested cells and processed for flow cytometry (a) and Immunoblot (b), respectively. (a) Flow cytometry analysis after propidium iodide staining was used to check the serum arrest at 0<sup>h</sup> and that cells had entered S phase at the 24<sup>h</sup> time point. (b) Cells were harvested at the indicated time points. Total protein was isolated, separated by PAGE and blotted onto nitrocellulose membrane. Spry-specific antibodies were used to detect Spry1, 2 and 4 protein levels, respectively. CyclinD1 and CyclinA were used, next to flow cytometry, to control proper cell cycle progression and β-actin was used as loading control.*

### Regulation of Spry cell cycle expression by cCbl

Fine tuning of signal duration and intensity is important for the cellular response to extracellular signals. Therefore, we next elucidated the role of the well described Spry-interacting protein c-Cbl on the expression of Spry proteins. Whereas under normal conditions, c-Cbl fulfills its evolutionary conserved role as a negative regulator of signal transduction via a mechanism involving polyubiquitination and degradation of protein

tyrosine kinases, dominant-negative mutations in cCbl's linker region lead to malignant transformation *in vitro*<sup>192</sup>. Since Spry levels differed markedly during cell cycle progression we investigated the role of cCbl in regulating these specific Spry expression patterns in WI38 cells.

Cells were arrested in G0 as described before and infected using wt (wt) and dominant negative  $\Delta 70Z$  ( $\Delta$ ) cCbl-expressing adenoviruses, as well as LacZ (Z) control virus on the day of serum deprivation. In preliminary tests, it was assured that the used adenovirus titers had no negative impact on cell cycle characteristics and flow cytometry analyses were added in each experiment to check proper cell cycle progression. Again the cells were released out of the cell cycle block in medium containing 20% serum. At different time points after the induction, cells were harvested and analyzed by flow cytometry (Figure 18a) and immunoblot (Figure 18b), respectively.

Cell cycle-specific Spry protein levels in cells overexpressing LacZ control virus was in accordance to the protein patterns described before (Figure 16, 17). Our data revealed that cCbl wt and  $\Delta 70Z$  protein increased Spry1 expression throughout the cell cycle (Figure 18b). A possible explanation is the ectopic expression of active and dominant-negative cCbl protein influence other, unknown regulators of Spry1 leading to higher expression levels. Spry4 protein was also induced by both cCbl forms in serum-deprived cells. During later G1 stages overexpression of either cCbl wt or cCbl  $\Delta 70Z$  protein, respectively had no effect Spry4 protein (Figure 18b). In the case of Spry2, ectopic expression of cCbl wt further reduced Spry2 protein, whereas dominant negative cCbl  $\Delta 70Z$  protein markedly increased Spry2 expression (Figure 18b). Therefore, our data clearly indicate that cCbl proteins are involved in repressing Spry2 expression before G1/S transition, whereas having a different and/ or opposing effect on Spry1 and Spry4.

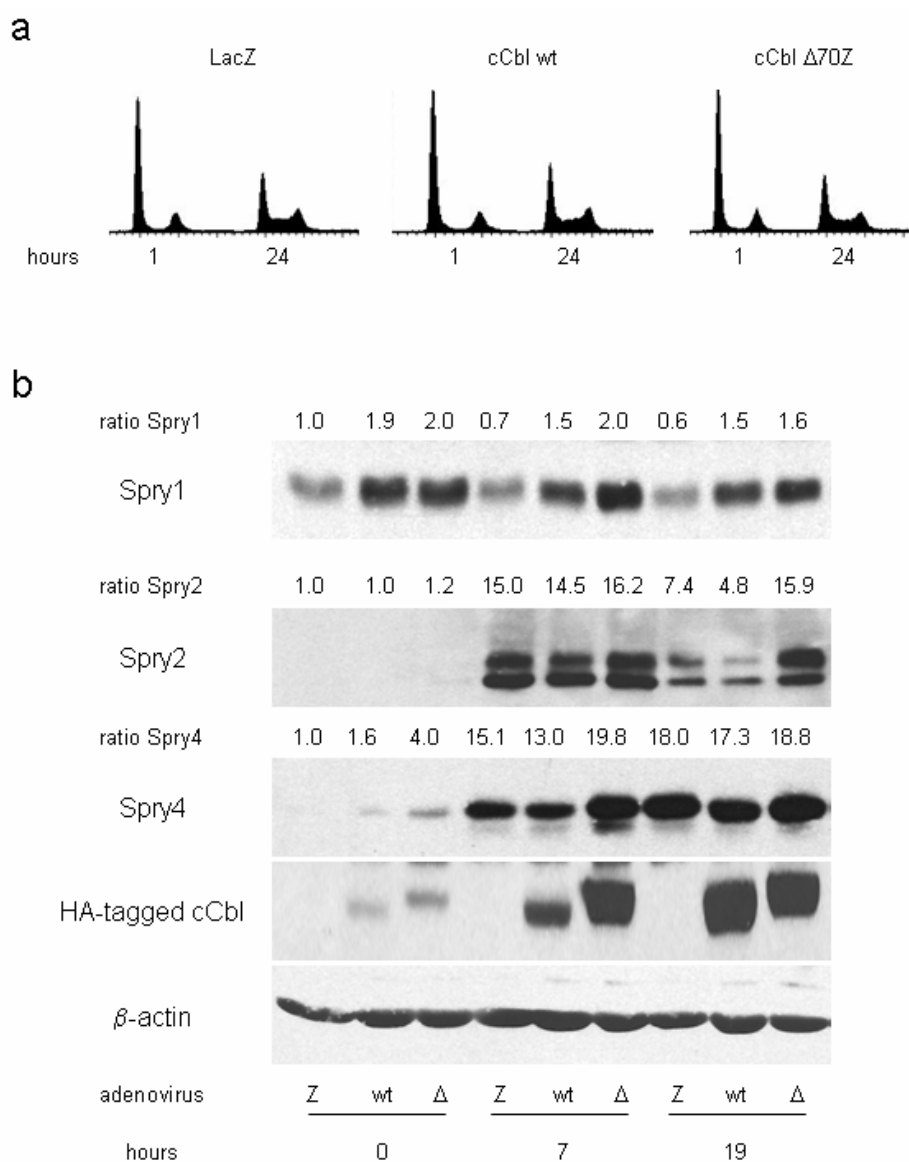


**Figure 18** Influence of *cCbl* on *Spry* cell cycle

(a) Flow cytometry analysis of cells harvested after 1<sup>h</sup> and 24<sup>h</sup> of induction. (b) Cells were harvested at the indicated time points. Total protein was isolated, separated by PAGE and blotted onto nitrocellulose membrane. *Spry*-specific antibodies were used to detect *Spry*1, 2 and 4 protein levels, respectively.  $\beta$ -actin was used as loading control. wt, *cCbl* wt.  $\Delta$ , dominant negative *cCbl*  $\Delta$ 70Z. Z, *LacZ* control virus.

### 5.3.2 Construction of a human lung cDNA library

To identify novel interaction partners of *Spry*2, a human lung cDNA library was synthesized in order to be used in Yeast-two hybrid screening assays.

1mg of total RNA was isolated from diverse logarithmically growing WI38 and NSCLC-derived fibroblasts and cells enriched in distinct phases of the cell cycle (G0, G1, S, or G2/M

phase). The accuracy was checked via gel electrophoresis and the amount measured via  $\eta$ -drop measurement.

poly(A)<sup>+</sup> mRNA was captured via biotinylated-oligo(dT) probes and streptavidin paramagnetic particles (SA-PMPs) and eluted by ddH<sub>2</sub>O to recover 6.4 $\mu$ g poly(A)<sup>+</sup> mRNA. The sample was restricted to final volume of 52 $\mu$ l (123ng/ $\mu$ l) using SpeedVac centrifugation at 30°C. 1<sup>st</sup> strand PCR synthesis was performed using oligo(dT) linker-primer followed by 2<sup>nd</sup> strand PCR reaction. After restriction digestion, the proceeded cDNA was size fractionated via size-exclusion chromatography (Figure 19).

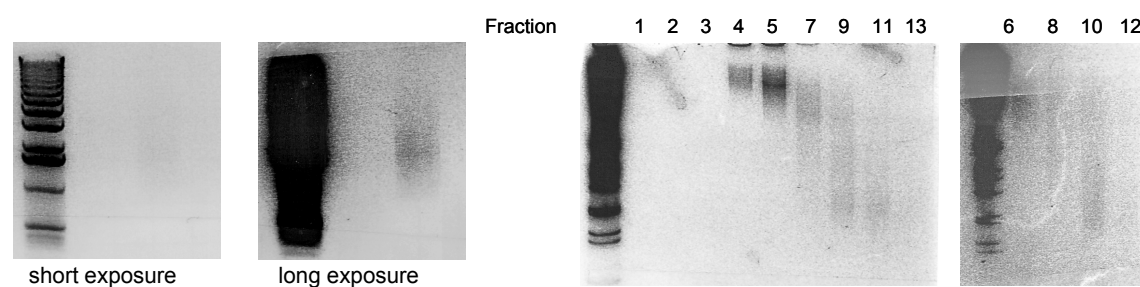


**Figure 19** *cDNA size fractionation.*

*Bulk cDNA separated by agarose gel electrophoresis (between 1.5-2.0kpbs) (left panels) and size fractionated cDNAs separated by PAGE (right panels).*

The cDNA fractions 4-6 and 7-12 were combined and extracted via phenol/chloroform. Afterwards the two samples were ligated into the phagemid vector HybriZAP-2.1 vector and packaged (Gigapack III Gold Packaging Extract - Stratagene #200201, Gigapack III Plus Packaging Extract - Stratagene #200205) generating a “long” (L) and “short” (S) primary phagemid cDNA library, respectively. Both were titrated to determine the plaque forming units (pfu)/ml (Figure 20).

titer primary phagemid library: L ( $1.7 \times 10^6$  pfu/ml), S ( $9.9 \times 10^5$  pfu/ml)

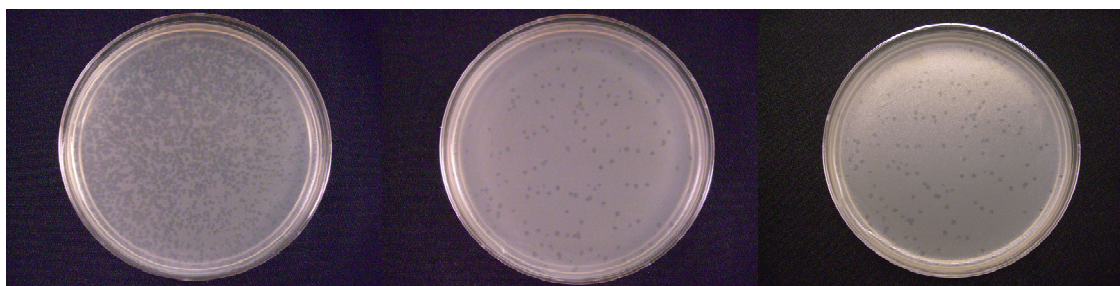


**Figure 20** *Plaque-Assay used to titer the phagemid library.*

Further, PCR reaction was used to determine the percentage and cDNA insert sizes of both primary libraries, respectively. The insert sizes of the primary library L varied between 500-2000bps, with an insert percentage of 100% (Note: sample 9, 10, 15, 17, 18 - PCR did not work). The insert sizes of the primary library S varied between 300-1000bps, with an insert percentage of about 50% (Figure 21).

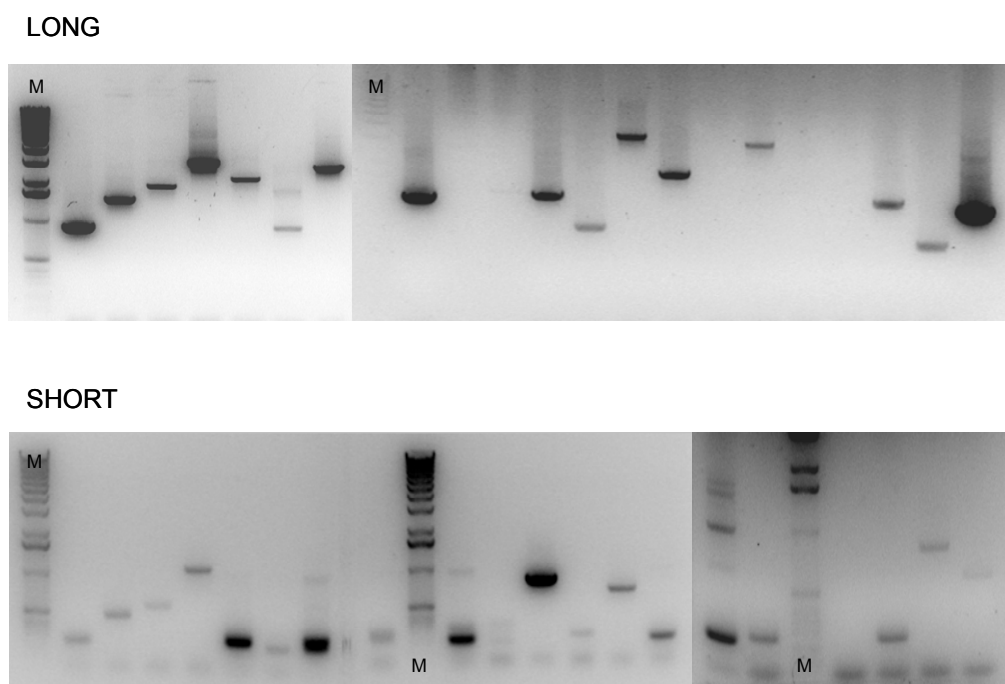


**Figure 21** PCR verification of percentage and insert size.

PCR products which are >237 bps in length represent the HybriZAP-2.1 vector with an cDNA insert, PCR products which are 237 bps in length represent empty HybriZAP-2.1 vector. M marker.

Both, primary libraries were amplified in XL-1 Blue MRF<sup>+</sup> to multiple L and S bacteriophage-derived secondary libraries. Each time the pfu/ml was determined

titer secondary phagemid library: L-a  $5.0 \times 10^9$  pfu/ml, L-b  $2.4 \times 10^{11}$  pfu/ml, L-c  $2.3 \times 10^{10}$  pfu/ml, L-d  $1.3 \times 10^{10}$  pfu/ml

S-a  $2.0 \times 10^8$  pfu/ml, S-b  $1.3 \times 10^{10}$  pfu/ml, S-c  $6.2 \times 10^9$  pfu/ml

Next, both 2<sup>nd</sup> phagemid libraries were amplified in XL-1 Blue MRF<sup>+</sup> cells and subsequently mass excised to pAD-GAL4-2.1 phagemid libraries, respectively, using an ExAssist Helper



Phage. The excised phagemids were titrated (colony forming units (cfu)/ml) and the percentage and cDNA insert sizes determined via PCR. The insert sizes in library L varied between 0.5-4.0 kbps and in S between 0.25-1.5 kpbs. The percentage of inserted cDNA fragments was in both pAD-GAL4-2.1 phagemid libraries close to 100% (Figure 22).

titer pAD-GAL4-2.1 phagemid library: L-a  $2.6 \times 10^8$  cfu/ml, S-a  $7.4 \times 10^7$  cfu/ml

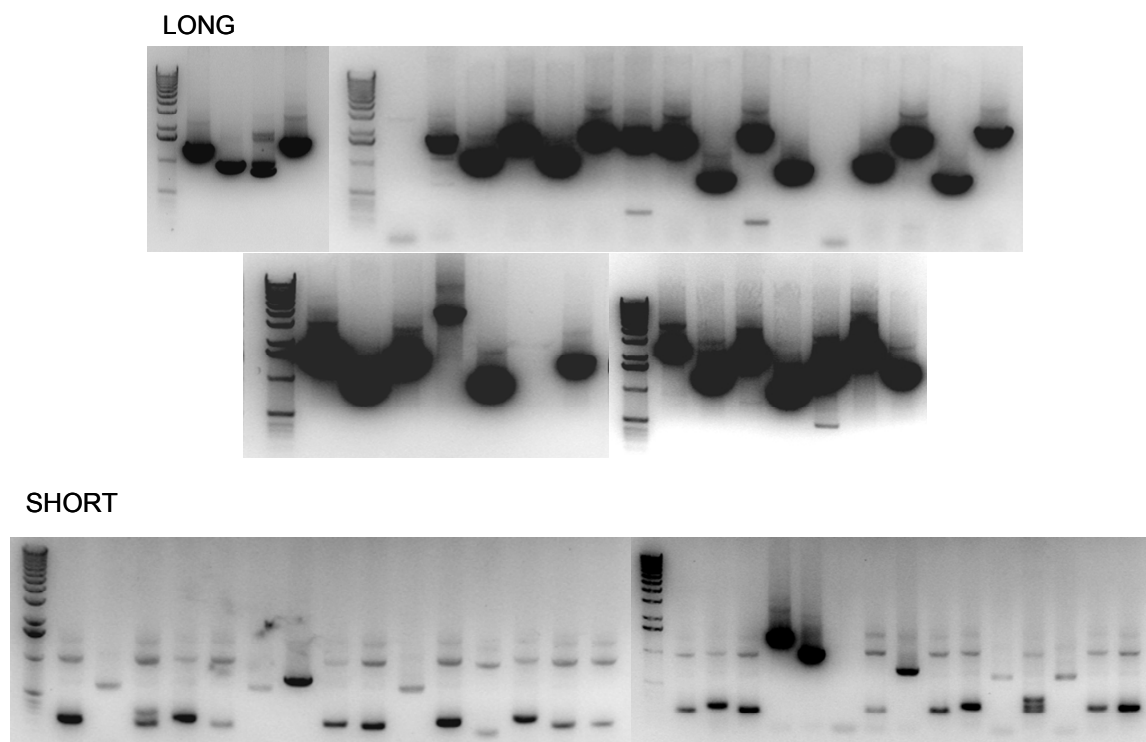


**Figure 22** PCR verification of percentage and insert size after mass excision. PCR products which are >237 bps in length represent the HybriZAP-2.1 vector with insert, PCR product which are 237 bps in length represent empty HybriZAP-2.1 vector.

Finally, L and S pAD-GAL4-2.1 phagemid libraries were amplified in XLOLR cells and isolated via MAXI Prep (Figure 23), respectively, to be used in a Yeast-two Hybrid Screen.

purified pAD-GAL4-2.1-cDNA vectors: L-a 1: 450ng/ $\mu$ l (200 $\mu$ l), L-a 2: 640ng/ $\mu$ l (180 $\mu$ l),  
L-a 3: 1.4 $\mu$ g/ $\mu$ l (200 $\mu$ l), L-a 4: 820ng/ $\mu$ l (250 $\mu$ l),  
L-a 5: 540ng/ $\mu$ l (250 $\mu$ l), L-a 6: 1.3 $\mu$ g/ $\mu$ l (250 $\mu$ l)  
  
S-a 1: 830ng/ $\mu$ l (200 $\mu$ l), S-a 2: 1.3 $\mu$ g/ $\mu$ l (250 $\mu$ l),  
S-a 3: 880ng/ $\mu$ l (250 $\mu$ l)

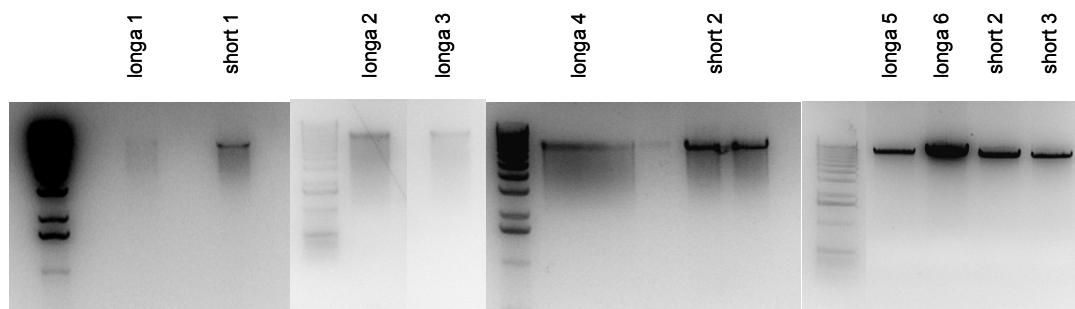


**Figure 23** MAXIPreps cDNA library.

*L-a 1-6 and S-a 1-3 after EcoRI digestion. Note the length of the pAD-GAL4-2.1-cDNA plasmids were 9-10kpbs.*

### 5.3.3 pBD-Gal4-hSpry2 bait LacZ screen

hSpry2 coding sequence was amplified by PCR using specific primers (5-AGTCGAATTCATGGAGGCCAGAGCTCAGAG-3 and 5-AGTCGTCGACCTATGTTGGTTTTTCAAAGT-3), cloned into the pBD-Gal4 bait vector and isolation of a positive clone was verified by sequencing. Then, pBD-Gal4- hSpry2 was transformed into YRG-2 yeast, plated on a SD-1 (-Trp) plate and incubated for 3-4 days in a 30°C incubator.

Using the LacZ assay, it was determined that Spry2 bait protein was not showing any auto-activity (by forming blue colonies) and therefore is suitable to successfully screen for interacting proteins in a yeast-two hybrid screen (Figure 24).

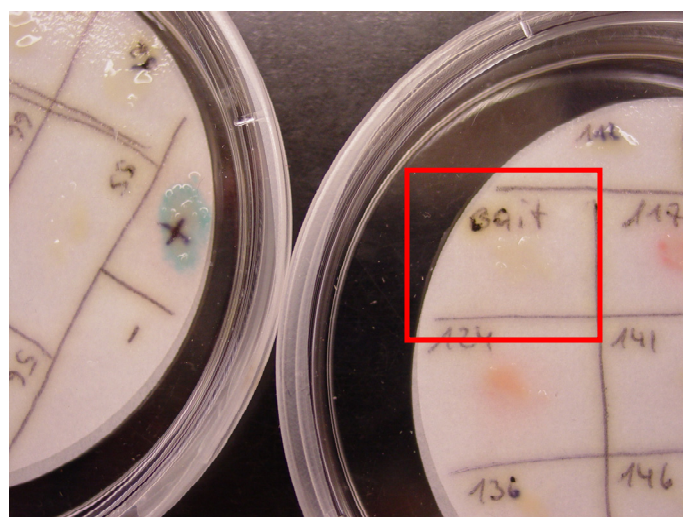


**Figure 24** Spry2 LacZ assay.

*LacZ assay of Spry2 bait (red square) after 5.5 hours in comparison to the positive (+) and negative (-) controls.*

## 6 Summary and Discussion

In the industrial world, cancer is the second highest cause of death after cardiovascular diseases. Although neoplastic transformation can be regarded as a disease of aging (the incidences increase with age) the pathogenic basis for developing tumours lies earlier in life<sup>193</sup> and theoretically any normal cell can become a cancer cell. Carcinogenesis is mediated via a multistep process accumulating genetic alterations for selective advantage<sup>194, 195</sup>. Even if cancer cells are very divergent concerning cell morphology and genetic instability, transformation of a normal to a tumor cell is characterized by a few characteristic features, such as enhanced mobility (migration and metastasis), autonomous growth and proliferation, and decreased cell immortality. Under non-malignant conditions, all these characteristics are tightly regulated by signal transduction pathways which convert extracellular signals into specific cellular responses<sup>14</sup>. Such signal-promoting cascades have to be tightly regulated to limit the negative consequences of aberrant activation, such as malformations during development and tumor formation during adult life. Thereby, negative feedback loops functioning to attenuate and terminate signaling processes play a central role. One of these negative feedback loops includes the members of the Spry protein family<sup>113, 130, 139, 140</sup>. Spry was first discovered in a *Drosophila* genetic screen as a novel antagonist of FGF-induced tracheal branching<sup>113</sup>. Homologues of Spry were found in *Xenopus laevis*<sup>115</sup>, chicken<sup>116, 117</sup>, zebrafish<sup>118</sup>, rat<sup>119</sup>, mouse<sup>116, 120, 121</sup> and humans<sup>113, 122</sup> based on sequence similarities. During organogenesis, Spry proteins are mainly expressed at sites of excessive FGF signaling organogenesis<sup>116, 117, 134-136</sup>. Further, induction of Spry expression, as well as Spry function was shown to be mediated by diverse growth factor stimuli, such as FGF2, EGF, PDGF, VEGF and HGF/SF<sup>106, 109, 111, 152, 153</sup>. Upon activation Spry proteins are localized to the plasma membrane and function mainly as inhibitors of RTK/Ras/MAPK-mediated processes to inhibit branching processes during embryogenesis, cell proliferation as well as cell growth and migration<sup>105</sup>. Correspondingly, the phenotypes observed in Spry knock-out mice are comparable to phenotypes observed when growth factors are overexpressed during embryonic development<sup>141, 142, 149, 150</sup>. Only in response to EGF signaling in mammals, ectopically expressed Spry sustained MAPK induction<sup>106, 126, 128, 166, 170-172</sup>. In this specific case, activated Spry was targeted and degraded by the ubiquitin E3 ligase cCbl instead of phosphorylated EGFR leading to prolonged EGFR-mediated signaling<sup>128, 175</sup>.

In human cancers, one of the systems almost generally found deregulated is the RTK/Ras/MAPK pathway. Consequently, multiple studies described tumor promoting

alterations in proteins functioning within this cascade, such as hyper-activated RTKs, or mutated Ras and bRaf<sup>189, 196, 197-201</sup>. Additionally, negative regulators, such as PTEN and c-Cbl, which guarantee multicellular surveillance, possess a high tumour suppressing potency<sup>22, 202, 203</sup> and are often found deregulated or lost in cancer. In this context, the aim of the study was to clarify the role of Spry proteins as negative regulators of RTK-mediated signaling.

In this study we report that expression of Spry2 is consistently downregulated on mRNA and protein levels in NSCLC compared to the respective normal adjacent epithelium. According to previous studies in rodents<sup>135, 204</sup>, Spry2 was primarily expressed in normal bronchial epithelium. Lowered levels of Spry2 protein, as found in NSCLC tumor specimens, are likely to cause a selective growth advantage of tumor cells. In contrast to Spry2, Spry1 even tended to be elevated in some tumor samples. The same situation was found in HCC<sup>159, 184</sup>, where Spry2 but not Spry1 was identified to be downregulated. In the prior report, Spry2 was downregulated in 9 of 11 (82%) specimens, whereas Spry1 was upregulated in 8/11 (73%) HCC samples compared to paired non-malignant liver<sup>159</sup>. With regard to other solid tumor types, it was shown that both Spry1 (38/50, 78%) and Spry2 (48/50, 96%) expression levels are frequently repressed in breast cancer<sup>160</sup>, while in prostate cancer a decrease in Spry1 (39% of 407 immunohistochemically analyzed prostate cancer tissue microarrays) and Spry4 (11 out of 25 cases, 44%) levels contribute to malignant transformation<sup>181, 183</sup>. Further, Spry2 expression was markedly reduced in metastasis-forming prostate cancer-derived sublines compared to their respective two parent prostate cancer cell lines<sup>182</sup>. These data indicate that diverse members of the signal-limiting family of Spry proteins are commonly downregulated during carcinogenesis, whereas which and how many of the Spry members are affected, depends on the tissue origin.

Many different mechanisms may account for Spry2 downregulation in NSCLC. Since it was shown that in prostate cancer cells (but not in breast cancer- and HCC-derived cells<sup>159, 160</sup>) silencing by promoter hypermethylation accounted for the reduced expression of Spry2<sup>182</sup>, and in some cases also for Spry4<sup>183</sup>, we checked the response of Spry2 expression in NSCLC-derived cells to treatment using AZA, which demethylates silenced promoter-regions to induce transcription. In our hands, only 3/12 cell lines exhibited slightly enhanced Spry2 expression following incubation in AZA-containing medium. Further, reduced gene doses did not significantly account for reduced Spry2 levels in NSCLC cells (data not shown). Contrary, in HCC, Spry2 was frequently deleted at the genomic DNA level<sup>184</sup> and in prostate cancer, 27-40% of LOH was analyzed using tightly flanking markers to the Spry2 gene<sup>182</sup>.

Nevertheless, as shown in both Manuscripts of this thesis, enhanced Spry2 and Spry4 levels correlated with activating K-Ras mutations, whereas Spry1 expression was only slightly upregulated in the background of constitutively active Ras. Using RFLP analyses, we solely detected K-Ras mutations in the NSCLC histological subtypes of adenocarcinoma (AC) and large-cell carcinoma (LCC), but non in squameous cell carcinoma (SCC). Correspondingly, K-Ras mutations were almost exclusively described in AC/ LCC and not in SCC<sup>58</sup>. Since Spry expression is regulated as part of an auto-regulatory feedback loop<sup>105</sup>, activating Ras mutations might explain why, with respect to histological subtypes, Spry2 levels tend to be higher in AC- and LCC- than in SCC-derived cell lines. Induced levels of Spry2 were also found in mice expressing dominant active K-Ras<sup>G12D</sup><sup>156</sup>. Furthermore, in melanoma cells expressing dominant active B-Raf<sup>V599E</sup>, Spry2 was also upregulated compared to low levels in melanocytes and wt B-Raf melanoma cells<sup>186</sup>. Nevertheless, the mechanisms responsible for downregulation of Spry2 in NSCLC cancer have to be elucidated in further, more mechanistic approaches.

To assess the contribution of Spry2 downregulation to the malignant phenotype of NSCLC cells, we investigated the effect of ectopically expressed Spry2 on inhibition of MAPK activity, cell migration and proliferation. Using an adenoviral expressing system, we demonstrated that Spry2-mediated repression of ERK activity was exclusively observed in those cells homozygous for K-Ras<sup>wt</sup> in contrast to mutated K-Ras<sup>G12</sup>. Also, in another report, Spry family member Spry4 failed to inhibit constitutive active Ras<sup>L61</sup> MAPK activation<sup>107</sup>. Accordingly, deceleration of cell migration by Spry2 was significantly more potent in NSCLC cell lines expressing K-Ras<sup>wt</sup> as compared to cell lines harboring K-Ras<sup>G12mut</sup>. Since initial attempts to immunoprecipitate Spry2 with K-Ras have been unsuccessful (data not shown) our data give further evidence that Spry proteins counteract RTK-Ras-MAPK-mediated signaling upstream of Ras. Focusing on MAPK activity and cell migration, reduced Spry proteins only serves as an selective advantage in cells expressing wt Ras during neoplastic formation, whereas constitutively active Ras can circumvent Spry2 MAPK inhibition. Further, Ras-MAPK induced Spry overexpression might be tolerated when activating mutations occur at the level or downstream of Ras.

Interestingly, cell proliferation was significantly inhibited by Spry2 in all tested NSCLC cell lines irrespective of the K-Ras status and completely abolished tumor formation in SCID mice. Also in urethane-induced NSCLC tumor development in mice<sup>185</sup> overexpression of Spry2 reduced tumor multiplicity and diameter in lung. Surprisingly, ectopic expression of dominant negative Spry2 (Spry2<sup>Y55F</sup>) unable to inhibit MAPK activation<sup>132, 153</sup>, also

significantly attenuated NSCLC cell proliferation. Nevertheless the effect was lower compared to overexpressed wt Spry2 protein, arguing for a possible cumulating contribution of MAPK-mediated signals. In the mutated K-Ras cell line A-549, a difference in the inhibition of cell proliferation between wt Spry2 and Spry2<sup>Y55F</sup> became visible from 72 hours onwards. Since activated K-Ras is lost due to degradation (reported half life of around 30 hours<sup>205</sup>) we suggest that Spry2<sup>wt</sup>, but not Spry2<sup>Y55F</sup>, interferes with the activation also of newly synthesized K-Ras. Nevertheless, we were the first to show that also Spry2<sup>Y55F</sup> significantly inhibits cell proliferation and suggest that at least Spry2 counteracts growth-factor induced cellular responses in a Ras-dependent and –independent manner by a yet unidentified mechanism. Since a study suggested the involvement of PTEN in Spry2-mediated effects<sup>206</sup>, we also checked the activity of PI3K-downstream signaling components. In our cells, AKT and S6 phosphorylations were rather increased by ectopic Spry2 which was also seen in a report studying the influence of Spry2 during muscle cell development<sup>207</sup>. Therefore, and in accordance with several other reports<sup>136</sup>, we conclude that also during NSCLC tumorigenesis, Spry2 expression is not involved in counteracting PI3K-mediated signals.

In our subsequent studies we focused on different mechanisms regulating Spry1, 2 and 4 expressions. Since all Spry family members were described to function and to be regulated in an autoregulatory feedback loop manner, our data proof the existence of distinct Spry member-specific differences.

Focusing on Spry1 we propose regulating mechanisms independent of the RTK/Ras/MAPK cascade. Elevated levels of Spry1 were found exclusively in serum-deprived, G0-resting cells, whereas a decrease of Spry1 mRNA and protein expression was observed immediately after cell cycle release and low levels were maintained throughout the remaining phases of the cell cycle. Also in other studies Spry1 mRNA levels were decreased as a consequence of growth factor induction<sup>106, 151, 152</sup>. Further, Spry1 protein levels were only slightly but not significantly enhanced by activating Ras mutations. Interestingly, dominant-negative versions of Ras moderately repressed Spry1 levels. Since Ras functions via divergent downstream cascades, it seems that inhibited signal transmission has secondary effects also on components involved in Spry1 regulation. Other data described the tumor suppressing transcription factor WT-1 to activate Spry1 promotor during kidney development<sup>151</sup>. Surprisingly, overexpression of both, wt and oncogenic cCbl, enhanced Spry1 expression during cell cycle. Since it was shown that

Spry1 is targeted by cCbl<sup>132</sup> our data indicate that cCbl stabilizes Spry1 by yet undefined mechanisms.

Induction of Spry2 expression is dominantly influenced via Ras/MAPK-mediated cascades. Using different approaches we detected upregulated Spry2 especially in those cell lines harboring activating Ras mutations. Further, ectopically expressed Ras proteins elevated Spry2 protein levels in serum-deprived and logarithmically growing cells. In earlier reports, knock in of an oncogenic Ras<sup>G12D</sup> variant in fetal lungs of mice as well as fibroblasts expressing active Raf-1 also caused increased Spry2 protein levels compared to wt cells<sup>155, 156</sup>. In resting cells, we were able to induce Spry2 expression in response to serum and EGF, FGF2 and FGF9 growth factor addition as a consequence of immediate Erk activation. Further, the induction of Spry2 expression was co-regulated on mRNA and protein levels. Since these growth stimuli also induced signaling via PI3K pathway, we used oncogenic Ras versions exclusively signaling either via MAPK or PI3K, to demonstrate that induction is exclusively mediated via the Ras/Erk signaling cascade. Accordingly, IGF, exclusively activating PI3K and not MAPK, failed to induce Spry2. An earlier report also showed that Erk activation is required for Spry2 expression, since Spry2 levels are decreased upon inhibition of MEK-1<sup>152, 153</sup>. On the other hand, Spry2 could not be further elevated in a cell line harboring activated Ras. Since serum still increased the slow migrating band, it is possible that some of the post-translational modifications such as phosphorylation<sup>105</sup> or farnesylation<sup>106</sup> are mediated by Ras-independent mechanisms. During cell cycle, again Spry2 mRNA and proteins levels were significantly co-regulated. Interestingly, Spry2 expression was upregulated early in G1 phase, downregulated before G1/S transition and peaked again during late S and G2/M phase. Introduction of ectopic wt cCbl did not interfere with upregulation of Spry2 after cell cycle release, but further reduced Spry2 levels before G1/S transition. Since cells expressing dominant-negative (oncogenic) cCbl failed to downregulate Spry2 expression, we propose that degradation of Spry2 via cCbl is crucial before cell entry into S-phase. Oncogenic cCbl  $\Delta$ 70Z lacks the linker region between cCbl's tyrosine binding and RING finger domain and was shown to induce rapid and acute transformation of NIH3T3<sup>192</sup>. Since the linker is thought to mediate multiple interactions between the bound substrate of cCbl and the ubiquitin-conjugating enzymes recruited by cCbl's RING finger, cCbl  $\Delta$ 70Z is unable to multi-ubiquitylate and downregulate RTKs<sup>208</sup>. Also in the case of Spry2, cCbl  $\Delta$ 70Z interferes with the ability of cCbl wt to mediate Spry2 ubiquitination.

In the literature, Spry4 was shown to be upregulated in response to activating mutations of Ras and within the MAPK cascade<sup>155, 156</sup>. In our studies, we also elucidated that Ras signaling

influences Spry4 expression. Comparable to Spry2, Spry4 was also upregulated in NSCLC cells harboring constitutively active Ras. Further, introduction of activating Ras proteins elevated Spry4 levels in both serum-deprived and logarithmically growing cells. Nevertheless, Spry4 induction was always less pronounced than Spry2. Testing the influence of diverse growth stimuli on Spry4 expression in response to Erk and PI3K activation in resting cells, Spry4 was only efficiently induced after serum addition on mRNA and protein levels. Despite of a slight increase of Spry4 upon EGF stimulation, all other growth factors used (including many FGFs, IGF and PDGF) failed to induce Spry4. Other reports described immediate induction of Spry4 expression in response to Wnt3a and Wnt7a and Fzd9 coexpression<sup>148, 157</sup>, while it was also reported that Spry4 mRNA is upregulated in response to EGF, FGF and PDGF and directly linked to Erk activation<sup>152, 153</sup>. In these reports, Spry4 expression was analyzed in cells starved for 48h in medium containing insulin and transferrin or to non-starved cells<sup>152, 153</sup>. In our hands, Spry4 does not fulfill the criteria of functioning as an immediate early gene. Since we assured that diverse growth factors were only applied to G0-resting cells, it is possible that unequal methodical approaches account for the differences seen in the case of Spry4 induction. Using activating Ras mutations exclusively targeting either Raf or PI3K, respectively, we could show that both Ras-downstream effector cascades elevate Spry4 levels in 72 hours serum-deprived cells and suggest that induction, extent and duration of Spry4 are differently regulated by diverse signaling pathways next to Erk activation. During cell cycle, Spry4 protein does not mimic the expression pattern of Spry4 mRNA. While Spry4 mRNA only peaked early in G1 and remained low during other cell cycle phases, Spry4 protein expression was enhanced during G1 (6-8<sup>h</sup> after serum addition in WI38 cells) remained high throughout the remaining cell cycle. Therefore, we suggest that Spry4 induction is dependent on diverse stimuli besides MAPK activation (achieved by the addition of single growth factors to G0 WI38 cells), while, once elevated, post-translatory events are responsible to stabilize Spry4 protein. Using ectopically expressed wt and oncogenic cCbl, Spry4 protein was moderately induced in G0/G1 cells by wt cCbl and even more by dominant negative cCbl. Nevertheless, before G1/S transition the high Spry4 expression peak was not much influenced by the cCbl proteins used. Since Spry4 was shown not to be a target of cCbl, it seems that according to the influence of different cCbl proteins on Spry1, cCbl alters the activities of other proteins influencing Spry4 protein expression.

In summary we could show that loss of Spry2 and not Spry1 expression contributes to the malignant phenotype of NSCLC by enhancing RTK-mediated processes like cell migration



and proliferation and propose that Spry2 re-expression might serve as a promising therapy of NSCLC even when K-Ras is mutated. Further we were able to point out differences concerning induction and regulation of different Spry family members. In our systems, only Spry2 mRNA and protein were exclusively activated by the Ras/Erk pathway. We could also show that downregulation via cCbl is occurring during G1 phase before G1/S transition. While Spry4 protein is stabilized by mechanisms secondary to Ras activation, Spry1 is downregulated by a yet unidentified mechanism. Since we demonstrate that Spry2 inhibits RTK-mediated signals upstream of Ras but also by mechanisms independent of the Ras/MAPK signaling axis, possibly via inhibiting  $\text{Ca}^{2+}$ -efflux<sup>115</sup> in response to Ras-independent activation of phospholipase-C<sup>209</sup>, the identification of new interaction partners will be necessary to clearly dissect function and regulation of Spry proteins. Correspondingly, we synthesized a human lung cDNA library suitable for Yeast-two hybrid screening using Spry proteins as baits.

We conclude that Spry proteins are important players to regulate cell and tissue homeostasis and in the future, activation of Spry proteins might be considered as a strategy for novel approaches in cancer therapy.

## 7 Abbreviations

4E-BP	eIF4E-binding protein
AC	adenocarcinoma
AP2	activator protein 2
AZA	5-aza-2'-deoxycytidine
Bnl	branchless
Btl	breathless
CAKUT	congenital anomalies of the urinary tract and kidney
cCbl	casitas B-lineage lymphoma
CREB	cyclicAMP response element-binding protein
EGF	epidermal growth factor
EGFR	epidermal growth factor receptor
eIF4E	eukaryotic translation initiation factor
ER	endoplasmic reticulum
Erk	extracellular-regulated kinase
FGF	fibroblast growth factor
FGFR	FGF receptor
FRS2	fibroblast growth factor receptor substrate 2
GAP	GTPase activating proteins
GDNF	glial cell line-derived neurotrophic factor
GEF	guanine-nucleotide exchange factor
Grb2	growth factor receptor-bound protein 2
GTPases	monomeric guanosine triphosphotases
HCC	hepatocellular carcinoma
HGF/ SF	hepatocyte growth factor/ scatter factor
HIF-1	hypoxia-inducible factor 1
Htl	heartless
LCC	large-cell carcinoma
LOH	loss of heterozygosity
MAPK	mitogen-activated protein kinase
MEFs	mouse embryonic fibroblasts
Mnk-1	MAPK-interacting kinase 1
MOI	multiplicity of infection

---

NF1	neurofibromin-1
NSCLC	non-small cell lung cancer (Nicht-kleinzelliges Lungenkarzinom)
PCR	polymerase chain reaction
PDGF	platelet-derived growth factor
PDK-1	3'-phosphoinositide-dependent kinase-1
PH	pleckstrin-homology
PI3K	phosphatidylinositol 3-kinase
PIP <sub>2</sub>	phosphatidylinositol 3, 4-biphosphate
PIP <sub>3</sub>	phosphatidylinositol 3, 4, 5-triphosphate
PKB	Akt/protein kinase B
PP2A	protein phosphatase 2A
pSer, pTyr	phosphorylated serine, tyrosine residue
PTB	phospho-tyrosine binding
PTP1B	protein-Tyr phosphatase-1B
PTEN	phosphatase and tensin homolog
Ret	rearranged during transfection
RT	room temperature
RTK	receptor tyrosine kinase
SCC	squameous cell carcinoma
Ser	serine
SH2/ 3	Src homology region 2/ 3
Shh	sonic hedgehog homolog
Shp2	SH2-containing Tyr phosphatase 2
Sos	son of sevenless
SP1	stimulating protein 1
Spry	sprouty
Stat	signal transducer and activator of transcription
Tesk	serine/threonine testicular protein kinase
Tyr	tyrosine
VEGF	vascular-endothelial growth factor
VEGFR	VEGF receptor
wt	wildtype (wildtyp)
WT1	wilms tumor suppressor gene 1

## 8 References

1. Maley, C. C. et al. Selectively advantageous mutations and hitchhikers in neoplasms: p16 lesions are selected in Barrett's esophagus. *Cancer Res* 64, 3414-27 (2004).
2. Nowell, P. C. Tumor progression: a brief historical perspective. *Semin Cancer Biol* 12, 261-6 (2002).
3. Vogelstein, B. & Kinzler, K. W. Cancer genes and the pathways they control. *Nat Med* 10, 789-99 (2004).
4. McCormick, F. Signalling networks that cause cancer. *Trends Cell Biol* 9, M53-6 (1999).
5. Duesberg, P. & Li, R. Multistep carcinogenesis: a chain reaction of aneuploidizations. *Cell Cycle* 2, 202-10 (2003).
6. Loeb, L. A. A mutator phenotype in cancer. *Cancer Res* 61, 3230-9 (2001).
7. Friedberg, E. C. DNA damage and repair. *Nature* 421, 436-40 (2003).
8. Fidler, I. J. Critical factors in the biology of human cancer metastasis: twenty-eighth G.H.A. Clowes memorial award lecture. *Cancer Res* 50, 6130-8 (1990).
9. Yokota, J. Tumor progression and metastasis. *Carcinogenesis* 21, 497-503 (2000).
10. Classon, M. & Harlow, E. The retinoblastoma tumour suppressor in development and cancer. *Nat Rev Cancer* 2, 910-7 (2002).
11. Ortega, S., Malumbres, M. & Barbacid, M. Cyclin D-dependent kinases, INK4 inhibitors and cancer. *Biochim Biophys Acta* 1602, 73-87 (2002).
12. Sherr, C. J. The Pezcoller lecture: cancer cell cycles revisited. *Cancer Res* 60, 3689-95 (2000).
13. Tlsty, T. D. & Hein, P. W. Know thy neighbor: stromal cells can contribute oncogenic signals. *Curr Opin Genet Dev* 11, 54-9 (2001).
14. Freeman, M. Feedback control of intercellular signalling in development. *Nature* 408, 313-9 (2000).
15. Ashcroft, M. & Vousden, K. H. Regulation of p53 stability. *Oncogene* 18, 7637-43 (1999).
16. Oren, M. Regulation of the p53 tumor suppressor protein. *J Biol Chem* 274, 36031-4 (1999).
17. Levine, A. J. p53, the cellular gatekeeper for growth and division. *Cell* 88, 323-31 (1997).
18. Hubbard, S. R., Mohammadi, M. & Schlessinger, J. Autoregulatory mechanisms in protein-tyrosine kinases. *J Biol Chem* 273, 11987-90 (1998).
19. Hunter, T. The Croonian Lecture 1997. The phosphorylation of proteins on tyrosine: its role in cell growth and disease. *Philos Trans R Soc Lond B Biol Sci* 353, 583-605 (1998).
20. Blume-Jensen, P. & Hunter, T. Oncogenic kinase signalling. *Nature* 411, 355-65 (2001).
21. McKay, M. M. & Morrison, D. K. Integrating signals from RTKs to ERK/MAPK. *Oncogene* 26, 3113-21 (2007).
22. Levkowitz, G. et al. Ubiquitin ligase activity and tyrosine phosphorylation underlie suppression of growth factor signaling by c-Cbl/Sli-1. *Mol Cell* 4, 1029-40 (1999).
23. Luo, J., Manning, B. D. & Cantley, L. C. Targeting the PI3K-Akt pathway in human cancer: rationale and promise. *Cancer Cell* 4, 257-62 (2003).
24. Malumbres, M. & Barbacid, M. RAS oncogenes: the first 30 years. *Nat Rev Cancer* 3, 459-65 (2003).
25. Rajalingam, K., Schreck, R., Rapp, U. R. & Albert, S. Ras oncogenes and their downstream targets. *Biochim Biophys Acta* 1773, 1177-95 (2007).

26. Bentires-Alj, M., Kontaridis, M. I. & Neel, B. G. Stops along the RAS pathway in human genetic disease. *Nat Med* 12, 283-5 (2006).
27. Roberts, A. et al. The cardiofaciocutaneous syndrome. *J Med Genet* 43, 833-42 (2006).
28. Tartaglia, M. & Gelb, B. D. Noonan syndrome and related disorders: genetics and pathogenesis. *Annu Rev Genomics Hum Genet* 6, 45-68 (2005).
29. Goody, R. S., Frech, M. & Wittinghofer, A. Affinity of guanine nucleotide binding proteins for their ligands: facts and artefacts. *Trends Biochem Sci* 16, 327-8 (1991).
30. Wittinghofer, A. & Nassar, N. How Ras-related proteins talk to their effectors. *Trends Biochem Sci* 21, 488-91 (1996).
31. John, J., Schlichting, I., Schiltz, E., Rosch, P. & Wittinghofer, A. C-terminal truncation of p21H preserves crucial kinetic and structural properties. *J Biol Chem* 264, 13086-92 (1989).
32. Gideon, P. et al. Mutational and kinetic analyses of the GTPase-activating protein (GAP)-p21 interaction: the C-terminal domain of GAP is not sufficient for full activity. *Mol Cell Biol* 12, 2050-6 (1992).
33. Downward, J. Control of ras activation. *Cancer Surv* 27, 87-100 (1996).
34. Quilliam, L. A., Khosravi-Far, R., Huff, S. Y. & Der, C. J. Guanine nucleotide exchange factors: activators of the Ras superfamily of proteins. *Bioessays* 17, 395-404 (1995).
35. Sondermann, H. et al. Structural analysis of autoinhibition in the Ras activator Son of sevenless. *Cell* 119, 393-405 (2004).
36. Freedman, T. S. et al. A Ras-induced conformational switch in the Ras activator Son of sevenless. *Proc Natl Acad Sci U S A* 103, 16692-7 (2006).
37. Margarit, S. M. et al. Structural evidence for feedback activation by Ras.GTP of the Ras-specific nucleotide exchange factor SOS. *Cell* 112, 685-95 (2003).
38. Roberts, A. E. et al. Germline gain-of-function mutations in *SOS1* cause Noonan syndrome. *Nat Genet* 39, 70-4 (2007).
39. Tartaglia, M. et al. Gain-of-function *SOS1* mutations cause a distinctive form of Noonan syndrome. *Nat Genet* 39, 75-9 (2007).
40. Boykevisch, S. et al. Regulation of ras signaling dynamics by Sos-mediated positive feedback. *Curr Biol* 16, 2173-9 (2006).
41. Bartel, D. P. MicroRNAs: genomics, biogenesis, mechanism, and function. *Cell* 116, 281-97 (2004).
42. Johnson, S. M. et al. RAS is regulated by the let-7 microRNA family. *Cell* 120, 635-47 (2005).
43. Burke, P., Schooler, K. & Wiley, H. S. Regulation of epidermal growth factor receptor signaling by endocytosis and intracellular trafficking. *Mol Biol Cell* 12, 1897-910 (2001).
44. Chiu, V. K. et al. Ras signalling on the endoplasmic reticulum and the Golgi. *Nat Cell Biol* 4, 343-50 (2002).
45. Jiang, X. & Sorkin, A. Coordinated traffic of Grb2 and Ras during epidermal growth factor receptor endocytosis visualized in living cells. *Mol Biol Cell* 13, 1522-35 (2002).
46. Mor, A. & Philips, M. R. Compartmentalized Ras/MAPK signaling. *Annu Rev Immunol* 24, 771-800 (2006).
47. Plowman, S. J. & Hancock, J. F. Ras signaling from plasma membrane and endomembrane microdomains. *Biochim Biophys Acta* 1746, 274-83 (2005).
48. Sorkin, A. & Von Zastrow, M. Signal transduction and endocytosis: close encounters of many kinds. *Nat Rev Mol Cell Biol* 3, 600-14 (2002).

49. Goodwin, J. S. et al. Depalmitoylated Ras traffics to and from the Golgi complex via a nonvesicular pathway. *J Cell Biol* 170, 261-72 (2005).
50. Rocks, O. et al. An acylation cycle regulates localization and activity of palmitoylated Ras isoforms. *Science* 307, 1746-52 (2005).
51. Bivona, T. G. et al. Phospholipase Cgamma activates Ras on the Golgi apparatus by means of RasGRP1. *Nature* 424, 694-8 (2003).
52. Fivaz, M. & Meyer, T. Reversible intracellular translocation of KRas but not HRas in hippocampal neurons regulated by Ca<sup>2+</sup>/calmodulin. *J Cell Biol* 170, 429-41 (2005).
53. Mukherjee, S. & Maxfield, F. R. Membrane domains. *Annu Rev Cell Dev Biol* 20, 839-66 (2004).
54. Prior, I. A. et al. GTP-dependent segregation of H-ras from lipid rafts is required for biological activity. *Nat Cell Biol* 3, 368-75 (2001).
55. Roy, S. et al. Individual palmitoyl residues serve distinct roles in H-ras trafficking, microlocalization, and signaling. *Mol Cell Biol* 25, 6722-33 (2005).
56. Leon, J., Guerrero, I. & Pellicer, A. Differential expression of the ras gene family in mice. *Mol Cell Biol* 7, 1535-40 (1987).
57. Bos, J. L. et al. Prevalence of ras gene mutations in human colorectal cancers. *Nature* 327, 293-7 (1987).
58. Mascaux, C. et al. The role of RAS oncogene in survival of patients with lung cancer: a systematic review of the literature with meta-analysis. *Br J Cancer* 92, 131-9 (2005).
59. Fujita, J. et al. Ha-ras oncogenes are activated by somatic alterations in human urinary tract tumours. *Nature* 309, 464-6 (1984).
60. Visvanathan, K. V., Pockock, R. D. & Summerhayes, I. C. Preferential and novel activation of H-ras in human bladder carcinomas. *Oncogene Res* 3, 77-86 (1988).
61. Luo, D. et al. Analysis of N-ras gene mutation and p53 gene expression in human hepatocellular carcinomas. *World J Gastroenterol* 4, 97-99 (1998).
62. Bos, J. L. et al. Mutations in N-ras predominate in acute myeloid leukemia. *Blood* 69, 1237-41 (1987).
63. Esteban, L. M. et al. Targeted genomic disruption of H-ras and N-ras, individually or in combination, reveals the dispensability of both loci for mouse growth and development. *Mol Cell Biol* 21, 1444-52 (2001).
64. Johnson, L. et al. K-ras is an essential gene in the mouse with partial functional overlap with N-ras. *Genes Dev* 11, 2468-81 (1997).
65. Koera, K. et al. K-ras is essential for the development of the mouse embryo. *Oncogene* 15, 1151-9 (1997).
66. Umanoff, H., Edelmann, W., Pellicer, A. & Kucherlapati, R. The murine N-ras gene is not essential for growth and development. *Proc Natl Acad Sci U S A* 92, 1709-13 (1995).
67. Barbacid, M. ras genes. *Annu Rev Biochem* 56, 779-827 (1987).
68. Bos, J. L. ras oncogenes in human cancer: a review. *Cancer Res* 49, 4682-9 (1989).
69. Scheffzek, K. et al. The Ras-RasGAP complex: structural basis for GTPase activation and its loss in oncogenic Ras mutants. *Science* 277, 333-8 (1997).
70. Graham, D. L., Eccleston, J. F. & Lowe, P. N. The conserved arginine in rho-GTPase-activating protein is essential for efficient catalysis but not for complex formation with Rho.GDP and aluminum fluoride. *Biochemistry* 38, 985-91 (1999).
71. Cichowski, K. & Jacks, T. NF1 tumor suppressor gene function: narrowing the GAP. *Cell* 104, 593-604 (2001).
72. Feig, L. A. & Cooper, G. M. Inhibition of NIH 3T3 cell proliferation by a mutant ras protein with preferential affinity for GDP. *Mol Cell Biol* 8, 3235-43 (1988).

73. Matallanas, D. et al. Differences on the inhibitory specificities of H-Ras, K-Ras, and N-Ras (N17) dominant negative mutants are related to their membrane microlocalization. *J Biol Chem* 278, 4572-81 (2003).
74. Sigal, I. S. et al. Mutant ras-encoded proteins with altered nucleotide binding exert dominant biological effects. *Proc Natl Acad Sci U S A* 83, 952-6 (1986).
75. Dhillon, A. S. & Kolch, W. Untying the regulation of the Raf-1 kinase. *Arch Biochem Biophys* 404, 3-9 (2002).
76. Wellbrock, C., Karasarides, M. & Marais, R. The RAF proteins take centre stage. *Nat Rev Mol Cell Biol* 5, 875-85 (2004).
77. Voice, J. K., Klemke, R. L., Le, A. & Jackson, J. H. Four human ras homologs differ in their abilities to activate Raf-1, induce transformation, and stimulate cell motility. *J Biol Chem* 274, 17164-70 (1999).
78. Garnett, M. J. & Marais, R. Guilty as charged: B-RAF is a human oncogene. *Cancer Cell* 6, 313-9 (2004).
79. Alessi, D. R. et al. Identification of the sites in MAP kinase kinase-1 phosphorylated by p74raf-1. *Embo J* 13, 1610-9 (1994).
80. Mansour, S. J. et al. Mitogen-activated protein (MAP) kinase phosphorylation of MAP kinase kinase: determination of phosphorylation sites by mass spectrometry and site-directed mutagenesis. *J Biochem* 116, 304-14 (1994).
81. Payne, D. M. et al. Identification of the regulatory phosphorylation sites in pp42/mitogen-activated protein kinase (MAP kinase). *Embo J* 10, 885-92 (1991).
82. Zheng, C. F. & Guan, K. L. Activation of MEK family kinases requires phosphorylation of two conserved Ser/Thr residues. *Embo J* 13, 1123-31 (1994).
83. Wu, Y. & Han, M. Suppression of activated Let-60 ras protein defines a role of *Caenorhabditis elegans* Sur-1 MAP kinase in vulval differentiation. *Genes Dev* 8, 147-59 (1994).
84. Kolch, W. Coordinating ERK/MAPK signalling through scaffolds and inhibitors. *Nat Rev Mol Cell Biol* 6, 827-37 (2005).
85. Morrison, D. K. & Davis, R. J. Regulation of MAP kinase signaling modules by scaffold proteins in mammals. *Annu Rev Cell Dev Biol* 19, 91-118 (2003).
86. Rodriguez-Viciana, P. et al. Phosphatidylinositol-3-OH kinase as a direct target of Ras. *Nature* 370, 527-32 (1994).
87. van Weering, D. H. et al. Protein kinase B activation and lamellipodium formation are independent phosphoinositide 3-kinase-mediated events differentially regulated by endogenous Ras. *Mol Cell Biol* 18, 1802-11 (1998).
88. Kauffmann-Zeh, A. et al. Suppression of c-Myc-induced apoptosis by Ras signalling through PI(3)K and PKB. *Nature* 385, 544-8 (1997).
89. Yan, J., Roy, S., Apolloni, A., Lane, A. & Hancock, J. F. Ras isoforms vary in their ability to activate Raf-1 and phosphoinositide 3-kinase. *J Biol Chem* 273, 24052-6 (1998).
90. Toker, A. & Newton, A. C. Cellular signaling: pivoting around PDK-1. *Cell* 103, 185-8 (2000).
91. Datta, S. R., Brunet, A. & Greenberg, M. E. Cellular survival: a play in three Akts. *Genes Dev* 13, 2905-27 (1999).
92. Samuels, Y. et al. High frequency of mutations of the PIK3CA gene in human cancers. *Science* 304, 554 (2004).
93. Jimenez, C. et al. Identification and characterization of a new oncogene derived from the regulatory subunit of phosphoinositide 3-kinase. *Embo J* 17, 743-53 (1998).
94. Shayesteh, L. et al. PIK3CA is implicated as an oncogene in ovarian cancer. *Nat Genet* 21, 99-102 (1999).

95. Bader, A. G., Kang, S., Zhao, L. & Vogt, P. K. Oncogenic PI3K deregulates transcription and translation. *Nat Rev Cancer* 5, 921-9 (2005).
96. Haas-Kogan, D. et al. Protein kinase B (PKB/Akt) activity is elevated in glioblastoma cells due to mutation of the tumor suppressor PTEN/MMAC. *Curr Biol* 8, 1195-8 (1998).
97. Celebi, J. T. et al. Phenotypic findings of Cowden syndrome and Bannayan-Zonana syndrome in a family associated with a single germline mutation in PTEN. *J Med Genet* 36, 360-4 (1999).
98. Dufner, A. & Thomas, G. Ribosomal S6 kinase signaling and the control of translation. *Exp Cell Res* 253, 100-9 (1999).
99. Aoki, M., Blazek, E. & Vogt, P. K. A role of the kinase mTOR in cellular transformation induced by the oncoproteins P3k and Akt. *Proc Natl Acad Sci U S A* 98, 136-41 (2001).
100. Zhu, J., Woods, D., McMahon, M. & Bishop, J. M. Senescence of human fibroblasts induced by oncogenic Raf. *Genes Dev* 12, 2997-3007 (1998).
101. Qiu, R. G., Chen, J., Kim, D., McCormick, F. & Symons, M. An essential role for Rac in Ras transformation. *Nature* 374, 457-9 (1995).
102. Gille, H. & Downward, J. Multiple ras effector pathways contribute to G(1) cell cycle progression. *J Biol Chem* 274, 22033-40 (1999).
103. Verheijen, M. H., Wolthuis, R. M., Defize, L. H., den Hertog, J. & Bos, J. L. Interdependent action of RalGEF and Erk in Ras-induced primitive endoderm differentiation of F9 embryonal carcinoma cells. *Oncogene* 18, 4435-9 (1999).
104. Kim, H. J. & Bar-Sagi, D. Modulation of signalling by Sprouty: a developing story. *Nat Rev Mol Cell Biol* 5, 441-50 (2004).
105. Mason, J. M., Morrison, D. J., Basson, M. A. & Licht, J. D. Sprouty proteins: multifaceted negative-feedback regulators of receptor tyrosine kinase signaling. *Trends Cell Biol* 16, 45-54 (2006).
106. Impagnatiello, M. A. et al. Mammalian sprouty-1 and -2 are membrane-anchored phosphoprotein inhibitors of growth factor signaling in endothelial cells. *J Cell Biol* 152, 1087-98 (2001).
107. Lee, S. H., Schloss, D. J., Jarvis, L., Krasnow, M. A. & Swain, J. L. Inhibition of angiogenesis by a mouse sprouty protein. *J Biol Chem* 276, 4128-33 (2001).
108. Zhang, C. et al. Regulation of vascular smooth muscle cell proliferation and migration by human sprouty 2. *Arterioscler Thromb Vasc Biol* 25, 533-8 (2005).
109. Gross, I., Bassit, B., Benezra, M. & Licht, J. D. Mammalian sprouty proteins inhibit cell growth and differentiation by preventing ras activation. *J Biol Chem* 276, 46460-8 (2001).
110. Yigzaw, Y., Cartin, L., Pierre, S., Scholich, K. & Patel, T. B. The C terminus of sprouty is important for modulation of cellular migration and proliferation. *J Biol Chem* 276, 22742-7 (2001).
111. Lee, C. C. et al. Overexpression of sprouty 2 inhibits HGF/SF-mediated cell growth, invasion, migration, and cytokinesis. *Oncogene* 23, 5193-202 (2004).
112. Sutterluty, H. et al. Down-Regulation of Sprouty2 in Non-Small Cell Lung Cancer Contributes to Tumor Malignancy via Extracellular Signal-Regulated Kinase Pathway-Dependent and -Independent Mechanisms. *Mol Cancer Res* 5, 509-20 (2007).
113. Hacohen, N., Kramer, S., Sutherland, D., Hiromi, Y. & Krasnow, M. A. sprouty encodes a novel antagonist of FGF signaling that patterns apical branching of the *Drosophila* airways. *Cell* 92, 253-63 (1998).



114. Sutherland, D., Samakovlis, C. & Krasnow, M. A. branchless encodes a Drosophila FGF homolog that controls tracheal cell migration and the pattern of branching. *Cell* 87, 1091-101 (1996).
115. Nutt, S. L., Dingwell, K. S., Holt, C. E. & Amaya, E. Xenopus Sprouty2 inhibits FGF-mediated gastrulation movements but does not affect mesoderm induction and patterning. *Genes Dev* 15, 1152-66 (2001).
116. Minowada, G. et al. Vertebrate Sprouty genes are induced by FGF signaling and can cause chondrodysplasia when overexpressed. *Development* 126, 4465-75 (1999).
117. Chambers, D. & Mason, I. Expression of sprouty2 during early development of the chick embryo is coincident with known sites of FGF signalling. *Mech Dev* 91, 361-4 (2000).
118. Furthauer, M., Lin, W., Ang, S. L., Thisse, B. & Thisse, C. Sef is a feedback-induced antagonist of Ras/MAPK-mediated FGF signalling. *Nat Cell Biol* 4, 170-4 (2002).
119. Hashimoto, S., Nakano, H., Singh, G. & Katyal, S. Expression of Sprouty genes 1, 2 and 4 during mouse organogenesis. *Gene Expr Patterns* 2, 347-53 (2002).
120. de Maximy, A. A. et al. Cloning and expression pattern of a mouse homologue of drosophila sprouty in the mouse embryo. *Mech Dev* 81, 213-6 (1999).
121. Zhang, S., Lin, Y., Itaranta, P., Yagi, A. & Vainio, S. Expression of Sprouty genes 1, 2 and 4 during mouse organogenesis. *Mech Dev* 109, 367-70 (2001).
122. Tefft, J. D. et al. Conserved function of mSpry-2, a murine homolog of Drosophila sprouty, which negatively modulates respiratory organogenesis. *Curr Biol* 9, 219-22 (1999).
123. Leeksa, O. C. et al. Human sprouty 4, a new ras antagonist on 5q31, interacts with the dual specificity kinase TESK1. *Eur J Biochem* 269, 2546-56 (2002).
124. Anteby, E. Y. et al. Human placental Hofbauer cells express sprouty proteins: a possible modulating mechanism of villous branching. *Placenta* 26, 476-83 (2005).
125. Chi, L., Itaranta, P., Zhang, S. & Vainio, S. Sprouty2 is involved in male sex organogenesis by controlling fibroblast growth factor 9-induced mesonephric cell migration to the developing testis. *Endocrinology* 147, 3777-88 (2006).
126. Hall, A. B. et al. hSpry2 is targeted to the ubiquitin-dependent proteasome pathway by c-Cbl. *Curr Biol* 13, 308-14 (2003).
127. Hanafusa, H., Torii, S., Yasunaga, T. & Nishida, E. Sprouty1 and Sprouty2 provide a control mechanism for the Ras/MAPK signalling pathway. *Nat Cell Biol* 4, 850-8 (2002).
128. Rubin, C. et al. Sprouty fine-tunes EGF signaling through interlinked positive and negative feedback loops. *Curr Biol* 13, 297-307 (2003).
129. Guy, G. R. et al. Sprouty: how does the branch manager work? *J Cell Sci* 116, 3061-8 (2003).
130. Casci, T., Vinos, J. & Freeman, M. Sprouty, an intracellular inhibitor of Ras signaling. *Cell* 96, 655-65 (1999).
131. Lim, J. et al. Sprouty proteins are targeted to membrane ruffles upon growth factor receptor tyrosine kinase activation. Identification of a novel translocation domain. *J Biol Chem* 275, 32837-45 (2000).
132. Mason, J. M. et al. Tyrosine phosphorylation of Sprouty proteins regulates their ability to inhibit growth factor signaling: a dual feedback loop. *Mol Biol Cell* 15, 2176-88 (2004).
133. Lim, J. et al. The cysteine-rich sprouty translocation domain targets mitogen-activated protein kinase inhibitory proteins to phosphatidylinositol 4,5-bisphosphate in plasma membranes. *Mol Cell Biol* 22, 7953-66 (2002).
134. Chambers, D., Medhurst, A. D., Walsh, F. S., Price, J. & Mason, I. Differential display of genes expressed at the midbrain - hindbrain junction identifies sprouty2: an

- FGF8-inducible member of a family of intracellular FGF antagonists. *Mol Cell Neurosci* 15, 22-35 (2000).
135. Mailloux, A. A. et al. Evidence that SPROUTY2 functions as an inhibitor of mouse embryonic lung growth and morphogenesis. *Mech Dev* 102, 81-94 (2001).
  136. Mason, J. M., Morrison, D. J., Albert Basson, M. & Licht, J. D. Sprouty proteins: multifaceted negative-feedback regulators of receptor tyrosine kinase signaling. *Trends Cell Biol* 16, 45-54 (2006).
  137. Tefft, D. et al. mSprouty2 inhibits FGF10-activated MAP kinase by differentially binding to upstream target proteins. *Am J Physiol Lung Cell Mol Physiol* 283, L700-6 (2002).
  138. Perl, A. K., Hokuto, I., Impagnatiello, M. A., Christofori, G. & Whitsett, J. A. Temporal effects of Sprouty on lung morphogenesis. *Dev Biol* 258, 154-68 (2003).
  139. Kramer, S., Okabe, M., Hacohen, N., Krasnow, M. A. & Hiromi, Y. Sprouty: a common antagonist of FGF and EGF signaling pathways in *Drosophila*. *Development* 126, 2515-25 (1999).
  140. Reich, A., Sapir, A. & Shilo, B. Sprouty is a general inhibitor of receptor tyrosine kinase signaling. *Development* 126, 4139-47 (1999).
  141. Taketomi, T. et al. Loss of mammalian Sprouty2 leads to enteric neuronal hyperplasia and esophageal achalasia. *Nat Neurosci* 8, 855-7 (2005).
  142. Shim, K., Minowada, G., Coling, D. E. & Martin, G. R. Sprouty2, a mouse deafness gene, regulates cell fate decisions in the auditory sensory epithelium by antagonizing FGF signaling. *Dev Cell* 8, 553-64 (2005).
  143. Goodnough, L. H., Brugmann, S. A., Hu, D. & Helms, J. A. Stage-dependent craniofacial defects resulting from Sprouty2 overexpression. *Dev Dyn* 236, 1918-28 (2007).
  144. Welsh, I. C., Hagge-Greenberg, A. & O'Brien, T. P. A dosage-dependent role for Spry2 in growth and patterning during palate development. *Mech Dev* 124, 746-61 (2007).
  145. Colvin, J. S., Feldman, B., Nadeau, J. H., Goldfarb, M. & Ornitz, D. M. Genomic organization and embryonic expression of the mouse fibroblast growth factor 9 gene. *Dev Dyn* 216, 72-88 (1999).
  146. Colvin, J. S., White, A. C., Pratt, S. J. & Ornitz, D. M. Lung hypoplasia and neonatal death in Fgf9-null mice identify this gene as an essential regulator of lung mesenchyme. *Development* 128, 2095-106 (2001).
  147. Klein, O. D. et al. Sprouty genes control diastema tooth development via bidirectional antagonism of epithelial-mesenchymal FGF signaling. *Dev Cell* 11, 181-90 (2006).
  148. Taniguchi, K. et al. Sprouty2 and Sprouty4 are essential for embryonic morphogenesis and regulation of FGF signaling. *Biochem Biophys Res Commun* 352, 896-902 (2007).
  149. Basson, M. A. et al. Sprouty1 is a critical regulator of GDNF/RET-mediated kidney induction. *Dev Cell* 8, 229-39 (2005).
  150. Basson, M. A. et al. Branching morphogenesis of the ureteric epithelium during kidney development is coordinated by the opposing functions of GDNF and Sprouty1. *Dev Biol* 299, 466-77 (2006).
  151. Gross, I. et al. The receptor tyrosine kinase regulator Sprouty1 is a target of the tumor suppressor WT1 and important for kidney development. *J Biol Chem* 278, 41420-30 (2003).
  152. Ozaki, K. et al. ERK pathway positively regulates the expression of Sprouty genes. *Biochem Biophys Res Commun* 285, 1084-8 (2001).

153. Sasaki, A., Taketomi, T., Wakioka, T., Kato, R. & Yoshimura, A. Identification of a dominant negative mutant of Sprouty that potentiates fibroblast growth factor- but not epidermal growth factor-induced ERK activation. *J Biol Chem* 276, 36804-8 (2001).
154. Rubin, C., Zwang, Y., Vaisman, N., Ron, D. & Yarden, Y. Phosphorylation of carboxyl-terminal tyrosines modulates the specificity of Sprouty-2 inhibition of different signaling pathways. *J Biol Chem* 280, 9735-44 (2005).
155. Courtois-Cox, S. et al. A negative feedback signaling network underlies oncogene-induced senescence. *Cancer Cell* 10, 459-72 (2006).
156. Shaw, A. T. et al. Sprouty-2 regulates oncogenic K-ras in lung development and tumorigenesis. *Genes Dev* 21, 694-707 (2007).
157. Winn, R. A. et al. Restoration of Wnt-7a expression reverses non-small cell lung cancer cellular transformation through frizzled-9-mediated growth inhibition and promotion of cell differentiation. *J Biol Chem* 280, 19625-34 (2005).
158. Li, X., Brunton, V. G., Burgar, H. R., Wheldon, L. M. & Heath, J. K. FRS2-dependent SRC activation is required for fibroblast growth factor receptor-induced phosphorylation of Sprouty and suppression of ERK activity. *J Cell Sci* 117, 6007-17 (2004).
159. Fong, C. W. et al. Sprouty 2, an inhibitor of mitogen-activated protein kinase signaling, is down-regulated in hepatocellular carcinoma. *Cancer Res* 66, 2048-58 (2006).
160. Lo, T. L. et al. The ras/mitogen-activated protein kinase pathway inhibitor and likely tumor suppressor proteins, sprouty 1 and sprouty 2 are deregulated in breast cancer. *Cancer Res* 64, 6127-36 (2004).
161. Ding, W., Bellusci, S., Shi, W. & Warburton, D. Functional analysis of the human Sprouty2 gene promoter. *Gene* 322, 175-85 (2003).
162. Ding, W., Bellusci, S., Shi, W. & Warburton, D. Genomic structure and promoter characterization of the human Sprouty4 gene, a novel regulator of lung morphogenesis. *Am J Physiol Lung Cell Mol Physiol* 287, L52-9 (2004).
163. Ding, W. & Warburton, D. Down-regulation of Sprouty2 via p38 MAPK plays a key role in the induction of cellular apoptosis by tumor necrosis factor-alpha. *Biochem Biophys Res Commun* 375, 460-4 (2008).
164. Ding, W. et al. Sprouty2 downregulation plays a pivotal role in mediating crosstalk between TGF-beta1 signaling and EGF as well as FGF receptor tyrosine kinase-ERK pathways in mesenchymal cells. *J Cell Physiol* 212, 796-806 (2007).
165. Lao, D. H. et al. A Src homology 3-binding sequence on the C terminus of Sprouty2 is necessary for inhibition of the Ras/ERK pathway downstream of fibroblast growth factor receptor stimulation. *J Biol Chem* 281, 29993-30000 (2006).
166. Sasaki, A. et al. Mammalian Sprouty4 suppresses Ras-independent ERK activation by binding to Raf1. *Nat Cell Biol* 5, 427-32 (2003).
167. Yigzaw, Y., Poppleton, H. M., Sreejayan, N., Hassid, A. & Patel, T. B. Protein-tyrosine phosphatase-1B (PTP1B) mediates the anti-migratory actions of Sprouty. *J Biol Chem* 278, 284-8 (2003).
168. Hanafusa, H., Torii, S., Yasunaga, T., Matsumoto, K. & Nishida, E. Shp2, an SH2-containing protein-tyrosine phosphatase, positively regulates receptor tyrosine kinase signaling by dephosphorylating and inactivating the inhibitor Sprouty. *J Biol Chem* 279, 22992-5 (2004).
169. Cabrita, M. A. & Christofori, G. Sprouty proteins: antagonists of endothelial cell signaling and more. *Thromb Haemost* 90, 586-90 (2003).
170. Egan, J. E., Hall, A. B., Yatsula, B. A. & Bar-Sagi, D. The bimodal regulation of epidermal growth factor signaling by human Sprouty proteins. *Proc Natl Acad Sci U S A* 99, 6041-6 (2002).

171. Wong, E. S. et al. Sprouty2 attenuates epidermal growth factor receptor ubiquitylation and endocytosis, and consequently enhances Ras/ERK signalling. *Embo J* 21, 4796-808 (2002).
172. Haglund, K., Schmidt, M. H., Wong, E. S., Guy, G. R. & Dikic, I. Sprouty2 acts at the Cbl/CIN85 interface to inhibit epidermal growth factor receptor downregulation. *EMBO Rep* 6, 635-41 (2005).
173. Fong, C. W. et al. Tyrosine phosphorylation of Sprouty2 enhances its interaction with c-Cbl and is crucial for its function. *J Biol Chem* 278, 33456-64 (2003).
174. Thien, C. B. & Langdon, W. Y. Negative regulation of PTK signalling by Cbl proteins. *Growth Factors* 23, 161-7 (2005).
175. Wong, E. S., Lim, J., Low, B. C., Chen, Q. & Guy, G. R. Evidence for direct interaction between Sprouty and Cbl. *J Biol Chem* 276, 5866-75 (2001).
176. Kowanz, K. et al. Identification of a novel proline-arginine motif involved in CIN85-dependent clustering of Cbl and down-regulation of epidermal growth factor receptors. *J Biol Chem* 278, 39735-46 (2003).
177. Chandramouli, S. et al. Tesk1 interacts with Spry2 to abrogate its inhibition of ERK phosphorylation downstream of receptor tyrosine kinase signaling. *J Biol Chem* 283, 1679-91 (2008).
178. Tsumura, Y., Toshima, J., Leeksa, O. C., Ohashi, K. & Mizuno, K. Sprouty-4 negatively regulates cell spreading by inhibiting the kinase activity of testicular protein kinase. *Biochem J* 387, 627-37 (2005).
179. DaSilva, J., Xu, L., Kim, H. J., Miller, W. T. & Bar-Sagi, D. Regulation of sprouty stability by Mnk1-dependent phosphorylation. *Mol Cell Biol* 26, 1898-907 (2006).
180. Lao, D. H. et al. Direct binding of PP2A to Sprouty2 and phosphorylation changes are a prerequisite for ERK inhibition downstream of fibroblast growth factor receptor stimulation. *J Biol Chem* 282, 9117-26 (2007).
181. Kwabi-Addo, B. et al. The expression of Sprouty1, an inhibitor of fibroblast growth factor signal transduction, is decreased in human prostate cancer. *Cancer Res* 64, 4728-35 (2004).
182. McKie, A. B. et al. Epigenetic inactivation of the human sprouty2 (hSPRY2) homologue in prostate cancer. *Oncogene* 24, 2166-74 (2005).
183. Wang, J., Thompson, B., Ren, C., Ittmann, M. & Kwabi-Addo, B. Sprouty4, a suppressor of tumor cell motility, is down regulated by DNA methylation in human prostate cancer. *Prostate* 66, 613-24 (2006).
184. Lee, S. A. et al. Integration of genomic analysis and in vivo transfection to identify sprouty 2 as a candidate tumor suppressor in liver cancer. *Hepatology* 47, 1200-10 (2008).
185. Minowada, G. & Miller, Y. E. Sprouty 2 gene in mouse lung tumorigenesis. *Chest* 125, 111S (2004).
186. Tsavachidou, D. et al. SPRY2 is an inhibitor of the ras/extracellular signal-regulated kinase pathway in melanocytes and melanoma cells with wild-type BRAF but not with the V599E mutant. *Cancer Res* 64, 5556-9 (2004).
187. Nishikawa, T. et al. A simple method of detecting K-ras point mutations in stool samples for colorectal cancer screening using one-step polymerase chain reaction/restriction fragment length polymorphism analysis. *Clin Chim Acta* 318, 107-12 (2002).
188. Hardy, S., Kitamura, M., Harris-Stansil, T., Dai, Y. & Phipps, M. L. Construction of adenovirus vectors through Cre-lox recombination. *J Virol* 71, 1842-9 (1997).
189. Zwick, E., Bange, J. & Ullrich, A. Receptor tyrosine kinases as targets for anticancer drugs. *Trends Mol Med* 8, 17-23 (2002).

190. Sutterluty, H. et al. p45SKP2 promotes p27Kip1 degradation and induces S phase in quiescent cells. *Nat Cell Biol* 1, 207-14 (1999).
191. Sutterluty, H. et al. Growth-regulated antisense transcription of the mouse thymidine kinase gene. *Nucleic Acids Res* 26, 4989-95 (1998).
192. Andoniou, C. E., Thien, C. B. & Langdon, W. Y. Tumour induction by activated abl involves tyrosine phosphorylation of the product of the cbl oncogene. *Embo J* 13, 4515-23 (1994).
193. Wick, G., Jansen-Durr, P., Berger, P., Blasko, I. & Grubeck-Loebenstien, B. Diseases of aging. *Vaccine* 18, 1567-83 (2000).
194. Hahn, W. C. & Weinberg, R. A. Rules for making human tumor cells. *N Engl J Med* 347, 1593-603 (2002).
195. Hanahan, D. & Weinberg, R. A. The hallmarks of cancer. *Cell* 100, 57-70 (2000).
196. Vlahovic, G. & Crawford, J. Activation of tyrosine kinases in cancer. *Oncologist* 8, 531-8 (2003).
197. Tateishi, M., Ishida, T., Mitsudomi, T., Kaneko, S. & Sugimachi, K. Immunohistochemical evidence of autocrine growth factors in adenocarcinoma of the human lung. *Cancer Res* 50, 7077-80 (1990).
198. Damstrup, L., Rygaard, K., Spang-Thomsen, M. & Poulsen, H. S. Expression of the epidermal growth factor receptor in human small cell lung cancer cell lines. *Cancer Res* 52, 3089-93 (1992).
199. Lei, W., Mayotte, J. E. & Levitt, M. L. Enhancement of chemosensitivity and programmed cell death by tyrosine kinase inhibitors correlates with EGFR expression in non-small cell lung cancer cells. *Anticancer Res* 19, 221-8 (1999).
200. Downward, J. Targeting RAS signalling pathways in cancer therapy. *Nat Rev Cancer* 3, 11-22 (2003).
201. Davies, H. et al. Mutations of the BRAF gene in human cancer. *Nature* 417, 949-54 (2002).
202. Sansal, I. & Sellers, W. R. The biology and clinical relevance of the PTEN tumor suppressor pathway. *J Clin Oncol* 22, 2954-63 (2004).
203. Yokouchi, M. et al. Ligand-induced ubiquitination of the epidermal growth factor receptor involves the interaction of the c-Cbl RING finger and UbcH7. *J Biol Chem* 274, 31707-12 (1999).
204. Hashimoto, S., Nakano, H., Singh, G. & Katyal, S. Expression of Sprad and Sprouty in developing rat lung. *Mech Dev* 119 Suppl 1, S303-9 (2002).
205. Tsai, F. M., Shyu, R. Y. & Jiang, S. Y. RIG1 inhibits the Ras/mitogen-activated protein kinase pathway by suppressing the activation of Ras. *Cell Signal* 18, 349-58 (2006).
206. Edwin, F., Singh, R., Endersby, R., Baker, S. J. & Patel, T. B. The tumor suppressor PTEN is necessary for human Sprouty 2-mediated inhibition of cell proliferation. *J Biol Chem* 281, 4816-22 (2006).
207. de Alvaro, C., Martinez, N., Rojas, J. M. & Lorenzo, M. Sprouty-2 overexpression in C2C12 cells confers myogenic differentiation properties in the presence of FGF2. *Mol Biol Cell* 16, 4454-61 (2005).
208. Zheng, N., Wang, P., Jeffrey, P. D. & Pavletich, N. P. Structure of a c-Cbl-UbcH7 complex: RING domain function in ubiquitin-protein ligases. *Cell* 102, 533-9 (2000).
209. Schlessinger, J. Cell signaling by receptor tyrosine kinases. *Cell* 103, 211-25 (2000).

## 9 Curriculum Vitae

# CHRISTOPH-ERIK MAYER

Datum und Ort der Geburt            24. Mai 1979, Wien, Österreich  
 Nationalität                            Österreich

### AUSBILDUNG

---

- 6/2007 – 9/2007                    Short-Term Fellowship im Labor von Ass. Prof. Dr. Mengiste, Department of Botany and Plant Pathology, Purdue University, West Lafayette, IN, USA – Erlernen der Yeast-Two Hybrid Technik und Synthese einer menschlichen Lungen-cDNA Library.
- seit 3/2005                            Dokorratsstudium an der Universität Wien unter der Betreuung von Ao. Prof. Dr. Pittner  
 Die Arbeit wurde im Labor von Priv. Doz. Dr. Sutterlüty am Institut für Krebsforschung, KIM I, Medizinische Universität Wien durchgeführt  
*Role of Sprouty proteins as antagonists of RTK signaling*
- seit 3/2005                            Universitätslehrgang Toxikologie für Postgraduierte an der Medizinischen Universität Wien
- 2/2005                                    Abschluß des Diplomstudiums Chemie/ Biochemie an der Universität Wien mit Auszeichnung
- 7/2003 – 2/2005                    Diplomarbeit an der Universität Wien unter der Betreuung von Ao. Prof. Dr. Pittner  
 Die Arbeit wurde im Labor von Ao. Prof. Dr. Berger am Institut für Krebsforschung, KIM I, Medizinische Universität Wien durchgeführt  
*Endogene Wachstumsfaktorinhibitoren (Sprouty Gene) in humanen Lungen- und Hirntumoren (Endogenous growth factor inhibitors (Sprouty genes) in human lung and brain tumours)*
- 10/1998 – 2/2005                    Diplomstudium Chemie an der Universität Wien
- 7/1997 – 1/1998                    Präsenzdienst

- 1989 – 1997 Realgymnasium mit musikalischem Schwerpunkt an der Höheren Internatsschule des Bundes, 1030 Wien.  
Matura bestanden im Juni 1997 mit ausgezeichnetem Erfolg
- 1985 – 1989 Volksschule des Instituts Sacré-Coeur, 1030 Wien

## PUBLIKATIONEN

Ras signaling has a clearly distinguishable impact on Sprouty1, 2 and expressions. Christoph-Erik Mayer, Barbara Haigl, Florian Jantscher, Gerald Siegwart, Walter Berger and Hedwig Sutterlüty. submitted to BBA-Molecular Cell Research

Down-Regulation of Sprouty2 in Non-Small Cell Lung Cancer Contributes to Tumor Malignancy via Extracellular Signal-Regulated Kinase Pathway-Dependent and -Independent Mechanisms. Hedwig Sutterlüty \*, Christoph-Erik Mayer \*, Ulrike Setinek, Johannes Attems, Slav Ovtcharov, Mario Mikula, Wolfgang Mikulits, Michael Micksche and Walter Berger. Mol Cancer Res. 2007 May;5(5):509-20. \*equally contributed.

Präsentationen auf Konferenzen:

Sprouty expression is regulated by multiple mechanisms: how are they altered in cancer? **Mayer CE**, Haigl B, Ovtcharov S, Micksche M, Berger W and Sutterlüty H. 100<sup>th</sup> Annual Meeting, American Association for Cancer Research, Los Angeles, USA, 2007

Sprouty expression is de-regulated at different levels in cancer cells. **C. Mayer**, C. Pirker, I. Fröhlich, S. Ovtcharov, J. Attems, M. Micksche, W. Berger, H. Sutterlüty. 19<sup>th</sup> Meeting of the European Association for Cancer Research, Budapest, Hungary, 2006.

Role of Sprouty2 Downregulation in Malignant Growth of Non-Small Cell Lung Cancer (NSCLC). **Christoph-Erik Mayer**, Hediwg Sutterlüty, Ulrike Setinek, Johannes Attems and Walter Berger. 1. PhD-Symposium 2005.

Influence of Sprouty2 on RTK-dependent Signalling in Non-Small Cell Lung Cancer (NSCLC). **Mayer C.E.**, Sutterlüty H. and Berger W. The 1<sup>st</sup> Vienna Meeting on Tumor Invasion and Metastasis 2005.

Beiträge zu Präsentationen auf Konferenzen:

Mechanisms involved in the regulation of Sprouty4 expression. Haigl B, **Mayer CE**, Attems J, Micksche M, Berger W and Sutterlüty H. 32<sup>nd</sup> FEBS Congress, Molecular Machines, Vienna, Austria, 2007.

A new function of Aurora A at the G1/S transition of the cell cycle. Jantscher F, Pirker C, **Mayer C**, Siegwart G, Micksche M, Berger W and Sutterlüty H. 32<sup>nd</sup> FEBS Congress, Molecular Machines, Vienna, Austria, 2007

Inhibition of cell migration and proliferation in non-small cell lung cancer (NSCLC) by Sprouty 2 (Spry2) via K-Ras dependent and independent pathways. Hedi Sutterlüty, **Christoph-Erik Mayer**, Johannes Attems, Ulrike Setinek, Mario Mikula, Wolfgang Mikulits,

Michael Micksche, Walter Berger. 97th Annual Meeting, American Association for Cancer Research, Washington DC, USA, 2006.

Role of Sprouty2 as negative regulator of RTK signalling in malignant growth of non-small cell lung cancer (NSCLC). Hedwig Sutterlüty, **Christoph-Erik Mayer**, Ulrike Setinek, Johannes Attens and Walter Berger. 96th Annual Meeting, American Association for Cancer Research, Anaheim, USA, 2005.

Role of Sprouty protein downregulation in non-small cell lung cancer (NSCLC) growth. Sutterlüty H, **Mayer CE**, Holzmann K, Micksche M and Berger W. 18<sup>th</sup> Meeting of the European Association for Cancer Research, Innsbruck, Austria, 2004.